STUDY ON CRITICAL SELF-IGNITION TEMPERATURE OF LOW RANK COAL TO PREVENT SPONTANEOUS COMBUSTION IN A COAL MINE GOAF

王, 永軍

https://doi.org/10.15017/1543980

STUDY ON CRITICAL SELF-IGNITION TEMPERATURE OF LOW RANK COAL TO PREVENT SPONTANEOUS COMBUSTION IN A COAL MINE GOAF

A dissertation presented

by

YONGJUN WANG

to

The Department of Earth Resources Engineering

Graduate School of Engineering

in partial fulfillment of the requirements

for the degree of

Doctor of Engineering

KYUSHU UNIVERSITY

2015-09

Abstract

Spontaneous combustion of low-rank coal, such as lignite, is a hot issue to promote their utilizations for a coal gasification power plant, because their reserves are huge and has not been fully developed due to high self-heating rate. It has been well-known that the spontaneous combustion of coal has been observed after the internal pile temperature is over the critical self-ignition temperature (*CSIT*) which strongly depends on the pile volume. Although previous laboratory measurements on self-heating rate of coal have been done using quite small amount of coal samples, it is required to carry upscale experiments using low-rank coal volume of $1m^3$ order, because the coal volume is the dominant physical factor than other factors to induce spontaneous combustion.

In the present study, the spontaneous combustion of lignite classified as low-rank coal has been investigated by both of laboratory experiment (pile size; 2.5 to 10 cm) and upscale experiment (pile size; 25 to 100 cm) using the wire-mesh basket test up to $1m^3$ in its volume in order to clear (a) temperature-time curves in the coal pile for different size of the baskets and ambient air temperature; (b) *CSIT* measurement for the coal pile volume; (c) extrapolate the *CSIT* value against 100 m^3 order in industrial stockpile volume. (d) simulate spontaneous combustion of residual coal in the mine goaf based on *CSIT* and thermal characteristics function of porosity in the goaf.

The dissertation is composed of six chapters as follows:

Chapter 1 describes the role of coal, especially low rank coal, in today's world energy demand. The problems of spontaneous combustion at coal mines in China, the largest coal production and consumption country in the world, are introduced from standing points of mine safety and Economic loss. Furthermore, this chapter

reviews experimental methodologies and theoretical approaches to investigate coal spontaneous combustion or self-heating presented by previous researches. The major physical parameters were defined based on the Frank-Kamenetskii (F-K) equation. The F-K equation was presented for combustible material piles by Frank Kameneskii (1959) to evaluate the critical self-ignition temperature (*CSIT*) which is the most substantial indicator to show the lowest temperature to lead spontaneous combustion. The F-K equation was formulated from Arrhenius equation on oxidation or heat generation and heat conduction equation to express heat balance in the pile.

Chapter 2 describes the apparatuses and methodologies for the wire-mesh basket tests with wide range of coal volume 10 to 10^6 cm^3 in laboratory and upscale experiments. The laboratory and upscale wire mesh baskets were filled with crushed coal 0.48 mm or 46 mm in average size, respectively. The baskets were installed in the chambers control its internal air to constant temperature (40 to 200 ºC) using electric heaters. In the experiments, coal temperatures in the pile and combustion gases (CO_2 and CO) from the coal were monitored continuously for 8 hour to 22 days depends on the basket size. Four lignite (low-rank coal) called LE-1, LE-2, NE and UE, and one sub-bituminous coal (SE) were pulverized with the average size of 0.48 mm or 46 mm were used for the wire-mesh basket experiments.

Chapter 3 describes the results laboratory experiment using three cubic wire-mesh baskets under different ambient temperatures (40 to 150 ºC) to find *CSIT* for coal samples. Based on the center temperature-time curves of three cubic piles 2.5, 5.0 and 10 cm in size, values of *CSIT* for LE-1 were obtained as 143, 124 and 117 ºC, respectively. From a comparison of relations between *CSIT* and pile size for LE-1 and UE, coal sample LE-1 showed lower *CSIT* than UE. Thus, the equation of *CSIT* vs. pile size depends on coal properties such as activation energy and moisture content.

Chapter 4 presents the upscale experimental results on *CSIT* for UE coal piles 25, 50 and 100 cm in size under the ambient temperature 75 or 85 ºC. The results of 100cm pile showed quite different temperature-time curves during the heating process. Besides, the pile height or volume reductions were also measured to analyze characteristic diversification of the coal piles. The most important result is the value of *CSIT* evaluated by the upscale experiment using the wire-mesh basket $1m^3$ in volume to extrapolate that of industrial coal stockpile with volume of 100 m^3 order.

Chapter 5 explains the numerical simulation on spontaneous combustion at a goaf area after longwall mining in the underground coal mine. The measured value of *CSIT* was applied to a practical numerical simulation to find a method to avoid spontaneous combustion of residual coals at the goaf. Based on the numerical simulation results the goaf area can be classified into three zones. It was also confirmed that the method injecting grouting slurry is effective to increase activation energy of residual coals and decrease porosity of goaf area consists residual coals and fall rocks. It was expected that the grouting slurry prevents the coal spontaneous combustion in the goaf. Measurement results of oxygen concentration using tube-bundle system also proved that the slurry grouting method is effective and economical to prevent spontaneous combustion by reducing porosity in goaf area.

Chapter 6 presents the conclusions of this study on spontaneous combustion of the low rank coal. It contains a summary of the findings on *CSIT* values vs. pile size or volume measured by the laboratory and upscale wire-mesh basket tests and numerical simulation results of spontaneous combustion of residual coal in a goaf area at a underground coal mine.

Table of Contents

Abstract II

Table of Contents V

List of Tables VII

List of Figures VIII

Acknowledgements XII

Chapter 1 : Introduction 1

1.1 Global Energy Status Including Coal 1

1.2 Coal and Its Distribution 2

1.3 Low Rank Coal 4

1.4 Spontaneous Combustion 7

1.5 Arrhenius Equation 8

1.6 Frank-Kamenetskii's Ignition Theory 9

1.7 Previous Accidents of Spontaneous Combustion 11

1.8 Evaluating Methods of Low Rank Coal Spontaneous Combustion 13

1.9 Objectives of Present Research 14

1.10 Dissertation Overview 16

Chapter 2: Experimental Apparatus and Methodology 20

2.1 Introduction 20

2.2 Experimental Design 20

2.2.1 Experimental setup 20

2.2.2 Experimental apparatus 23

2.3 Definitions of Parameters 25

2.4 Material Details 32

2.5 Equation for Critical Temperature 34

2.6 Conclusions 37

Chapter 3: Laboratory Experiments on Critical Self-Ignition Temperature 39

3.1 Introduction 39

3.2 Experimental Results and Discussions 40
3.2.1 Samples continues heating test 40
3.2.2 Wire-mesh basket test 43
3.3 Equation Analysis 52
3.4 Conclusions 54
Chapter 4 : Upscale Experiments on Critical Self-Ignition Temperature 55
4.1 Introduction 55
4.2 Experimental Apparatus 57
4.3 Measurement Results and Discussions 59
4.4 Critical Self-ignition Temperature for L = 100 cm Basket 72
4.5 Evaluation of Critical Self-ignition Temperature for Upscale Stockpiles 74
4.6 Conclusions 77
Chapter 5: Preventing Spontaneous Combustion of Residual Coal in Goaf 79
5.1 Introduction 79
5.2 Coal Properties 82
5.3 Mine Ventilation Network Analysis and Goaf Area Three Zones 83
5.4 Oxidized Zone Border Demarcation in Goaf Area 84
5.4.1 Oxygen concentration detection in goaf 85
5.4.2 Goaf air flow simulation 86
5.4.3 Simulation results and analysis 90
5.5 Preventing Method for Goaf Fire 93
5.5.1 Injecting grouting slurry into goaf area 93
5.5.2 Grouting simulation result verification 95
5.6 Conclusions 96
Chapter 6 : Conclusions 98
REFERENCES 101

List of Tables

Table 1- 1 Coal classification by standard 5

Table 2- 1 Characteristics of coal pile in wire-mesh baskets 29

Table 2- 2 Specific heat capacity and density of coal sample 32

Table 2– 3 Properties of coal samples 33

Table 2- 4 Critical value of δ in different shapes 37

Table 4- 1 Properties of UE 56

Table 4- 2 Environment temperatures (T_E) of upscale experiments 60

Table 5- 1 Density, specific heat capacity and proximate analyses of coal sample 82

Table 5- 2 Chinese safety standards for divided goaf zones 83

List of Figures

Figure 1- 1 Coal consumption per capita 2013 (Million tonnes oil equivalent) ... 3
Figure 1- 2 Distribution of coal field in China ... 4
Figure 1- 3 The ranks of coals ... 6
Figure 1- 4 The temperature profile in reacting system ... 11
Figure 1- 5 Photos of coal spontaneous combustion ... 12
Figure 1- 6 Coal spontaneous combustion distributions in China (2014) ... 12
Figure 1- 7 Schematic figure of coal pile temperature measurement apparatus . 15
Figure 2- 1 Schematic figure of experimental apparatus (Laboratory experiment) ... 21
Figure 2- 2 Schematic figure of experimental apparatus (Upscale experiment) . 21
Figure 2- 3 Photo of the constant temperature system for laboratory experiment (Jan. 2013) ... 22
Figure 2- 4 Photo of the constant temperature system for upscale experiment (Jun. 2014) ... 22
Figure 2- 5 Photograph of coals placed in wire-mesh baskets ... 23
Figure 2- 6 Specific heat capacity of coal samples measurement ... 24
Figure 2- 7 Coal samples density measurement ... 24
Figure 2- 8 DTA monitor system (Nov. 2012) ... 25
Figure 2- 9 Definition of different thermal environment temperatures ... 26
Figure 2- 10 Dimensions of wire-mesh basket and thermocouple positions in the experiments ... 26
Figure 2- 11 Schematic figure of natural air convection in coal pile ... 27
Figure 2- 12 Schematic figure of critical self-ignition temperature test ... 30
Figure 2- 13 Test coal size and thermocouple length definition ... 31
Figure 2- 14 Measurement method of thermocouple position changes and coal pile height in the upscale experiment ... 31
Figure 2- 15 DTA curves of coal samples in air atmosphere ... 33

Figure 2- 16 Internal temperature curve of spontaneous combustion based on Frank-Kamenetskii's model 34
Figure 3- 1 Laboratory experimental apparatus (Mar. 2013) 40
Figure 3- 2 Center temperature-time increase curve of LE-1 (lignite) 41
Figure 3- 3 Center temperature-time increase curve of LE-2 (lignite) 42
Figure 3- 4 Center temperature-time increase curve of NE (lignite) 42
Figure 3- 5 Center temperature-time increase curve of SE (sub-bituminous) 43
Figure 3- 6 Center temperature-time increase curve of UE (lignite) 43
Figure 3- 7 Critical ignition temperature for LE-1 (L = 2.5 cm) 44
Figure 3- 8 Critical ignition temperature for LE-1 (L = 5 cm) 45
Figure 3- 9 Critical ignition temperature for LE-1 (L = 10 cm) 45
Figure 3- 10 Internal temperature-time curves for T_E = 50°C using different size coal piles 47
Figure 3- 11 Internal temperature-time curves for T_E = 140°C using different size coal piles 47
Figure 3- 12 Temperature rising vs. time after placing in different ambient air temperature environment 49
Figure 3- 13 Comparison supercritical and subcritical state of two coal samples 50
Figure 3- 14 Critical self-ignition temperature comparison of LE-1 and UE 52
Figure 3- 15 Self-heating curve of LE-1 and UE 53
Figure 4- 1 DTA curve of UE in air atmosphere 57
Figure 4- 2 Photo of wire-mesh baskets (25, 50, 100 cm) for upscale experiment 58
Figure 4- 3 Photos of wire-mesh basket and loaded coal in the test (Aug. 2014) 59
Figure 4- 4 Schematic figure of pile temperature of upscale experiment 60
Figure 4- 5 Temperature profiles for coal sample (L = 25 cm) 61
Figure 4- 6 Temperature profiles for coal sample (T_E = 75ºC) 61
Figure 4- 7 Examples of the coal sample changes in 110 ºC environment (Jun. 2014) 64

Figure 4- 8 Coal pile height vs. reciprocal temperature 64

Figure 4- 9 Temperature-time profiles at different vertical positions in the coal pile (T_E = 85ºC)..... 65

Figure 4- 10 Results of temperature profiles for coal sample (L = 50 cm) 66

Figure 4- 11 Coal pile height vs. reciprocal temperature 67

Figure 4- 12 Gas concentration and temperature at pile center..... 67

Figure 4- 13 Photos of coal smoking..... 68

Figure 4- 14 Photos of thermocouples position and coal pile height 69

Figure 4-15 Water condensation observed on the window 69

Figure 4- 16 Schematic of thermocouple position change 72

Figure 4- 17 Temperature distribution of thermocouple position 73

Figure 4- 18 Critical self-ignition temperature measured by center temperature (T_C) using the wire-mesh basket (L = 100cm)..... 73

Figure 4- 19 Coal weight loss ratio of coal (W_L) versus size of wire-mesh basket 75

Figure 4- 20 Plotting $\ln\left(\delta_c (T_{CSIT})^2 / r^2\right)$ against $(T_{CSIT})^{-1}$ based on critical self-ignition temperature, $x = \dfrac{1000}{T_{CSIT}}$; $y = \ln\left(\dfrac{\delta_c (T_{CSIT})^2}{r^2}\right)$ 75

Figure 4- 21 *CSIT* vs. coal stockpile volume 76

Figure 4- 22 Prediction of critical self-ignition temperature expanding to coal pile volume up to 1,000 m^3 77

Figure 5- 1 Plan of mining in Haizi coal mine..... 80

Figure 5- 2 Three Dimensional network airways diagram provided by the MIVENA system 81

Figure 5- 3 Plotting $\ln\left(\delta_c (T_{CSIT})^2 / r^2\right)$ against $(T_{CSIT})^{-1}$ based on critical self-ignition temperature, $x = \dfrac{1000}{T_{CSIT}}$; $y = \ln\left(\dfrac{\delta_c (T_{CSIT})^2}{r^2}\right)$ 81

Figure 5- 4 Schematic of three zones in the goaf..... 83

Figure 5- 5 The tube bundle gas monitoring system for goaf area in the coal mine (Dec. 2013) 84
Figure 5- 6 Schematic of the tube bundle gas monitoring system 85
Figure 5- 7 Distribution of oxygen concentration in #3205 goaf area (by Measurement, Dec. 2013) 86
Figure 5- 8 Gird block model of analysis area and definition of coordinate (*X,Y*) (by Gambit) 87
Figure 5- 9 Numerical model of goaf area and boundary conditions for FLUENT simulations 89
Figure 5- 10 Air leakage flow velocity vector in goaf simulated by FLUENT .. 91
Figure 5- 11 Contour lines of air leakage velocity in a goaf (unit: m/sec) simulated by FLUENT 91
Figure 5- 12 Schematic of "Three zones" in goaf area 92
Figure 5- 13 Grouting area and pipe bury diagram 93
Figure 5- 14 Contour lines of air leakage velocity after grouting slurry (goaf porosity is 0.1) 96
Figure 5- 15 Area of oxidation zone vs. goaf porosity 96

Acknowledgements

My deepest gratitude goes first and foremost to Professor Kyuro Sasaki, my supervisor, for his constant encouragement and guidance. He has walked me through all the stages of the writing of this thesis. Without his consistent and illuminating instruction, this thesis could not have reached its present form.

High tribute shall be paid to my co-supervisor Professor Xiaoming Zhang, whose profound knowledge of my research field triggers my immense zeal plunged into the research work and whose earnest attitude tells me how to explore the forward way in my study. Without his guidance this dissertation would not have been possible.

I am also deeply indebted to Associate Professor Yuichi Sugai for his patient guidance and technical support in this research. Especially for his ideas and discussions on DTA test, without his useful comments and kind instruction this work could not be finished.

I would like to express my heartfelt gratitude to Professor Toshiaki Kitagawa for his meticulous review and useful comments to improve my thesis. I also owe a special debt of Dr. Amin Yousefi, who gives me suggestions and help to work out the thesis.

My sincere thanks should also go to Ms. Mingchun Zhao, Mr. Li Zhang, Engineer Xiangtie Lin, and Engineer Jiaxing Cai for their guidance and support during my internship and for their cooperation on coal samples collecting.

I also wish to express my gratitude to the Monbukagakusho: MEXT for financial support to pursue my study in Kyushu University. The Global Center of Excellence program (G-COE), Green Asia program (GA), Kyushu University to give me opportunities and financial support on internship, international conferences.

Special thanks should go to all formers and present members of Resources Production and Safety Engineering Laboratory for their assistances and kind supports.

Last my thanks would go to my beloved family for their loving considerations and great confidence in these years. I would like to express my sincere gratitude to my wife Xinhui Li and my cute son Zimu Wang.

Chapter 1 : Introduction

1.1 Global Energy Status Including Coal

Energy is an important foundation of economic and social development. Especially with the development of world economy and continuous improvement of living standards, the world demand for energy continues growing. Thus, it is leading to increasingly fierce competition for energy resources followed by heavy environmental pollution and degradation. Since 2013, the global economic recovery has weakened, and international energy supply and demand patterns have changed with the trends of consumption. Despite a stagnant global economic growth, global primary energy consumption increased by 2.3% in 2013, showing 1.8% acceleration compared to 2012.

Although the global consumption growth of oil, coal, and nuclear power has been accelerated in 2013, it remained below the 10-year average of 2.5%. All fuels except oil, nuclear power and renewables in power generation sector at below-average rates. With 32.9% of global energy consumption, oil remains the world's leading fuel, but for the fourteenth consecutive year, it also continued to lose market share (BP statistical review of world energy, 2014).

Coal consumption kept increasing because of its lower price, but regional imbalance became greater and trade flow shows new changes. The relative price fluctuation of coal and natural gas lead to structural changes in power supply. In particular, after global coal prices have fallen for two consecutive years coal is extending its competitive edge in power generation and the competitive balance has begun to shift. Coal was the fastest-growing fossil fuel in the past couple of years, with China and India accounting for 88% of its global growth.

Consumption and production has been increased for all fuel types except

nuclear power. In addition, the consumptions rate rose more rapidly than production rate. Nowadays, fossil fuels are still playing an important role in terms of global energy demand. Statistical data suggests that growth in global CO_2 emissions from energy use is also accelerating year by year.

1.2 Coal and Its Distribution

Coal is a combustible brownish-black or black sedimentary rock formed by lithification of plant debris usually occurring in rock strata in layers or veins (Ambedkar, 2012; Ussiri et al., 2014). It has been used as an energy resource, primarily burned for the production of electricity and generating heat, and is also used for industrial purposes, such as refining metals. Coal is the largest source of energy for worldwide electricity generation, as well as one of the largest anthropogenic sources of CO_2 emission. In 1999, world gross CO_2 emissions from coal usage were 8,666 million tonnes (EIA, 2008; IEA, 2006). However, in 2011 it was 14,416 million tonnes, indicating a significant growth (International energy statistics, 2014).

Human use of coal can be traced back to Before Christ (BC) era. The earliest recognized coal use is from the Shenyang area of China 4000 BC where neolithic inhabitants had begun carving ornaments from black lignite (Golas et al., 1999). Coal from the Fushun mine in northeastern China was used to smelt copper as early as 1000 BC (Encyclopedia Britannica, 2014).

Currently, coal is an important resource for global energy system. It is the world's major source of power generation, accounting for 40% of electricity production. In 2013, global coal production increased by 0.8%, that was below the 10-year average (3.0%) but it is still the fastest-growing fossil fuel. The domination of coal in global energy mix is associated with its abundance, widely distribution, and cheap price (World Energy Council, 2013). Wide distribution of coal is

demonstrated in Figure 1-1 with major coal deposits existing on every continent.

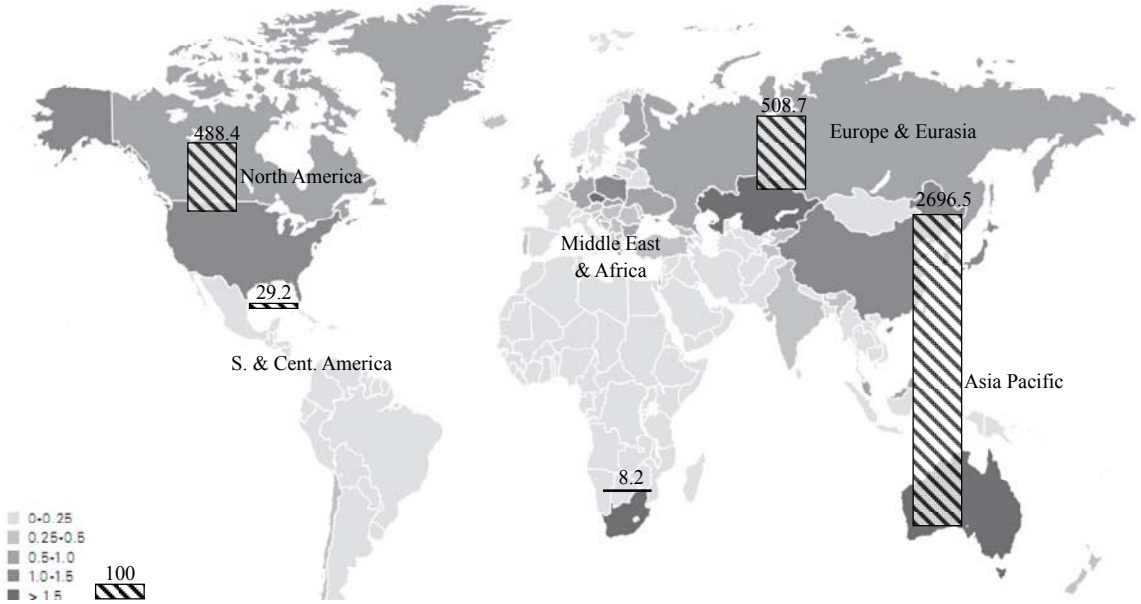

Figure 1- 1 Coal consumption per capita 2013 (Million tonnes oil equivalent)

Source: BP statistical review of world energy 2014

As shown in Figure 1-1, global fossil energy (e.g. coal) consumption is mainly concentrated in Americas, Europe and Asia Pacific. China had a total proven coal reserve of 114,500 million tonnes at the end of 2013, followed with 62,200 million tonnes of anthracite & bituminous, 33,700 million tonnes of sub-bituminous, and 18,600 million tonnes of lignite. China holds 12.8% of the world's total coal reserves but accounts for 47.4% of world's coal production (BP statistical review of world energy 2014).

As statistical data shows in Figure 1-2, China is rich in coal resources. In addition to Shanghai, other provinces and autonomous regions all have distributed coal field, though the distribution is quite uneven. The major coal resources accounting to almost 50% of proved reserves are distributed in north China area, between Daxing'anling-Taihang Mountain, and Helan Mountain and most parts of Inner Mongolia, Shanxi Province, Shaanxi Province, Ningxi Province, Gansu Province, and Henan Province.

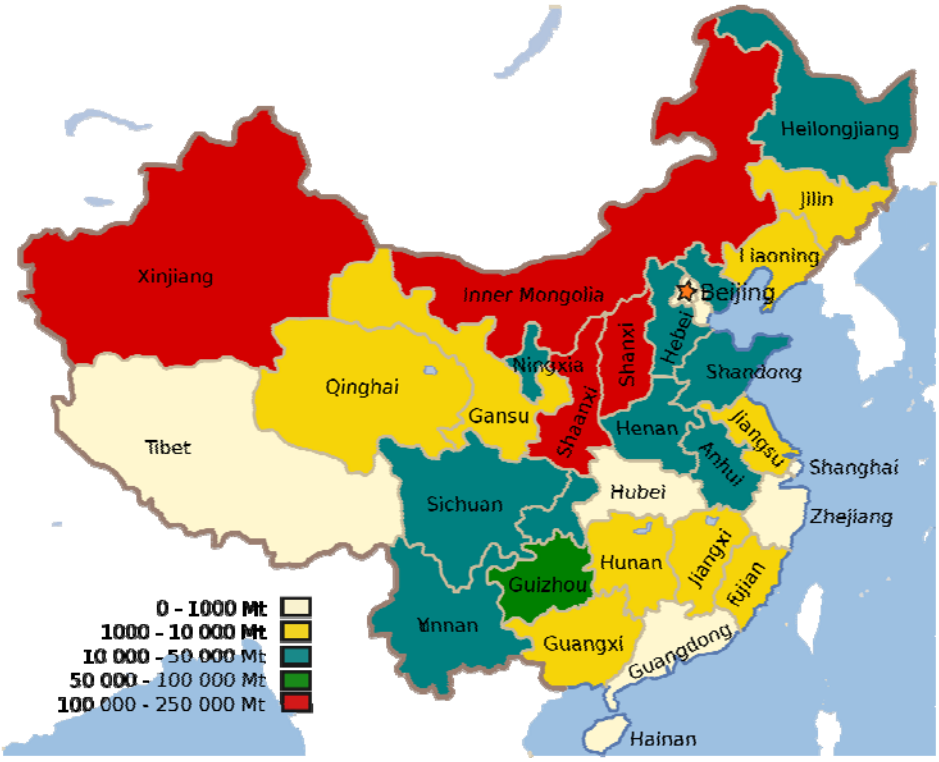

Figure 1- 2 Distribution of coal field in China

Source: en.wikipedia.org/wiki/Coal_in_China

1.3 Low Rank Coal

Coal is fossilized plant life, created over millions of years. As geological processes applied pressure to dead biotic material over time, under suitable conditions, its metamorphic grade increases successively into Peat, Lignite, Sub-bituminous coal, Bituminous coal, Anthracite and Graphite (Ambedkar, 2012). The classification of coal is generally based on the content of volatiles. However, the exact classification varies between countries. According to Karlsruhe (2008), coal is classified by different standard classification (Table 1-1).

Table 1- 1 Coal classification by standard

Coal Types and Peat					Total Water Content (%)	Energy Content a.f.* (kJ/kg)	Volatiles d.a.f.** (%)	Vitrinite Reflection in Oil (%)
UNECE	**USA(ASTM)**	**Germany(DIN)**						
Peat	Peat	Torf			75	6,700		
Orho-Lignite	Lignite	Weichbraunkohle			35	16,500		0.3
Meta-Lignite		Mattbraunkohle						
Sub-bituminous Coal	Sub-bituminous Coal	Glanzbraunkohle			25	1,900		0.45
Bituminous Coal	High Volatile Bituminous Coal	Flammkohle	Steinkohle	Hartkohle	10	2,500	45	0.65
		Gasfammkohle					40	0.75
	Medium Volatile Bituminous Coal	Gaskohle					35	1.0
		Fettkohle				36,000 Hard Coking Coal	28	1.2
	Low Volatile Bituminous Coal	Esskohle					19	1.6
							14	1.9
Anthracite	Semi-Anthracite	Magerkohle			3	36,000	10	2.2
	Anthracite	Anthrazit						

*a.f. =ash-free
**d.a.f. =dry, ash-free

UNECE: Ortho-Lignite up to 15,000 kJ/kg
Meta-Lignite up to 20,000 kJ/kg
Sub-bituminous Coal up to 24,000 kJ/kg
Bituminous Coal up to 2% average Vitrinite Reflection

USA: Lignite up to 19,300 kJ/kg

Source: BGR

The physical and chemical properties of coal depends on the degree of change it underwent while maturing from peat to anthracite (known as coalification), and generally the ranking of coal is based on its water and energy content (Dave and Tipre, 2012). In other words, "The rank of a coal describes the degree of the metamorphism undergone by it upon coalification as it matures from peat to anthracite" (Pandit et al., 2011). The rate of oxidation decreases with increase in rank of coal (Banerjee, 2000). The top of rank scale is placed by anthracite which has lower level of moisture and higher carbon and higher energy content (Pandit et al., 2011). Low-rank coals, such as lignite and sub-bituminous coal, are typically softer and friable materials with a dull, earthy appearance (Huang and Finkelman, 2008). They are geologically the youngest ones and have higher proportions of hydrogen and oxygen, and are characterized by high moisture levels and low carbon and low energy content.

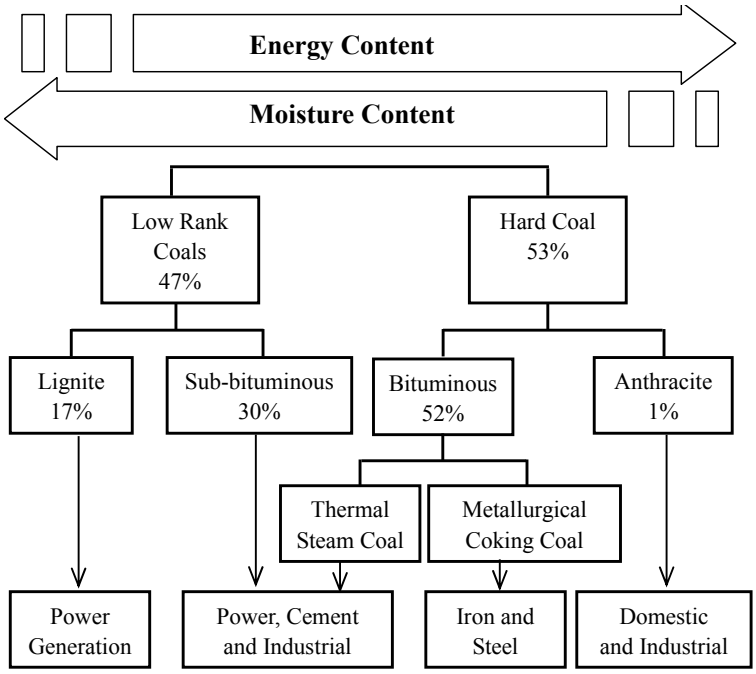

Figure 1- 3 The ranks of coals

Source: riverbasinenergy.com

Low rank coal constitutes around 47% of the global coal reserve (see Figure 1-3). They are known with lower mining cost, high reactivity, and low ash. On the other hand, they are associated with limitations such as high moisture content, low calorific value, high transportation cost, and potential safety hazards. To overcome such limitations, it is necessary to remove considerable amount of moisture using thermal, mechanical, or chemical methods. Although low-ranked coals have lower carbon content and consequently lower energy content, they are easier to ignite due to having higher volatile compounds. If the moisture of low rank coals is removed they will be dried but on the other hand they will be much easier to ignite. Nowadays, with increasing demand for energy, the low rank coal production is increasing year after year because of its benefits. However there are certain drawbacks such as environmental pollutions and spontaneous combustion during mining, transportation and storage.

In China, low rank coal is mainly distributed in the northern parts of the

country such as Inner Mongolia Autonomous Region and Southwestern parts such as Yunnan Province. Most of the low rank coal in China is used for generating electricity (Zhao et al., 2007).

1.4 Spontaneous Combustion

Since low rank coal is a main topic of this thesis, spontaneous combustion should be explained in more details. Spontaneous combustion occurs in three stages; a) self-heating; which is temperature increase because of exothermic internal reactions, b) thermal runaway; through which self-heating accelerates to high temperatures, and c) ignition (Babrauskas, 2003).

Coal is a self-heating material, meaning that the combustion can occur in underground mine, open pit mines, coal stockpiles, transportation and the site of disposal of coal wastes (see Figure 1-5). Coal reactions have been divided into two distinct components: devolatilization of raw coal and oxidation of residual char (Gray et al., 1976).

For industrial use, coal stockpiles are prone to spontaneous combustion particularly where large amounts are stored for long periods (Ray et al., 2014). Low rank coal exhibited the greatest tendency to self-heat because of its special characteristics. According to recorded statistical data, self-heating occurs more commonly at power plants than transfer points or ports (IEA, 2011).

In the spontaneous combustion process, first oxygen reacts with the fuel (i.e. coal) and thus oxidation occurs and produces heat (if the heat is dissipated the temperature of the coal will not increase). If the temperature is very high the oxidation reaction proceeds at a higher rate until the internal temperature causes ignition of the material. So the ignition of the material is the most important aspect to control the spontaneous combustion.

Self-heating of coal is a naturally occurring process caused by the oxidation of coal (IEA 2010). Self-heating of coal occurs because of some complex exothermic reactions. If the produced heat is not dissipated and there is a continuous air supply, self-heating of coal will be continued (Beamish and Blazak, 2005). The factors contributing to the self-heating of the coal can be divided into two major types: intrinsic factors (i.e. properties of the coal) and extrinsic factors (i.e. environment or storage conditions) (Speight, 2012).

Bacterial action in coal also can encourage self-ignition especially in haystacks and wood. Chemist M. Lin mentioned that these kinds of bacteria can convert ordinary coal to an environmentally attractive resource (Yap, 2004). However, there is no conclusive proof to authenticate or dispose this theory. Electro-chemical theory describes auto-oxidation of coals as oxidation-reduction processes happens in micro galvanic cells created by the coal components (Lakra, 2011; Ray, 2014).

1.5 Arrhenius Equation

Coal self-heating is a complex process which results in an increase in temperature, a loss of mass and weathered blocks. Heat generation results in chemical reaction, physical reaction, and microbial activity and so on. If the surrounding environment removes or absorbs the generated heat only low temperature oxidation will occur (Riley, 1996). Hence, applying Arrhenius equation on coal self-heating process to analysis temperature increase phenomenon is reasonable and useful. The Arrhenius equation is a well-known formula for the temperature dependence of thermally induced reaction rates (Deckers et al., 2012).

The equation gives the dependence of the rate constant k of a chemical reaction on the absolute temperature T (K).

$$k = Ae^{-E/(RT)} \tag{1-1}$$

Where, A is pre-exponential factor; E is activation energy; R is the universal gas constant. On the other hand, taking the natural logarithm of Arrhenius' equation yields:

$$\ln(k) = \frac{-E}{R}\frac{1}{T} + \ln(A) \quad (1\text{-}2)$$

So, when a reaction has a constant rate that obeys Arrhenius' equation, a plot of $\ln(k)$ versus $(1/T)$ gives a straight line, whose gradient and intercept can be used to determine E and A . This procedure is common in experimental chemical kinetics by which the activation energy for a reaction. The activation energy is equal to $(-R)$ times of the slope of a plot of $\ln(k)$ vs. $(1/T)$ and the pre-exponential factor A can be obtained from the equation intercept. This indicates that coal self-heating reaction can be determined by quantize activation energy (E) and pre-exponential factor (A).

1.6 Frank-Kamenetskii's Ignition Theory

Spontaneous combustion of accumulated solid material is a common way of ignition. Spontaneous combustion in self-heating materials, such as coal piles, wood and other combustible sedimentary dust is quite common in our life. Based on this, there are a number of theories for coal spontaneous combustion. According to coal-oxygen complex theory, oxidation of coal is initiated at native radical sight. Oxygen and moisture incorporate into organic matrix through the formation of peroxyl radical and hydro peroxides. This is followed by some reactions or decompositions which may lead to wide range of oxygen functionality in the matrix or gaseous product (Jain, 2009). Pyrite theory suggested that heating of coal could be caused by the existence of iron pyrites in finely powdered and dispersed state in the presence of moisture. However, if the present pyrite is less than 5%, then its effect is negligible (Münzner, 1975).

Given that the spontaneous combustion of accumulated solids has a larger scale

and a longer incubation period etc., it is hard to verify the ignition's actual cause through full-size experiment in the laboratory. However, application of Frank-Kamenetskii theory on the simulation of accumulated solids' spontaneous combustion can solve this tough problem. For a given accumulated solid, in the case of boundary conditions and ambient temperature, Frank-Kamenetskii model can be used to predict the risk of spontaneous combustion ignition.

Frank-Kamenetskii (1959) theory is a model based on equation proposed a high Biot number model.

In certain circumstances such as where there is a considerable resistance to heat transfer in the reacting system, or in a system with highly conducting walls that has a low thermal conductivity, the temperature gradient can be taken into account through the Frank-Kamenetskii theory (Wang et al., 2008).

Otherwise, if there is no temperature gradient between the reacting mass outside of the system and inside the system the Semenov model can be used (Wang et al., 2008). Semenov (1928) developed a model for thermal explosion of a spatially homogeneous system, which demonstrates the principles of the thermal ignition phenomenon in a quantitative way. In such a system, pressure, temperature, and composition are uniform. Furthermore, the chemistry is approximated by a one-step reaction from fuel to produces after reactions (Warnatz et al., 2001).

The temperature T, of the reacting system is assumed to be uniform and constant through the whole volume of the system. The external temperature and the walls of the system are both assumed to be the same temperature T_E (Lu et al., 2009). This is shown in Figure 1- 4. This means that there is no gradual temperature gradient but a sudden change between inside and outside of the system (Combustion, 2006).

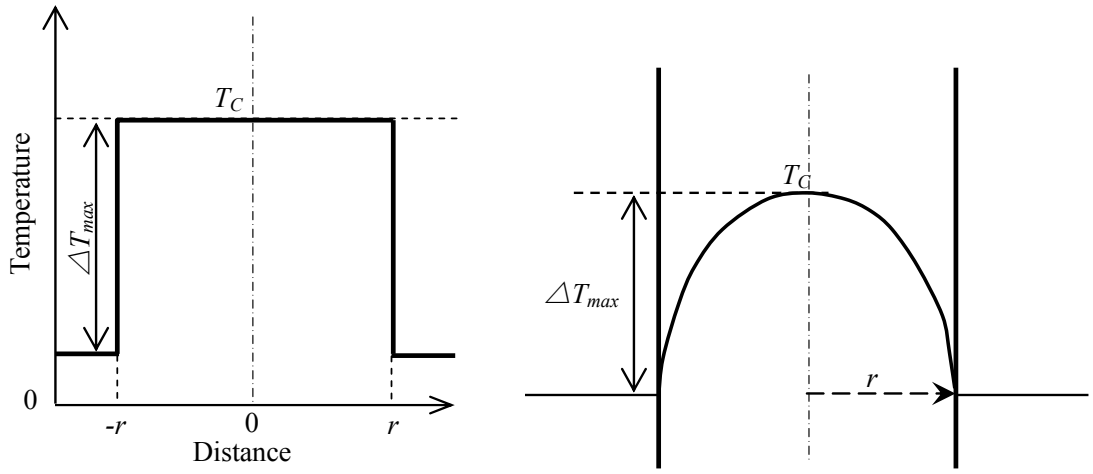

(a) Semenov Model (b) Frank-Kamenetskii Model

Figure 1- 4 The temperature profile in reacting system

T_0: Initial temperature; T_C: Maximum temperature; ΔT_{max}: Maximum temperature difference; T_E: Environment (external) temperature; r: Equivalent radius

1.7 Previous Accidents of Spontaneous Combustion

The extensive use of coal in turn brings about more incidental troubles. The most ticklish one is coal self-heating as shown in Figure 1-5.

On the other hand, this phenomenon reflects the relative of exposure time and storage size of coal pile. Spontaneous combustion in stockpiles has major environmental, economic and safety problems (Krishnaswamy et al., 1996). Rather than huge economic loss of coal ignition, the released heat-affected coal may become partially or totally unsuitable for its intended use. Thus early detection and prevention of spontaneous combustion is of vital importance. It is not always clear how frequently combustion occurs and where ignition starts as there is a lack of information published on this topic.

Figure 1- 5 Photos of coal spontaneous combustion

(the photos were presented from coal mines with permissions to use for this PhD thesis)

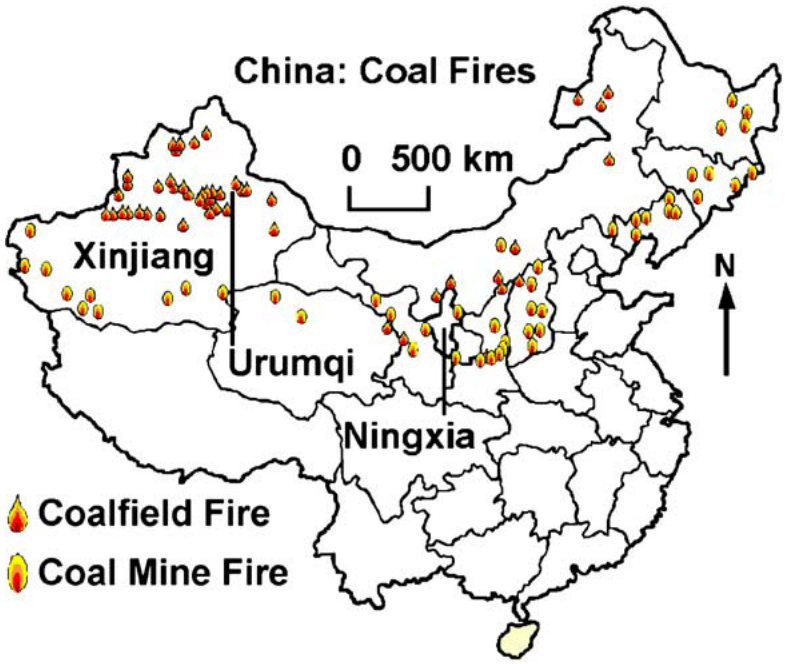

Figure 1- 6 Coal spontaneous combustion distributions in China (2014)

Source:/www.guancha.cn/FaZhi/2015_02_06_308726.shtml

In China, as Figure 1-6 shows, spontaneous combustion in coalfields and coal mines is mainly distributed in the North part region. Remote sensing data shows

more than 50 coalfields and coal mines with potentials for spontaneous combustion exist in North China, such as Xinjiang, Ningxia, Inner Mongolia, Gansu, Shanxi, Shaanxi provinces and so on (Tan, 2000). Coal fire burning area is up to 720 km^2, approximately. The destruction followed by spontaneous combustion can prevent the exploitation of a part of coal resources in coal seams. Currently, spontaneous combustion disasters directly threaten the security of Chinese coal-dominated energy structure.

1.8 Evaluating Methods of Low Rank Coal Spontaneous Combustion

As mentioned before, self-heating or spontaneous combustion of coal is a naturally-occurring process caused by the oxidation of coal (Cox et al., 1984). There are so many physical and chemical reactions in the process. Many kinds of exothermic processes exist in coal stockpiles which contribute to the self-heating of coal (Thomas et al., 1992, Pisupati et al., 1993). According to the observations, the spontaneous combustion of coal initiates at the spots of coal seam surfaces called “hot spots”. These hot spots are rooted to deeper zones of the seam and smolder in a combustion event because of the low oxygen concentration (Sasaki et al., 2011). So coal heat generation measurement is the most important work to evaluate spontaneous combustion. Based on micro calorimeter, the equation guiding heat generation in crushed coal via oxygen adsorption has been proposed to evaluate coal self-heating (Miyakoshi et al., 1984). Besides, another approach is coal self-heating thermic effect quantification by measuring heat generation rate and oxygen consumption rate in different types of crushed coal at constant temperatures (Kaji et al. 1987). On the other hand, natural convection caused by air permeability in coal pile is significantly important for self-heating (Brooks et al., 1988, Bradshaw et al., 1991). To a certain extent, the natural air convection caused by temperature difference promotes coal initial heat generation and conduction (Krishnaswamy et

al., 1996). Fierro et al., (2001) developed a one-dimensional model to show that the porosity and wind speed play an important role in coal piles, and verified his simulation results by applying it to stockpiles of a mixture of lignite coal. These researches indicate that in coal spontaneous combustion research environmental conditions and properties must be considered.

Recently, coal spontaneous combustion by using the systematic application of an anti-oxidant and testing the fixed particle size coal sample self-heating rates in the laboratory was successfully practiced to develop an appropriate principal hazard management plan for law-rank coal (Beamish et al., 2013). This research proposed the idea of using Frank-kamenetskii model to carry out calculations about large coal piles by testing the small size coal critical self-ignition temperature in the laboratory. The analysis of the laboratory experiment results enabled the critical ignition-temperature of the coal sample to be presented as a function of stockpile volume.

1.9 Objectives of Present Research

There are very limited studies on the estimation of the critical ignition temperatures of bulky stocks of coal. Gray and Lee (1967) measured the subcritical and supercritical conditions around 300°C and measured pre-ignition temperatures at different positions in a cylindrical reaction vessel. They used Frank-Kamenetskii's ignition theory to test different methods for determining the radius of the equivalent sphere then comparing and contrasting the results. Bowes (1984) also presented simplified self-heating models based on Frank-Kamenetskii's ignition theory. These studies, however, did not clearly find accurately critical ignition temperatures.

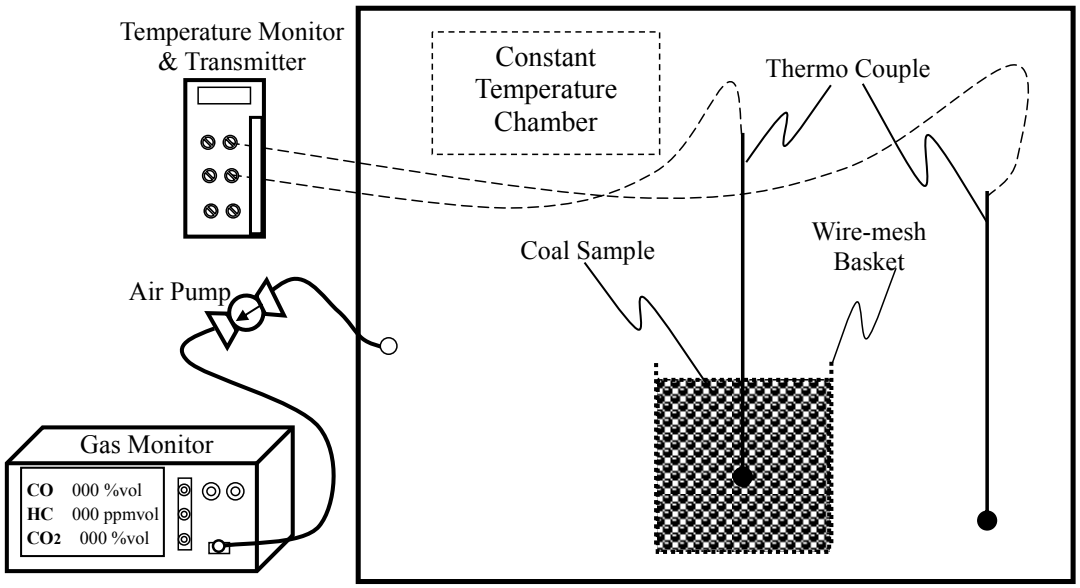

Figure 1- 7 Schematic figure of coal pile temperature measurement apparatus

Many researchers investigate self-heating or spontaneous combustion of coal stockpiles from various aspects. In the present research, an equation was derived from the Frank-Kamenetskii model for estimating critical temperature of self-ignition in order to express heat balance and heat generation rate in different parts of a coal pile and heat transfer from the outer surface of the pile.

The critical ignition-temperatures of low-rank coals for establishing safety criteria for storing and transporting of this kind of coal is not identified yet. In this dissertation, experimental apparatus and measurement procedures of thermal diffusivity and establishing temperature in the different parts of coal pile have been presented to evaluate the critical self-ignition temperature of different types of coal samples (see Figure 1- 7).

Based on the Frank-Kamenetskii's model, Critical Self-Ignition Temperature (*CSIT*) can be formulated from heat balance between heat generation and heat loss rates of the coal pile. Suppose the heat generation rate is expressed by the Arrhenius equation consisting of parameters for activation energy, frequency factor, and critical radius of the coal pile, then by plotting linear relationship of convert equations, it is

easily possible to calculate the coal activation energy and other important parameters. Until now, it is clear that the key variable is experimental test of *CSIT*. In coal spontaneous combustion investigation, it is an important value for molar heat of reaction, apparent activation energy and frequency factor calculation and quantization.

Hence, focus of this study is on the measurement and analysis of the coal samples' inside temperature changes with different volumes and different ambit air temperatures. Then, Fourier equation boundary conditions to calculate the self-heating data of the coal sample is a matter of investigation. Finally, by using experimental results to estimate *CSIT* of an actual coal stockpile from theoretical equations for scaling, critical ignition-temperature of the coal sample can be evaluated as a function of stockpile volume. Thus, applying this function can be used to predict *CSIT* of larger stockpile volumes, and to evaluate and realize the huge coal stockpile risk and weight loss.

1.10 Dissertation Overview

The dissertation mainly investigates the coal pile spontaneous combustion by analyzing coal samples *CSIT.* It is composed of six parts as follows:

Chapter 1: Introduction

This chapter illustrates an overview of the world energy status. It describes the coal distribution and classification, especially explains the specifications of low rank coal. Furthermore, it reviews the methods and useful tips from the literature, and discusses coal spontaneous combustion and closely related theories related to prediction and prevention of coal self-ignition.

Chapter 2: Experimental apparatus and methodology

In this chapter, different sets of experimental apparatus, such as Differential Thermal Analysis (DTA), gas emission analysis, special ordered wire-mesh baskets, and electrical hot air generator and so on, were applied in the test. Two of six types of coal samples were selected for the further analysis. The coal samples with average particle distribution of around 0.48 mm and 46 mm were filled in the wire-mesh basket. Then the sample properties and DTA measurement results are reported. Moreover, some necessary parameter definitions are presented in this chapter in order to preclude the possibility of confuse in result analysis. Furthermore, parameters analyzing for affecting factors of the coal critical self-ignition temperature (*CSIT*) was mentioned. It was concluded that the volume and temperature difference are the main reason to affect the coal pile *CSIT*. Finally, Frank-Kamenetskii's model based on Arrhenius equation was evaluated to analyze measured data. Linear equation of $\ln\left(\frac{\delta_c T_{CSIT}^2}{r^2}\right)$ against $\frac{1}{T_{CSIT}}$ was also evaluated in this chapter.

Chapter 3: Laboratory experiments on critical self-ignition temperature

Since coal critical self-ignition temperature (*CSIT*) theory analysis is feasible, laboratory small size tests were practiced based on Frank-Kamenetskii's model. By analyzing the temperature curve in different environments, coal samples self-heating law and a variety of heat transfer parameters was obtained based on which the coal samples critical self-ignition temperature can be decided. Furthermore, two different coal samples comparison was done to evaluate the activation energy. UE sample which has larger activation energy needed more heat to start combustion. Finally, the critical self-ignition temperature as a function of pile size or volume was determined.

Chapter 4: Upscale experiments on critical self-ignition temperature

Following the previous chapter, chapter 4 is an investigation on critical self-ignition temperature to evaluate the feasibility of coal pile self-heating risk. Critical self-ignition temperature (*CSIT*) of large size coal piles in upscale experiment was carried out with establishing a large thermostatic chamber to simulate coal internal heat environment. Due to the time, environments and other inconvenient problems, for upscale experiments only UE was chosen for continuing the measurement of internal temperature of coal pile and following the idea of applying Frank-kamenetskii model on coal critical self-ignition temperature in order to verify the feasibility of the model.

The upscale experiment result fully proved that the method and theory used in the study is reliable and useful. From the test result it can be found that the larger the wire-mesh basket size, the lower the critical self-ignition temperature. Furthermore, the calculated activation energy of UE sample was 200.7 kJ/mol and the measured calorific value of coal sample was 3434 kcal/kg. Temperature and gas composition together with the decrease in height of the pile shows that the preheating, rapid heating and decline stage should be gone through during the heating process. Moreover, coal pile (UE) weight loss ratio and size relationship was evaluated as $W_L\% = -6.28 \lg(L) + 34.39$ and critical self-ignition temperature and stockpile volume V extrapolated over $1m^3$ has been obtained as $T_{CSIT} - 273 = -12.73 \lg(V) + 81.6$. Finally, the function of critical temperature has been applied to predict critical self-ignition temperature of larger stockpile volumes less than 1,000 m^3.

Chapter 5: Preventing spontaneous combustion of residual coal in coal mine goaf

In this chapter, field practice was carried out by the theory of critical self-ignition temperature, and it was fully proved that reducing porosity in the goaf area to prevent spontaneous combustion of residual coal is useful. The MIVENA was used to analyze mine ventilation network airflows to control airflows in and out

of working faces and goafs. As the second approach, numerical simulations were carried out by the simulator FLUENT in order to predict spontaneous combustion of residual coal with leakage flow in the #3205 goaf and dividing the goaf into three zones based on oxygen concentration. Finally, the numerical simulation results showed that the slurry grouting method is able to be an effective and economical method, which reduces porosity in the goaf area to prevent spontaneous combustion of residual coal.

Chapter 6: Final conclusions

The conclusions of the study are presented in this chapter.

Chapter 2: Experimental Apparatus and Methodology

2.1 Introduction

Prior to start the laboratory experiment and upscale experiment, the design of experiments and several important parameters must be considered at the beginning. In this chapter, the experimental setup of monitoring system for laboratory and upscale experiments, coal sample characteristic parameters (the density, porosity, specific heat capacity and thermal diffusivity) measurement system and coal sample Differential Thermal Analysis (DTA) were put forward initially to accomplish the experimental preparations and characteristics definition of the samples. In the upscale experiment, special ordered large size (25, 50, 100 cm in length) wire-mesh baskets were made to meet the present experimental requirement. Furthermore, the electrical hot air generator and internal electric heaters were equipped to maintain the inside temperature balance. By means of the advanced measure of DTA thermal analysis, evidences of coal sample activities in different heating process were obtained which can provide useful reference to the next step of the tests.

2.2 Experimental Design

2.2.1 Experimental setup

In the present work, temperature profiles at different positions of the coal pile in each ambient air temperature environment were measured. Six sets of wire-mesh baskets divided into two parts (one for laboratory experiment another for field test) are placed in different temperature environments. The low-rank coal with average particle distribution around 0.48 or 46mm was filled in the wire-mesh basket. Special-ordered thermocouples (Figure 2-13) were continuously monitoring coal temperature changes

in the basket. The schematic figure of experimental apparatus in laboratory experiments and upscale experiment are shown in Figure 2-1 and 2-2, respectively. The cube wire-mesh baskets were set in the constant temperature chambers (in size of 60×70×85 cm and 2×2×2 m) where ambient air temperature was controlled to be constant.

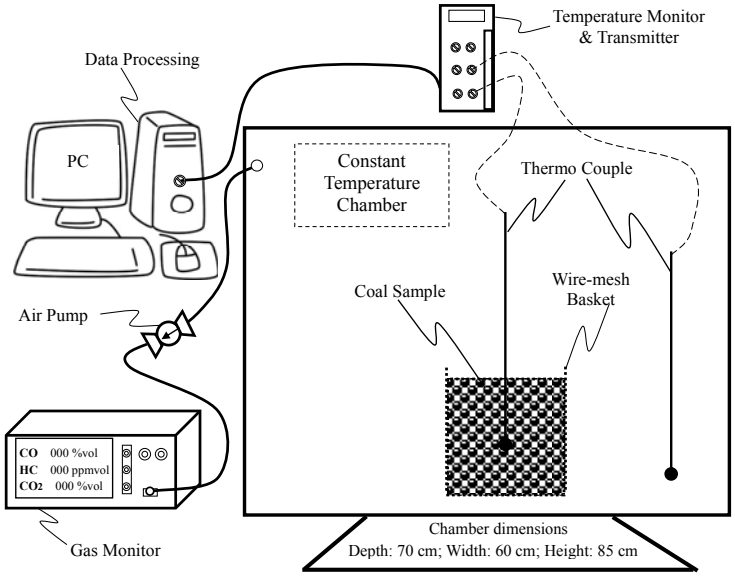

Figure 2- 1 Schematic figure of experimental apparatus (Laboratory experiment)

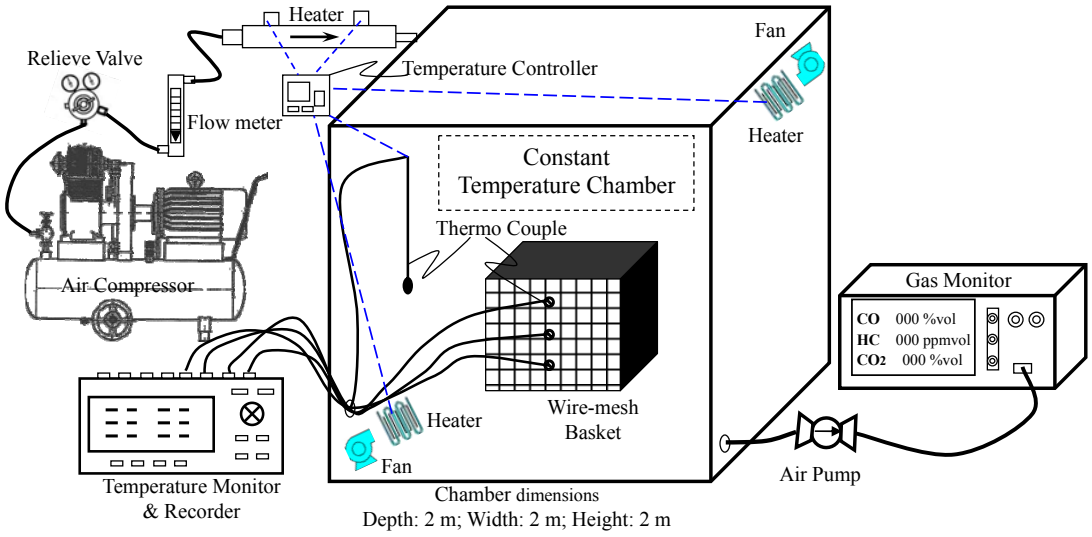

Figure 2- 2 Schematic figure of experimental apparatus (Upscale experiment)

In order to reduce the fluctuation range of temperature of constant chamber in

field test, the electrical hot air generator and internal electric heaters were equipped to maintain the inside temperature balance as shown in Figures 2-3 and 2-4.

Figure 2- 3 Photo of the constant temperature system for laboratory experiment (Jan. 2013)

Figure 2- 4 Photo of the constant temperature system for upscale experiment (Jun. 2014)

As showed in Figure 2-5, the cube wire-mesh baskets were set in the controllable constant ambient air temperature chamber. Thermocouples were used to

detect internal temperatures at 3 to 9 positions including the center of the coal pile.

(a) Laboratory experiment case (b) Upscale experiment case

Figure 2- 5 Photograph of coals placed in wire-mesh baskets

The coal was loaded into the constant temperature chamber at room temperature T_0. The coal heating experiments using the cube wire-mesh baskets were done under constant temperature conditions to establish the self-heating characteristics of coal samples if ignition occurred.

2.2.2 Experimental apparatus

Prior to monitoring the internal temperature changes of coal samples in different temperature environments, density and specific heat capacity of each coal sample were evaluated. The measurement instruments used to measure the specific heat capacity and density of coal samples are shown in Figure 2-6 and Figure 2-7, respectively.

Pure water is commonly used in the measurement because of its clear characteristics. In specific heat capacity measurements, pure water was preheated at

the temperature of 50°C beforehand (for at list 10 hours heating time). The coal sample temperature was equal to the environment temperature T_0. After full heat exchange of water and coal sample in an adiabatic box, the specific heat capacity of the coal samples were calculated by measuring the equilibrium temperature.

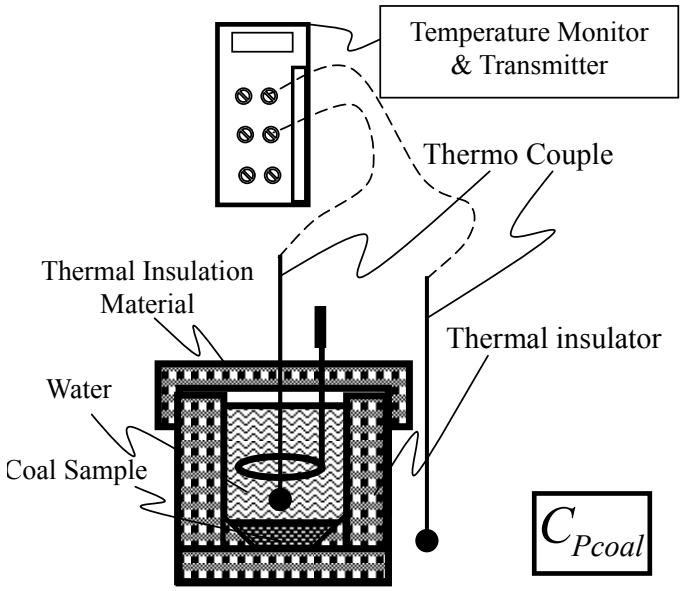

Figure 2- 6 Specific heat capacity of coal samples measurement

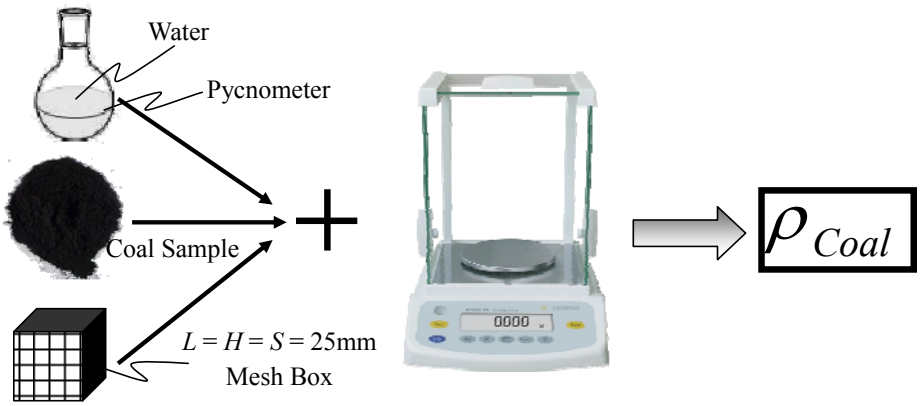

Figure 2- 7 Coal samples density measurement

Density is the measure of the mass per volume of a substance. It can be determined by measuring the volume and the density of a substance. Because the shapes of crushed coal samples can make it difficult to measure volume directly,

volume is often measured indirectly through subtraction. Water and specific capacity pycnometer (e.g. 50 ml) was used to measure the real density of coal samples.

Figure 2- 8 DTA monitor system (Nov. 2012)

On the other hand, DTA test (see Figure 2- 8) also was carried out to define the coal samples. By using the DTA curve the endotherm peak (which accompanied by the chemical reaction and water evaporation) can easily be found. Moreover, the critical process or points of heat absorption & exotherm and evidence of coal sample activities in different heating process also can be obtained by analyzing the recorded temperature curve. The analysis of DTA data can provide useful reference to the following tests.

2.3 Definitions of Parameters

In order to preclude the possibility of confusion in the result analysis, definitions of parameters must be considered at first. During the heating process, different thermal environment temperatures were defined as shown in Figure 2-9. Moreover, characteristics of the wire-mesh baskets and thermocouple positions were decided. Figure 2-10 shows the wire-mesh baskets dimensions parameters and thermocouple

positions in details. Besides, each size and volume of wire-mesh basket is listed in Table 2- 1.

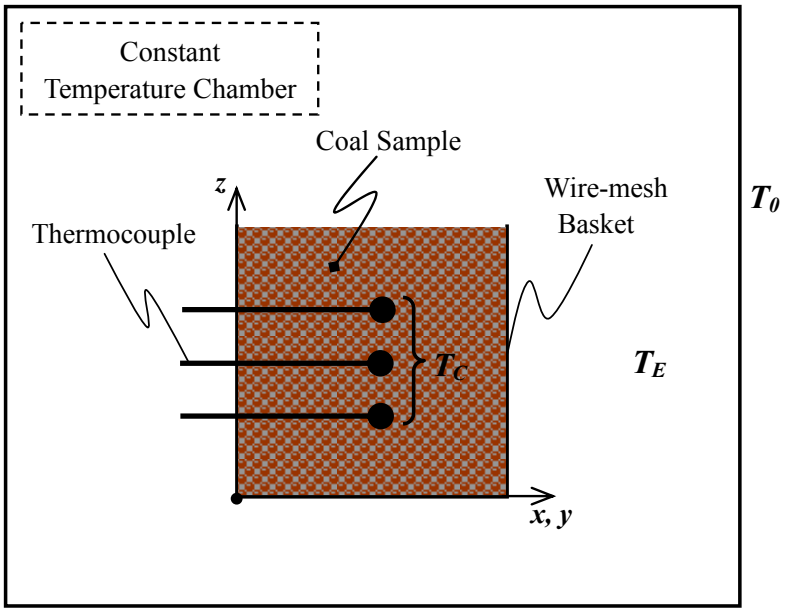

Figure 2- 9 Definition of different thermal environment temperatures

T_C : Inside Coal Temperature; T_E : Ambient Air Temperature in Constant Chamber; T_0 : Outside Environment Temperature. (Unit: °C)

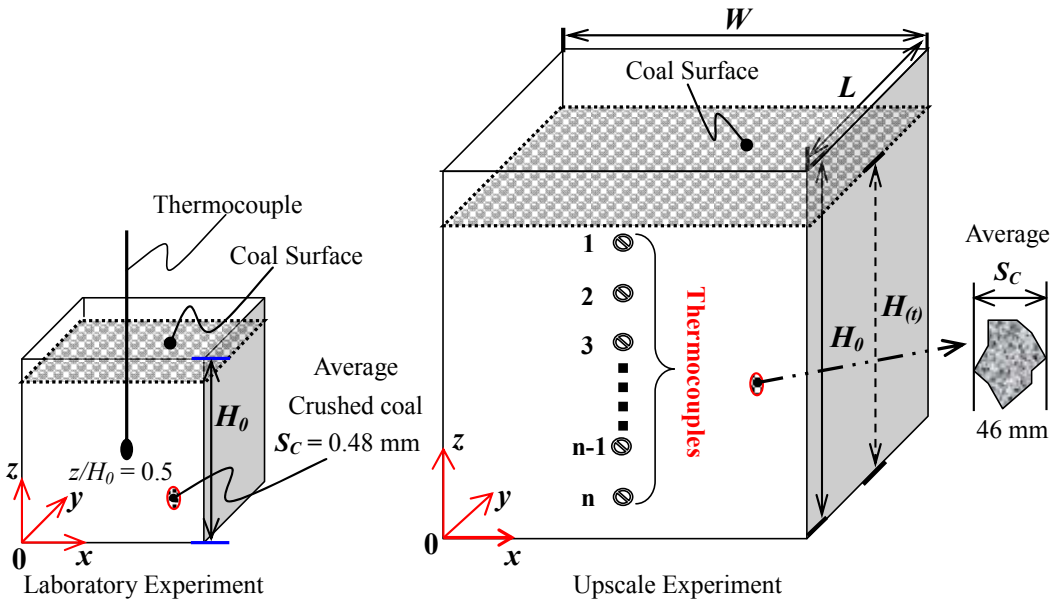

Figure 2- 10 Dimensions of wire-mesh basket and thermocouple positions in the experiments

$L = H_0 = W$ (Unit: cm*), $H_0 = H(0)$, t : Elapsed time*

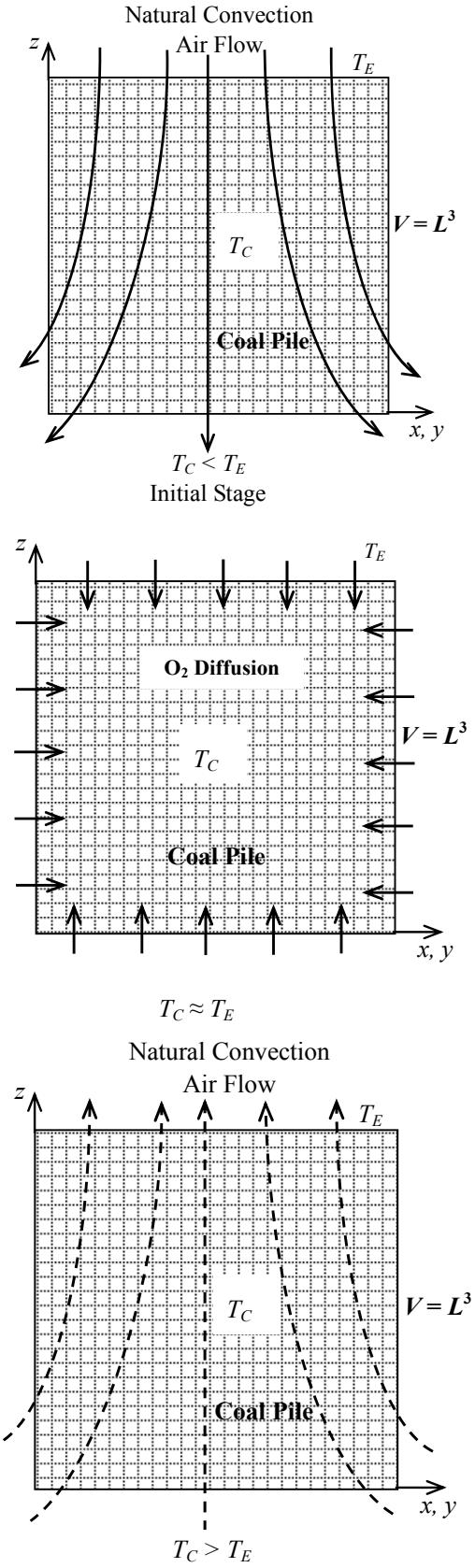

Figure 2- 11 Schematic figure of natural air convection in coal pile

In general, coal critical self-ignition temperature (*CSIT*) is mainly affected by the coal pile volume (V) and thermal diffusivity (α) of the sample. Moreover, coal samples thermal conductivity is depended on the coal pile porosity and specific internal surface in it (Sasaki, et al,. 2011). In the test, the effective thermal conductivity of coal pile can be estimated as, $\lambda = \lambda coal\ (1- \varepsilon) + \varepsilon \lambda air$. Along with the coal pile the volumetric heat capacity and thermal diffusivity is expressed as

$$\rho Cp = \varepsilon \rho_{air} Cp_{air} + (1-\varepsilon)\rho_{coal} Cp_{coal}, \quad \alpha = \lambda / \rho Cp \tag{2-1}$$

where,

ρCp: Volumetric heat capacity;

ε: Coal pile porosity;

α: Thermal diffusivity;

λ: Effective thermal conductivity;

λair: Effective thermal conductivity of air;

ρ_{coal}: Coal density;

ρ_{air}: Air density;

Cp_{coal}: Coal specific heat capacity;

Cp_{air}: Air specific heat capacity.

Based on the test results analysis and heat transfer theory, coal pile volume and thermal diffusivity have dominated the effects of coal pile critical self-ignition temperature (*CSIT*) which can be wrote as $T_{CSIT} = f\ (V, \alpha)$. In this study, the coal sample has same density and heat capacity in laboratory and upscale experiment (see Table 2-2), and the thermal conductivity effect on the different volumes of *CSIT* can be offset. Hence, it was noticed that in this test only coal pile volume can restrict the critical self-ignition temperature.

Moreover, another minor phenomenon is natural air convection (see Figure

2-11). In the experiment test, natural air convection is induced by the temperature difference of heating environment and coal sample. So the temperature difference ($\Delta T = |T_E - T_0|$) is the main reason for the coal sample inside natural air convection. In that case, the natural air convection could be the main effect on coal pile heat exchange. When the air motion starts automatically and naturally, it is an indication of being buoyancy driven.

On the other hand, coal size rate (S_C / L) calculation result in laboratory experiment and for upscale experiment are approximately the same (e.g. L = 10cm; S_C / L = 0.0048, L = 100cm; S_C / L = 0.0046), which means size effects of coal samples are similar and it can be expected that size effect has almost no effect on the critical self-ignition temperature. Hence, for the experiment purpose coal size rate (S_C / L) affecting is much less than that of the porosity.

Table 2- 1 Characteristics of coal pile in wire-mesh baskets

Basket L (cm)	Basket Volume	Basket Meshes (inch)$^{-1}$	Coal Pile Porosity ε	Initial Coal Weight	Coal Size Ratio S_C / L
Laboratory wire-mesh basket (2.5 to 10 cm)					
2.5	15.625 cm^3	35	0.41	12 g	0.0192
5.0	125 cm^3	35	0.45	90 g	0.0096
10	1000 cm^3	35	0.42	751 g	0.0048
Upscale wire-mesh basket (25 to 100 cm)					
25	0.015625 m^3	2.5	0.47	10.8 kg	0.0184
50	0.125 m^3	2.5	0.47	86 kg	0.0092
100	1 m^3	2.5	0.46	706 kg	0.0046

So the assumption can be made in the tests that the coal piles have same thermal-conditions on thermal diffusivity in the piles. In such case, coal sample can be oxidized exothermically at around critical temperature. The unique affecting factor of coal critical self-ignition temperature (*CSIT*) in the test environment is coal pile volume (V). Therefore, it can be stated that test data were valid for expansion to

predicting spontaneous combustion in large coal stockpile.

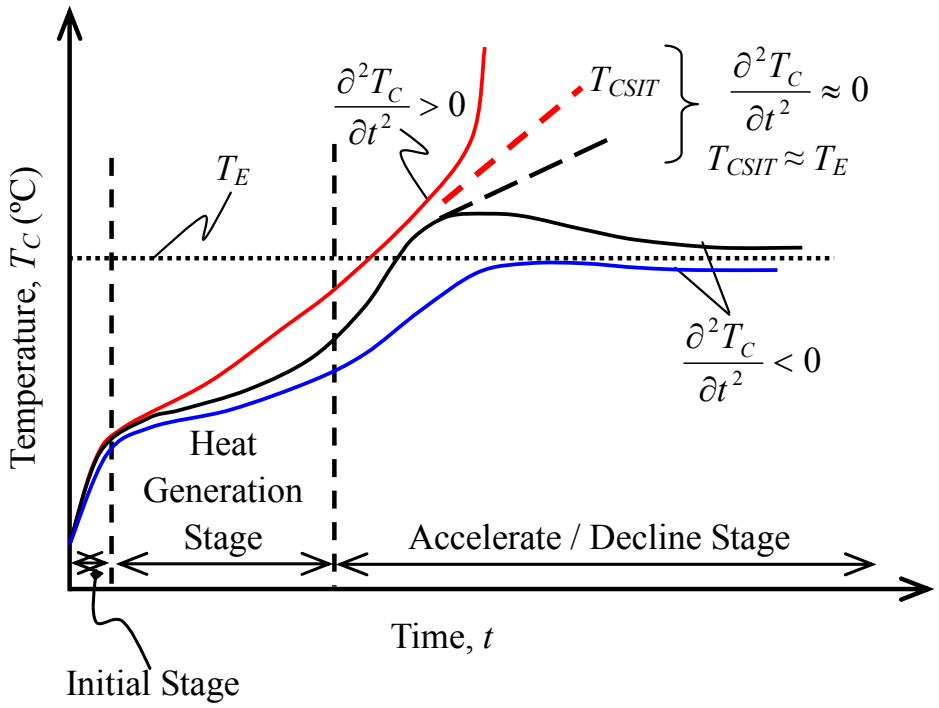

Figure 2- 12 Schematic figure of critical self-ignition temperature test

The graphical description of the process of critical self-ignition temperature measurement is presented in the Figure 2-12. The total heat exchange process can be divided into three stages as shown in the Figure 2-12. In the test process, any heating environment temperature higher than the critical self-ignition temperature is termed "supercritical" and lower is termed "subcritical". If the heating environment temperature (T_E) is close to T_{CSIT}, then the heat generated from coal pile inside would be closer to promoting continued reaction of sample for starting self-ignition. We call this range of heating environment temperature (T_E) as subcritical, which finally shifts to a declining stage. On the contrary, if $T_E > T_{CSIT}$ coal sample generating heat over loss, and inside temperature climbing will continue. This instability state (called supercritical) speeds up the chemical reaction rate and finally reaches thermal runaway. Here, this is an accelerate stage. Hence, the critical self-ignition temperature is between subcritical and supercritical states, around

where the environment temperature (T_E) is equal to T_{CSIT} approximately. After clearing the definition of critical self-ignition temperature of coal sample, experiment can be carried out.

Figure 2- 13 Test coal size and thermocouple length definition

Left: Typical size of the coal sample and thermocouple length; Right: L_T (unit: cm*)*

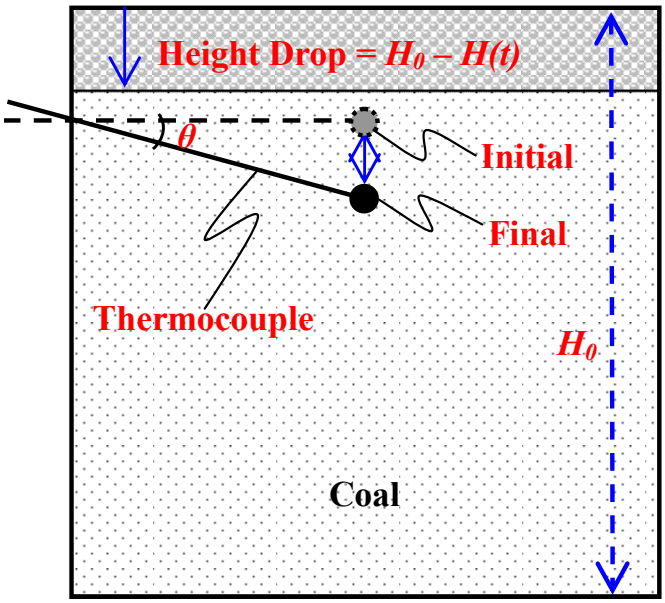

Figure 2- 14 Measurement method of thermocouple position changes and coal pile height in the upscale experiment

In order to evaluate whether the coals are weathered and crushed clearly, an

experiment was carried out. Different sizes of fresh coal samples were placed in test temperature environment to evaluate and determine the sample's weathered or crushed degree. Before the start of experiment, the coal samples were measured and photographed to make it possible to compare the changes after enduring the heating environment (see Figure 2-13). During the hearing process, large size coal pile height and thermocouples position change also should be considered. Figure 2-14 illustrates the definition of these parameters.

2.4 Material Details

The test chose 5 types of coal samples named LE-1, LE-2, NE, SE and UE from different areas in the word. All the coal samples were low rank coal except SE coal. In order to get a better test result, coal samples several characteristics was measured before the start of experiment. The 5 types of coal samples specific heat capacity and density measuring results are listed in Table 2-2.

Table 2- 2 Specific heat capacity and density of coal sample

Name	Density (g/cm^3)	*Cp* (kJ/(kg·°C))	Rank	Use Lab/Upscale/Simulation
LE-1	0.74	1.27	Lignite	Lab & Upscale
LE-2	1.028	3.825	Lignite	Lab
NE	1.29	2.181	Lignite	Lab & Simulation
SE	1.384	2.33	Sub-bituminous	Lab
UE	1.298	3.371	Lignite	Lab & Upscale

Besides, coal samples properties also can contribute to the heat generation. Different coal samples properties are measured by special oven (highest temperature 2,000°C) in proper order. The results are depicted in the Table 2-3.

In DTA test, the lignite and sub-bituminous coal samples were crushed for proximate analysis. The thermal analyses were carried out with the powdered samples with the weight of approximately 28 mg and with a heating rate of 10°C/min. DTA was carried out in air atmosphere and from room temperature to 800°C by using Al_2O_3 as the reference material. According to recorded data several analyses were repeated under identical conditions to meet the reproducibility of the results. The results for the DTA analyses are presented in Figure 2-15.

Table 2– 3 Properties of coal samples

Name	Fixed Carbon (%)	Ash (%)	Volatile Matter (%)	Moisture (%)	Average Diameter (mm)
LE-1	30.7	10.54	55.76	3.0	0.48
LE-2	6.26	0.62	24.12	59.0	0.48
NE	54.0	6.98	33.62	5.53	0.48
SE	42.7	14.43	38.87	4.0	0.48
UE	24.7	8.3	39.8	27.2	0.48

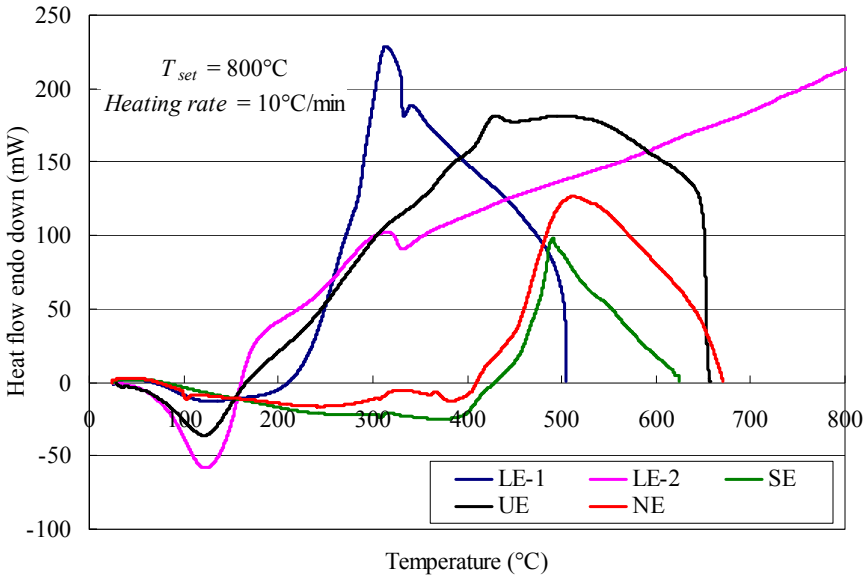

Figure 2- 15 DTA curves of coal samples in air atmosphere

Evidence of each coal sample activities in different heating process can be

obtained in the DTA curve. As shown in Figure 2-15, all coal samples showed an endotherm peak at 130°C, approximately. This phenomenon indicated that mass loss and blocks crushing was started in this process. Then, coal samples were located inside reactions and heat exchange was speeded up to promote DTA recorded heat flow to the exothermal climax. By analyzing the DTA recorded data (heat flow and elapsed time), coal sample calorific value can be roughly calculated.

2.5 Equation for Critical Temperature

Based on the Frank-Kamenetskii's model and Arrhenius equation, critical self-ignition temperature can be formulated from heat balance at the temperature between heat generation and heat loss rates of the coal pile. Frank-Kamenetskii (1959) theory is a model based on Equation 2-1, which propose a high Biot number model ($Bi > 10$; $Bi = hr/\lambda$). The Frank-Kamenetskii theory allow for the temperature gradient in the reacting system to be considered, while the Semenov model ignores temperature gradient between the reacting mass inside and outside of the reaction system that causes a substantial decline problem.

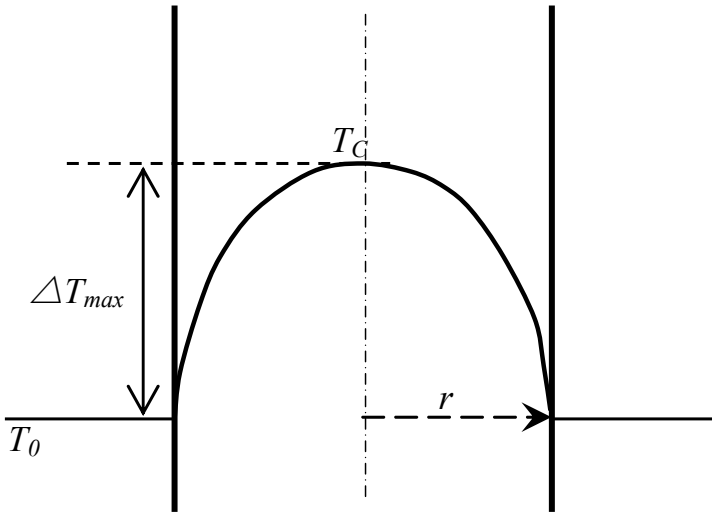

Figure 2- 16 Internal temperature curve of spontaneous combustion based on Frank-Kamenetskii's model

Assume the analysis model is one-dimensional continuous with double-sided heat, then

$$\alpha\left(\frac{\partial^2 T}{\partial r^2}+\frac{\kappa}{r}\frac{\partial T}{\partial r}\right)+\frac{Q}{\rho Cp}=\frac{\partial T}{\partial t} \tag{2-2}$$

where,

r: Critical (Equivalent) radius, m;

Q: Heat generating, J/kg;

λ: Thermal conductivity, W/(m·K);

a: Thermal diffusivity, m^2/s;

κ: Frank-Kamenetskii parameter (dimensionless)

T: Temperature, K

ρCp: Volumetric heat capacity, $J/m^3 \cdot K$.

can be calculated. Suppose the heat generation rate is expressed by the Arrhenius equation and the system has reactants with a low thermal conductivity and also it has highly conducting walls, the Equation (2-2) can be expressed as

$$\frac{\partial^2 \theta}{\partial z^2}+\frac{\kappa}{z}\frac{\partial \theta}{\partial z}=\frac{r^2 E\Delta H_c A C_i^n}{\lambda R T^2}\cdot\exp\left(-\frac{E}{RT}\right)\exp(\theta) \tag{2-3}$$

$$\nabla^2\theta=-\delta\exp(\theta) \tag{2-4}$$

The equation giving the δ (m^2/K^2) value is

$$\delta=\frac{r^2 E\Delta H_c A C_i^n}{\lambda R T^2}\cdot\exp\left(-\frac{E}{RT}\right) \tag{2-5}$$

Here, δ describes the reaction system including chemical heat generating rate and the rate of heat dissipating to the environment from boundaries. The value of δ

depends on the degree of self-heating. Moreover, only within a range of δ values, the Equation (2-4) is solvable. If the actual situation is beyond the range ($\delta \geq \delta_c$), the reaction system will start self-ignition. For different solid shapes, δ value can be calculated by the equation, as shown in Table 2-4. It clearly shows that Equation (2-5) can be used to evaluate the relationship between size and critical self-ignition temperature in the system.

Returning to Equation (2-5), that equation can be rewritten as

$$\ln\left(\frac{\delta_c T_{CIST}^2}{r^2}\right) = \ln\left(\frac{E\Delta H_c A C_i^n}{\lambda R}\right) - \frac{E}{RT_{CIST}} \tag{2-6}$$

It is clear that in the Equation (2-6) left-hand-side has a linear relationship with $\frac{1}{T_{CSIT}}$. This relation is widely used in spontaneous combustion survey and prevention of solid accumulations. By plotting $\ln\left(\frac{\delta_c T_{CSIT}^2}{r^2}\right)$ against $\frac{1}{T_{CSIT}}$, $\ln\left(\frac{E\Delta H_c A C_i^n}{\lambda R}\right)$ and activation energy, *E*, can be obtained from the intercept and slope of the linear equation, respectively. Finally, heat generating rate, ΔH_c, critical self-ignition temperature (T_{CIST}) and function of the pile radius (r) can be obtained (as shown in Equation (2-6)). The value of T_{CIST} can be obtained to predict critical self-ignition temperature for larger volume of coal piles. Coupled with the DTA measured results it can be easily found that each coal sample has its own level of temperature change and energy conversion. Arrhenius equation can explain this phenomenon legitimately. Every coal sample needs different level of activation energy to give impetus to the reaction start. Then, the wide variety of constituent of coal samples were put in reactions to find different orders and energy requirements. Activation energy (E) and pre-exponential factor (A) can describe these two

important parts more intuitively. Thus, E and A quantization are important to expand the results by the tests to the large size stockpiles and industrial utilization.

Table 2- 4 Critical value of δ in different shapes

Shape	κ	δ_c
Plate (thickness = 2 r)	0	0.88
Cylinder (radius = r)	1	2.00
Sphere (radius = r)	2	3.32
Cube (side length = 2 r)	3.28	2.52

The method used in this study requires repeated tests several times to obtain the best critical temperature. The point of critical ignition can also be problematic to recognize, as there is not always a sharp rise in temperature. Hence, some judgment must be considered. As the equation shows, the method mainly focus on establishing good values for $\frac{E}{R}$ and $\ln\left(\frac{E\Delta H_c AC_i^n}{\lambda R}\right)$. It is effective to use a convective oven with good circulation to produce high velocities around the sample to give high convective heat transfer accomplish a faster heating environment. Moreover, the radiation exchange between the wire-mesh baskets and the walls of the oven must also be determined. Hence, Biot number in the experimental heating system is needed to establish. In addition, the thermal conductivity for the different types of coal materials were measured in this study to defined the Biot number as well. Convective heat transfer coefficient as a function of oven velocity and wire-mesh baskets size (Tamborello, 2011) was also considered for the identifying heat transfer characteristics of the intelligent oven used in the test.

2.6 Conclusions

In this chapter, different types of apparatus were equipped to measure the inside

temperature changes of coal samples in different temperatures environment (T_E) under standard atmospheric pressure. In the study, experimental measurement procedures of thermal diffusivity and sample properties have been presented in advance. Besides, parameters definition was considered beforehand to preclude confusion in the result analysis.

Five coal samples consist four lignite samples (low-rank coal) and one sample of sub-bituminous coal taken from different coal mining areas were used to evaluate the critical self-ignition temperature. The DTA data were measured were promoted to define each coal sample characteristics. All samples showed an endotherm peak at 130°C, approximately. Mass loss and powdering with cracking of coal blocks was started during the endotherm process. Then, heat dynamic equilibrium was reached and the series of reactions were speeded up until getting to the exothermal climax. By analyzing DTA curves useful reference to the following experiments can be obtained.

According to the analysis result, the coal pile critical self-ignition temperature is mainly affected by the volume and temperature difference under the same condition of the pile porosity. Coal sample inside each unit has the same heat exchange with same thermal diffusivity in the laboratory and upscale experiments, and for practical engineering it can be neglected. Based on actual statistics of coal size data, the test used common size, which proved it has same thermal condition in the test.

Frank-Kamenetskii's model based on Arrhenius equation was used to analyze the measured temperature data. By plotting $\ln\left(\frac{\delta_c T_{CSIT}^2}{r^2}\right)$ against $\frac{1}{T_{CSIT}}$, activation energy (E) and pre-exponential factor (A) can be obtained from the intercept and slope of the linear equation, respectively. Quantize E and A is helpful to expand the laboratory experiment results to the large size stockpiles and industrial scales.

Chapter 3: Laboratory Experiments on Critical Self-Ignition Temperature

3.1 Introduction

The experimental studies on the critical ignition temperatures of bulky stocks of coal were carried out for the first time in 1960s. Gray and Lee (1967) measured the subcritical and supercritical conditions around 300°C and measured pre-ignition temperatures at different positions in a cylindrical reaction vessel. Bowes (1984) also presented simplified self-heating models based on Frank-Kamenetskii's ignition theory. But they all didn't find accurate critical ignition temperatures.

In this chapter, critical ignition temperatures of coal samples assuming each to be placed in hot surroundings in air at normal pressure were estimated by heating tests. The laboratory small size test was done (oven testing) with specific size samples in a wire-mesh basket suspended in the constant temperature oven. This corresponds to the test method discussed in chapter 2, i.e. a low temperature coal (T_C = T_0) placed in a hot environment (T_E) with inserting 2 to 5 thermocouples. Obviously, the tests should be conducted under safety considerations. The test is repeated by changing the oven set temperature until the critical temperature is found for a given basket size, usually a cube. However, once a minimum of three critical values have been found an analysis can be conducted. The objective was to find a fundamental law for preventing the phenomenon of coal spontaneous combustion. In the test, five coal samples were pulverized as the size-graded to 0.25 to 0.76 mm (average was 0.48 mm). Experiments of heating coal samples have been done by distinct conditions to check self-heating characteristics of coal samples. The experiment apparatus are shown in Figure 3-1.

Figure 3- 1 Laboratory experimental apparatus (Mar. 2013)

3.2 Experimental Results and Discussions

3.2.1 Samples continues heating test

To get some insight in the comparison of coal samples, the difference of lignite coal and sub-bituminous coal heat exchange process was tested by continuously heating the environment (step by step increasing T_E) from room temperature T_0 to 140°C with temperature gradient of 10°C/hour (except LE-1). Every test was started with uniform coal particle size (average 0.48 mm) and equivalent coal weight (90g). The coal samples were filled in the wire-mesh basket as a coal pile. The heating environment was constant and adjustable. By using the thermocouple record system the coal sample internal temperature was measured on time. Figures 3-2 to 3-6 illustrate the coal samples inside temperature changes curve (L = 5 cm).

It clearly shows that during the primary heating stage (T_E < 80°C); the temperature curves at the center position in the basket are very smooth. However,

when T_C is goes up to 100°C the measured temperature reaches thermal runaway phenomenon and eventually the combustion starts. Especially around the temperature of 160°C, the increasing slope of temperature curve is nearly equal to 30 ºC/min.

On the other hands, these coal samples also have their own unique phenomenon during heating period. Directly recorded data are shown in Figure 3-2; LE-1 has a faster rate of temperature rise which indicates that coal sample with higher thermal conductivity was existed in the basket. That is also the reason of testing 20 minutes as the time step. The other 4 tests were carried out with the time stage of 120 minutes. It clearly shows that LE-2 always delayed to get to the environmental setting temperature (T_E). By considering the DTA analysis, it can be concluded that moisture content of coal has an influence on the temperature-dependent thermal conduction and heat capacity. In the rest of coal samples such as NE, UE and SE the temperature rise was almost on a reasonable step-wise time scale in each time gap. No significant differences in temperature rise during heating process until T_E were observed up to critical self-ignition temperature range.

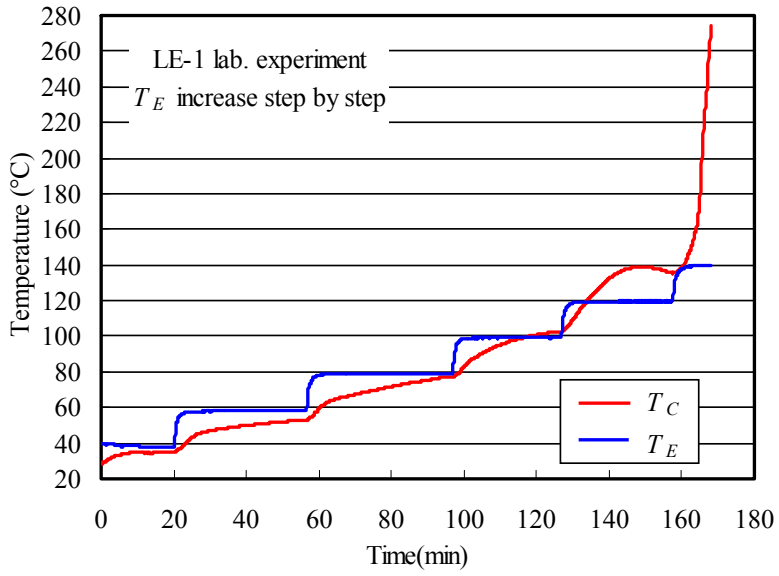

Figure 3- 2 Center temperature-time increase curve of LE-1 (lignite)

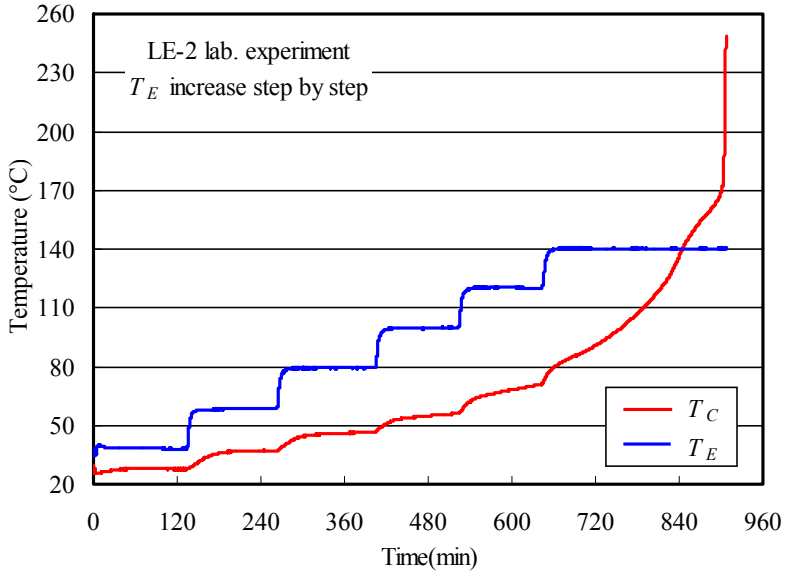

Figure 3- 3 Center temperature-time increase curve of LE-2 (lignite)

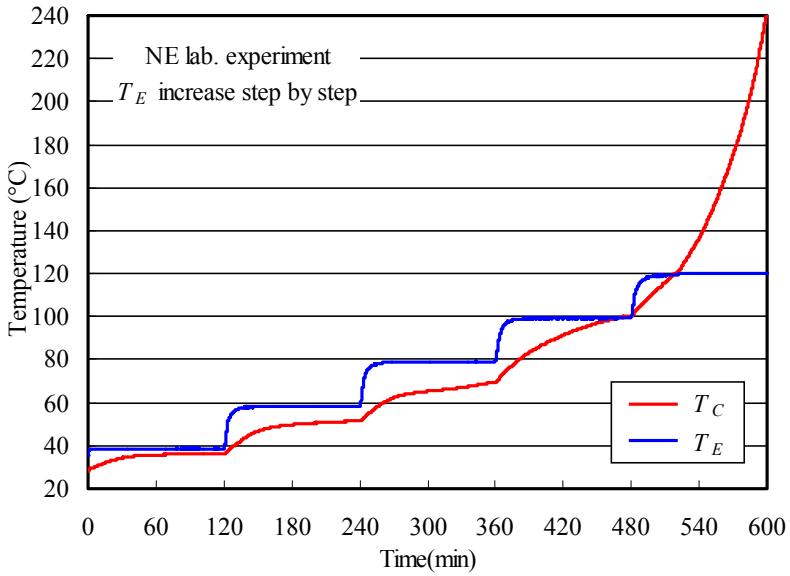

Figure 3- 4 Center temperature-time increase curve of NE (lignite)

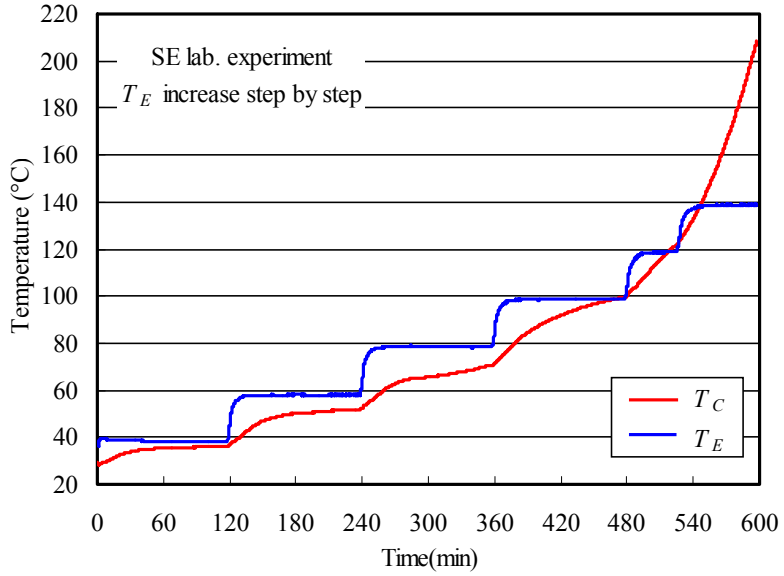

Figure 3- 5 Center temperature-time increase curve of SE (sub-bituminous)

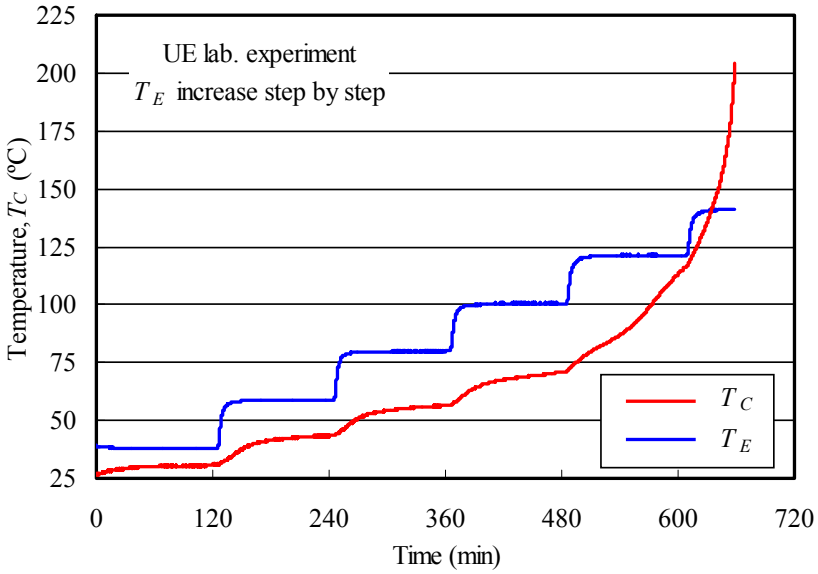

Figure 3- 6 Center temperature-time increase curve of UE (lignite)

Based on the above data and information, the study mainly analyzed two representative coal samples to examine the effect of wire-mesh basket different sizes on the coal spontaneous combustion.

3.2.2 Wire-mesh basket test

Figure 3-7 shows temperature measurement results of LE-1 for different ambient air

temperatures with wire-mesh basket length of 2.5 cm, to find the critical point of self-ignition temperature (*CSIT*). In this case, the value of the *CSIT* is determined to be 141 ºC (414 K). Directly from the Figure 3-7 it can be found that during the first 30 minutes all three same coal samples were tested in different oven temperature (T_E). The same temperature rising trend was observed. After passing 140ºC, temperatures start to show differences. Furthermore, in the T_E =140ºC case, the center temperature increases for a while with a smooth gradient until the heat balance, and then starts to decrease and eventually returns back to environment temperature. On the contrary, T_E =143 ºC and T_E =145 ºC show quite different trend with case of 140ºC. The measured samples' center temperature rises steadily, reaching thermal runaway in just a very short time. To get some insight in the possible influence of the heating environment, in T_E =140ºC and T_E =143ºC cases, analysis of temperature-time curve is particularly appropriate. It clearly shows that when the center temperature goes up to 160ºC, one sample has a high self-heating energy leading to temperature-rise acceleration appreciably, and in the other sample natural convection induces heat loss making the temperature level off, then the sample cools down.

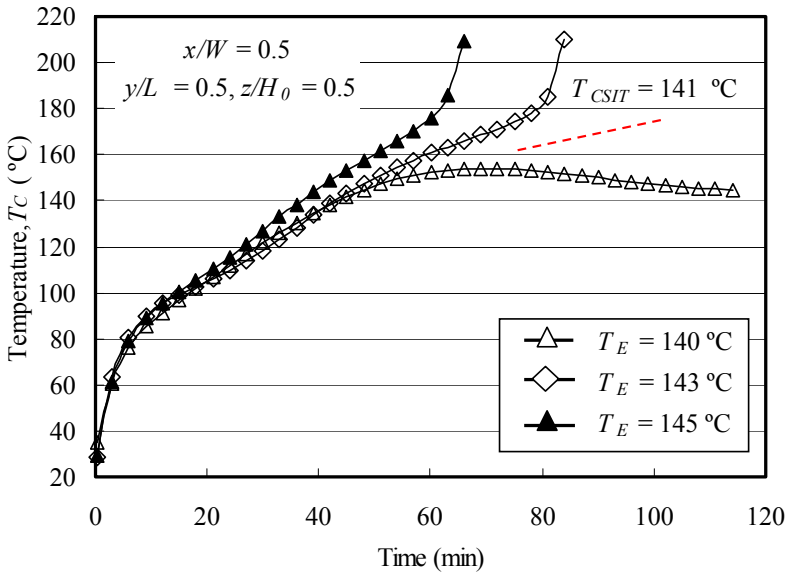

Figure 3- 7 Critical ignition temperature for LE-1 (L = 2.5 cm)

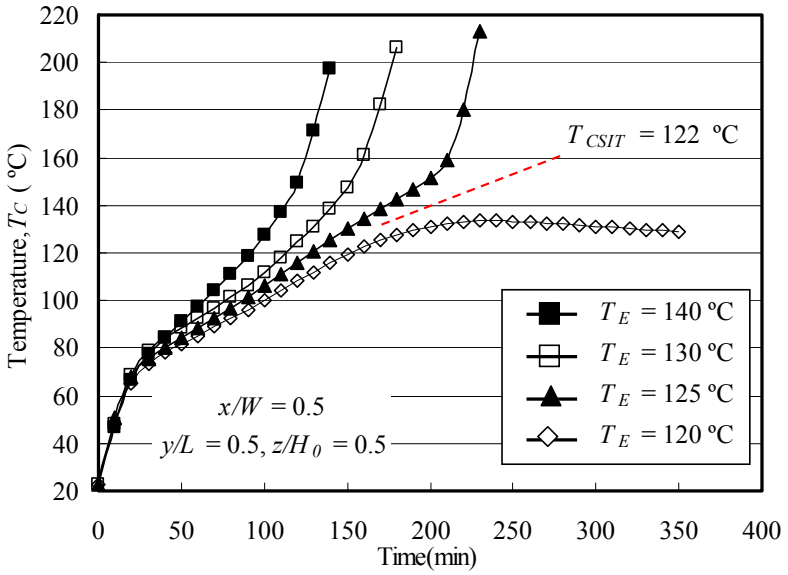

Figure 3- 8 Critical ignition temperature for LE-1 (L = 5 cm)

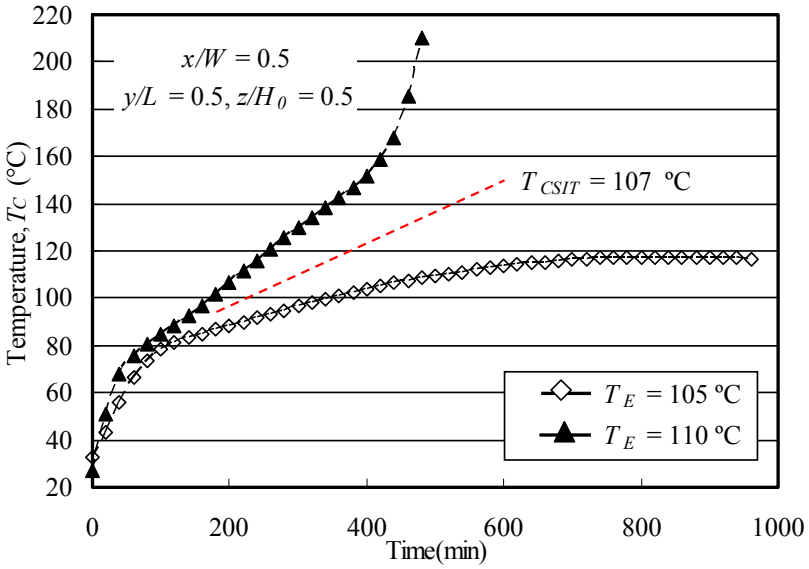

Figure 3- 9 Critical ignition temperature for LE-1 (L = 10 cm)

Figure 3-8 shows the different heating temperature of coal sample's center temperature curve in wire-mesh basket (L = 5 cm). The temperature curves appear to be different when the environment temperature goes up to 70°C after 25 minutes. From the phenomenon indicated by the temperature difference, it can be indicated that coal heat generation started in this temperature range. Then, if self-heating dominated the temperature increase, the spontaneous combustion may be started,

otherwise natural convection occupies heat exchange process leading to temperature level off and then back to T_E. Overall, the value of critical self-ignition temperature for the basket size; 5 cm is determined to be 124 ºC (397 K).

On the other hand, the center temperature curve in the 10 cm wire-mesh basket is illustrated in Figure 3-9. The critical self-ignition temperature of this case is determined to be 107ºC (380 K). As shown in the figure, it can be understood that the temperature rise against time is similar to the former two cases (2.5 and 5 cm baskets). During the whole heating process, if coal pile heat loss is less than the generated heat, the temperature will continue climbing up. This feedback between an increase in chemical reaction rate and the increase in temperature can lead to an instability and thermal runaway to a new state of equilibrium. Figure 3-9 fully demonstrates the process for T_E = 110°C case. This figure depicts the coal pile center temperature rising over environment temperature; T_E, which finally leads to the start of spontaneous combustion. Otherwise, as mentioned before the heat loss from coal pile would dominate the heat exchange process, and temperature would be leveled off and eventually coal pile would be cooled.

To get some insight in the LE-1 sample's self-heating, the experiments were compared to show the differences caused by varied sizes and center temperatures of wire-mesh basket based on the experiments of two quite different environmental temperatures.

It clearly shows that when the environment temperature is set as 50°C, the samples internal temperature-time curves are almost identical. However, with increasing in coal pile size the elapsed time to achieve a uniform temperature is longer (see Figure 3-10). Since there was a corresponding temperature sensor errors existed in the experiment, the slightly fluctuation of the final temperature was found around 50°C. From the result of laboratory measurement on the temperature changes for different coal pile sizes, it can be concluded that for each size of coal piles the

weak chemical energy in T_E = 50°C could not keep up with the heat loss, and this leads to the coal pile temperature to be leveled off after reaching to the T_E.

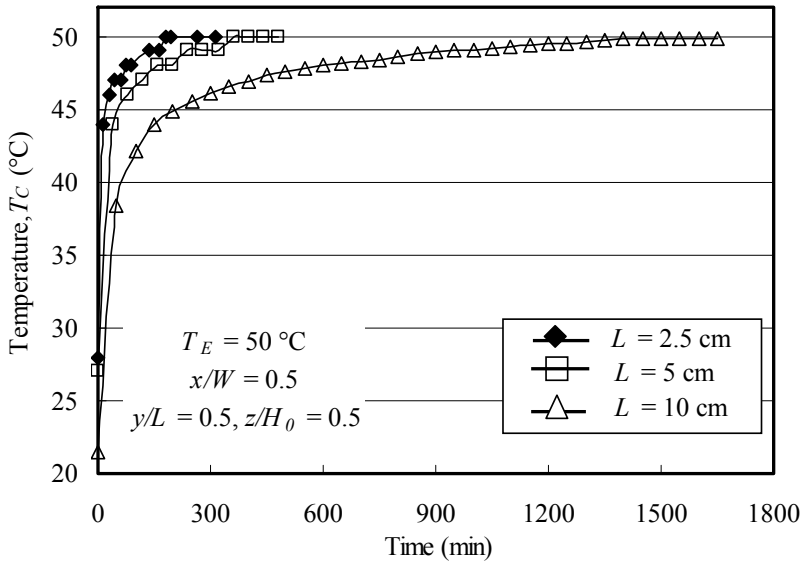

Figure 3- 10 Internal temperature-time curves for T_E = 50°C using different size coal piles

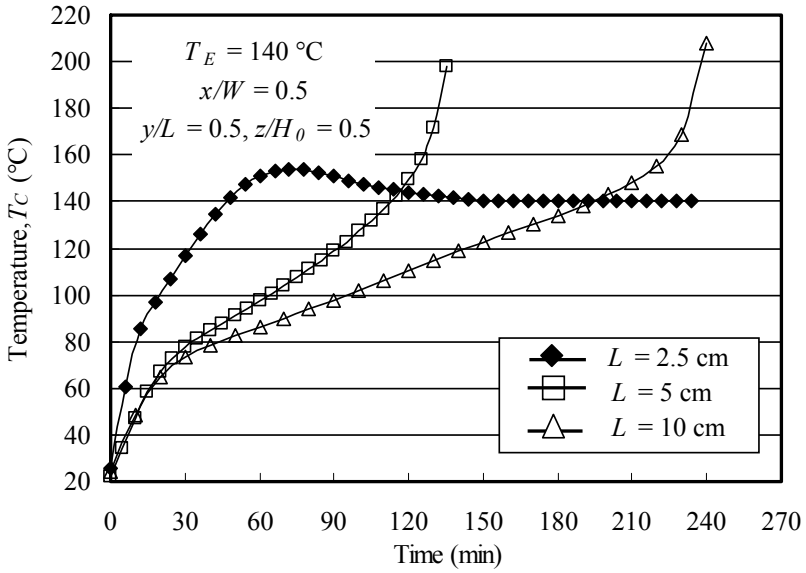

Figure 3- 11 Internal temperature-time curves for T_E = 140°C using different size coal piles

As shown in Figure 3-11, for the heating environment of T_E = 140°C

temperature-time curves for three sizes of wire-mesh basket are compared. Owing to the higher environment temperature T_E (T_E = 140°C), the self-heating appears after around 30 minutes. Once self-heating starts, the coal pile temperature speeds up which feedback an increase in chemical reaction rate. The coal pile can undergo two distinct situations about the reaction rate. If the heat loss keeps up with the chemical energy, the temperature reaches the equilibrium then levels off as shown in Figure 3-11 (L = 2.5 cm). Otherwise, it may continue rising to thermal runaway. Form the figure; it can be also summarized that the coal samples can be clearly distinguished from one species to another under natural convective conditions.

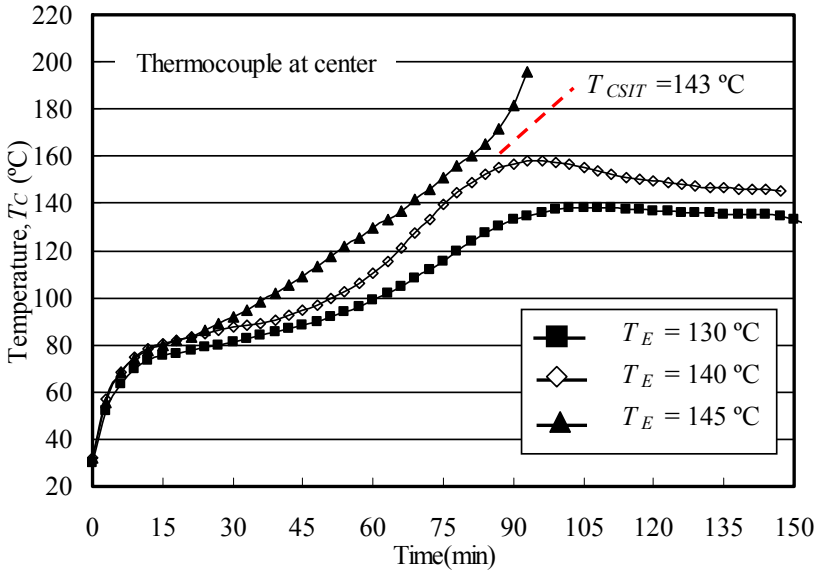

(a) L = 2.5 cm

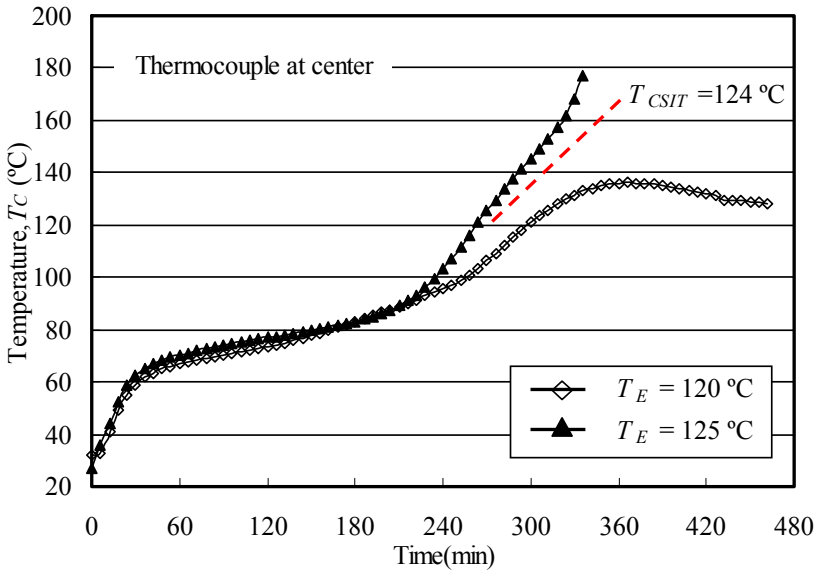

(b) L = 5 cm

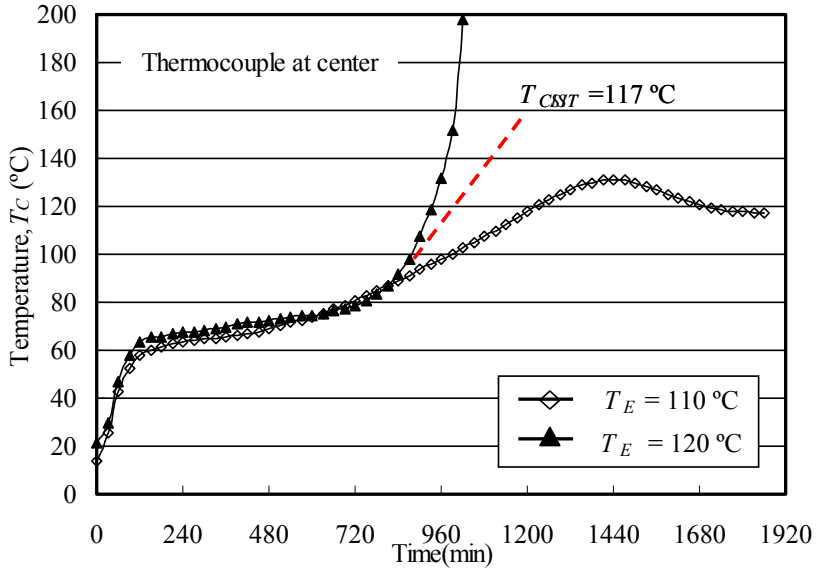

(c) L = 10 cm

Figure 3- 12 Temperature rising vs. time after placing in different ambient air temperature environment

In another test series, with fresh sample at an initial temperature of T_0, the center temperature rise curves for UE are shown in Figure 3-12. For each size of the basket the critical temperature of self-ignition is written in the figure. Take the L = 10 cm case for example, in which the intermediate combustion state of smoldering is short lived (apparently commencing at about 100°C) in T_E = 120°C heating

environment. This phenomenon was also observed in subcritical state (T_E =110 °C), but with a much weaker chemical reaction rate. It should be noticed that even in the subcritical state the coal pile's internal temperature is higher than its environmental temperature T_E, thus directly proves that self-heating is exceeding internal temperature of coal pile.

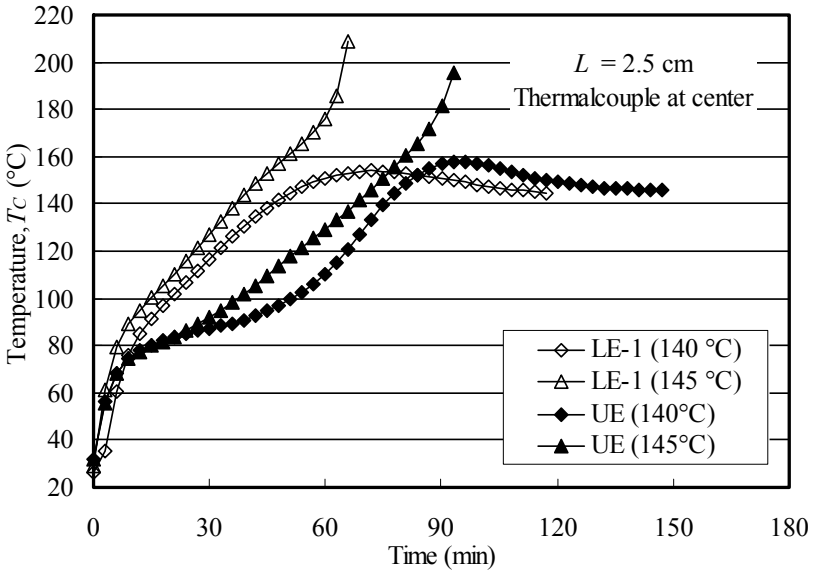

(a) 2.5 cm in length wire-mesh basket case

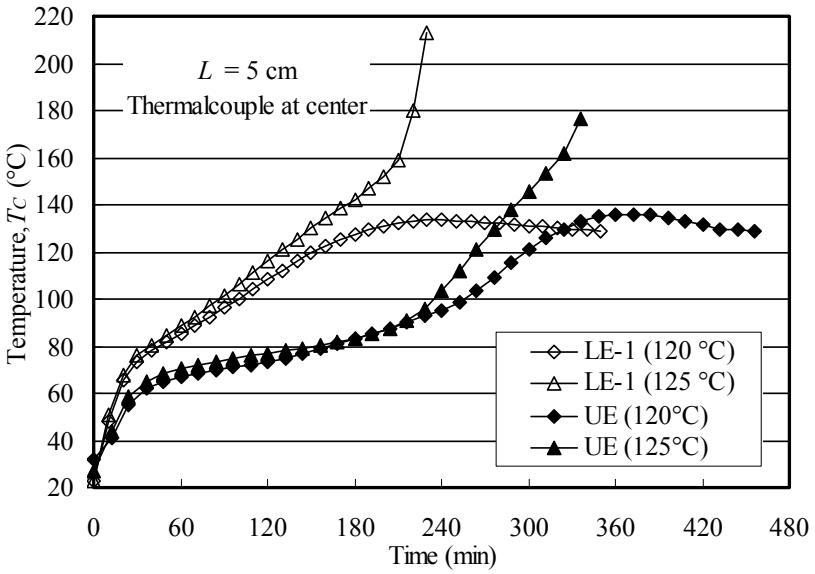

(b) 5 cm in length wire-mesh basket case

Figure 3- 13 Comparison supercritical and subcritical state of two coal samples

In the definition of coal sample critical self-ignition, accrediting the heat generated by coal is the basic step to assess the possibility of spontaneous combustion. Figure 3-13 shows measured data for two different coal samples. When the heating environmental temperature, T_E, is subcritical for the cases of L = 2.5 cm, T_E = 140 °C and L = 5 cm, T_E = 120 °C the center temperature is exceeded the T_E (heat exchange dynamic equilibrium), then it decays due to lack of energy and material in the self-heating reaction. But for the process that is supercritical (L = 2.5 cm, T_E = 145 °C; L = 5 cm, T_E = 125 °C), the coal samples have enough energy to promote the chain reactions. It shows a rapidly temperature rise over 200°C. Figure 3-13 also represents a distinct temperature delay of UE sample. When the coal samples start to generate heat against T_E, the two samples show different trends. Therefore, for this phenomenon, coal characteristics are particularly important. As shows in Table 2-2, UE sample's specific heat capacity is approximately 2 times larger than that of LE-1. Of course, large heat capacity should absorb more energy to raise the temperature. It is more clearly showed in Figure 3-12 that the large specific heat capacity delayed the rising temperature and decayed the temperature climbing up gradient. This depletion of energy is indicated by the specific heat and moisture content of the coal. Table 2-3 illustrates the properties of two samples. As this table shows, moisture content of LE-1 is around 3%, but UE is much higher than 27%. By evaporating or drying of coal moisture in a rate corresponding to the complete saturation of the air, the moisture content of the coal continues until practically reaching to zero (Schmal, 1987). The heat evaporates water from the coal at first. It means that the heat generated by the chemical reaction of coal is almost equal to the heat depleted by moisture evaporation. Hence, the coal temperature is leveled off until finishing the moisture evaporation. In such a case, UE with moisture content of nearly 30% shows a delay in temperature increase (see Figure 3-13).

After analyzing the center temperature curve of the former wire-mesh baskets with three different sizes, it is realized that the relative liability of coal samples

under heat oxidation can be recognized by thermal analysis. The results are plotted in Figure 3-14.

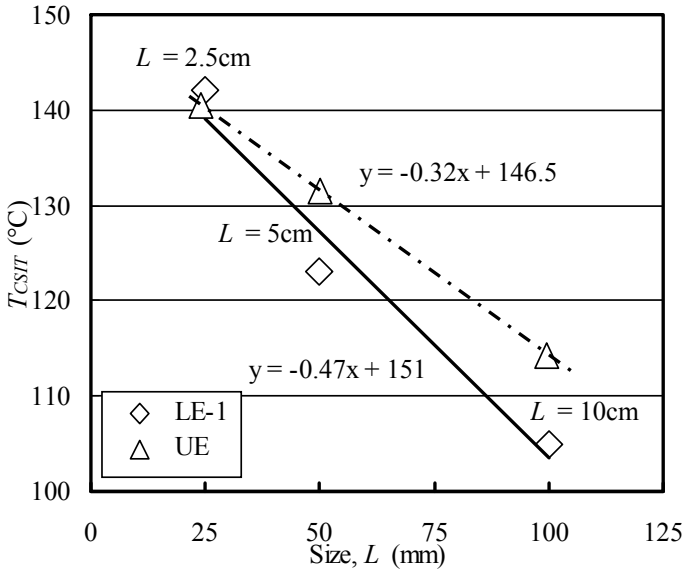

Figure 3- 14 Critical self-ignition temperature comparison of LE-1 and UE

There is a relationship between the critical ignition temperature and the size of wire-mesh basket within a certain range. The larger the wire-mesh basket the lower critical ignition temperature of coal sample (see Figure 3-14). With the different critical ignition temperature for different sizes of wire-mesh basket it can be concluded that coal stockpile size affects its critical ignition temperature.

3.3 Equation Analysis

As previously mentioned, the Frank-Kamenetskii theory with one-dimensional heat conduction

$$\ln\left(\frac{\delta_c T_{CSIT}^2}{r^2}\right) = \beta - \frac{E}{RT_{CSIT}};\quad \beta = \ln\left(\frac{EQA\rho}{R\lambda}\right) \tag{3-1}$$

was considered to analyze the coal self-heating with experimental measurement data.

According to the physical definition, by measuring elapsed time, surface area and temperature change rate the coal thermal diffusivity can be calculated. However in the actual experimental conditions the porosity may be critical. As calculated results show, the coal pile thermal diffusivity is approximately 0.42 m^2/s. In general, the active energy of coal sample can be evaluated by using the correlation between wire-mesh basket size and the corresponding critical spontaneous ignition temperature. The Frank-Kamenetskii equation is used for present test results with measured the critical ignition temperature of coal piles. It dispense with the individual values of molar heat of reaction Q, apparent activation energy E, frequency factor A, thermal conductivity λ, and specific heat of the coal samples ρCp. By analyzing the coal internal temperature and application of Fourier equation boundary conditions, the self-heating data of the coal samples can be calculated. Therefore, the self-heating curve of coal sample can be obtained from the calculation (see Figure 3-15).

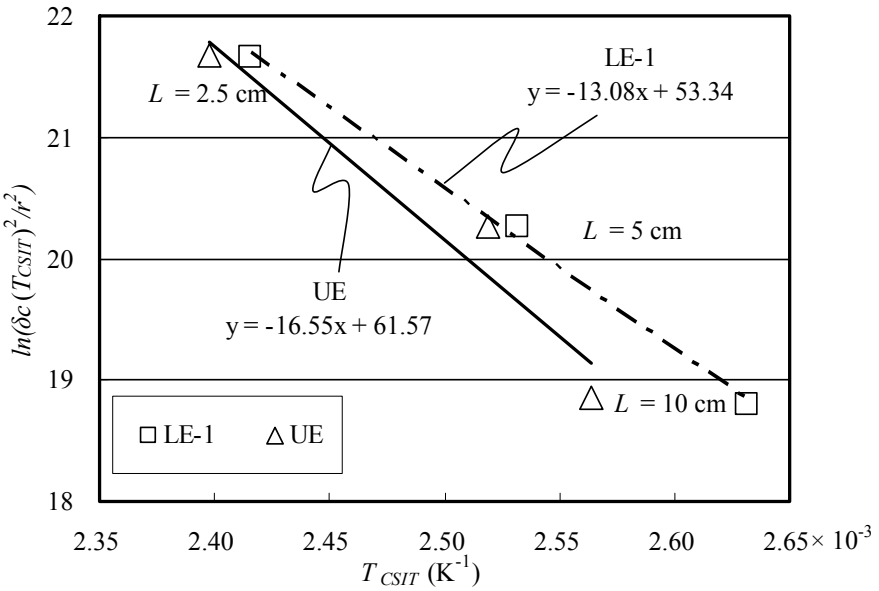

Figure 3- 15 Self-heating curve of LE-1 and UE

The activation energy of coal samples can be evaluated by calculating their asymptote from the slope $-\frac{E}{R}$ of the line. For coal samples, the line slope equation

can be evaluated as

$$\text{LE-1:}\quad \ln\left(\frac{\delta_c T_{CSIT}^2}{r^2}\right) = 53.34 - 13080\frac{1}{T_{CSIT}},\ E = R \times 16550\ \text{J/mol} = 108.7\ \text{kJ/mol} \quad (3\text{-}2)$$

$$\text{UE:}\quad \ln\left(\frac{\delta_c T_{CSIT}^2}{r^2}\right) = 61.57 - 16550\frac{1}{T_{CSIT}},\ E = R \times 16550\ \text{J/mol} = 137.5\ \text{kJ/mol} \quad (3\text{-}3)$$

As the calculation result shows UE has a larger activation energy which means it needs to absorb more heat to undergo combustion. In such case, larger activation energy accompanies a higher critical self-ignition temperature. This result is clearly seen in Figures 3-14 and 3-15. For further analysis of the result, an effect of coal pile size is considered. As Figures show, the effect of activation energy on coal critical self-ignition temperature can be easily found in larger size of coal pile.

3.4 Conclusions

The temperature-time curves in coal piles were measured by the laboratory experiment using three cubic wire-mesh baskets under different ambient temperatures (40 to 150ºC) to evaluate values of *CSIT* for coal samples. Based on the center temperature-time curves of three cubic piles 2.5, 5.0 and 10 cm in length, values of *CSIT* for the coal sample LE-1 were obtained as 143, 124 and 117 ºC, respectively. From a comparison of relations between *CSIT* and pile size for coal samples LE-1 and UE, LE-1 showed lower *CSIT* than UE. The equation of *CSIT* vs. pile size depends on coal properties such as activation energy and moisture content.

Chapter 4 : Upscale Experiments on Critical Self-Ignition Temperature

4.1 Introduction

For a long time, studies of coal spontaneous combustion has been done by laboratory measurements, thus upscaling to outdoor large piles monitoring is necessary. Owing to the influence and restriction of various inconvenient factors, such as occupying a huge space, complex slow phenomenon, long test period etc., large coal piles tests to investigate inner self-heating and spontaneous combustion characteristics have not carried out. Clear understanding of internal temperature distribution in large low-rank coal piles and developing an effective control method of coal pile spontaneous combustion are important based on coal oxidation and heat generation.

In the chapter 3, measurement results by the laboratory experiments provided in the critical self-ignition temperature to evaluate coal pile self-heating risks. Hence, the critical self-ignition temperature (*CSIT*) of large size coal piles was investigated by upscale experiment to extend the laboratory experiments. In this chapter, the experiments on the internal temperature of coal piles are presented and the idea of applying the Frank-kamenetskii model on coal critical self-ignition temperature by upscale is examined to verify feasibility of the model. Since the experiment required large amount of coal samples which are not oxidized by long time placing, vacuum package processes was used to transport the new coal sample.

The UE coal sample was transported from Baiyinhua coal filed. Baiyinhua coal filed is located in the northeast part of Inner Mongolia Autonomous Region, China. The coalfield exploration area is 24.98 km^2 and the amount of proven coal reserves is about 1.04251 billion tons. The open pit surface north-south trend is 7.17 km and east-west tends is 3.35 km with surface area of 22.14 km^2. According to coal mine

bore histogram, the largest mining depth is 330 meters. The coal of Baiyinhua coal filed is brown coal and the characteristics of sample are listed in Table 4-1.

Table 4- 1 Properties of UE

Item	Lignite coal	
Proximate analysis	Ash (%)	8.3
	Fixed carbon (%)	24.7
	Volatile Matter (%)	39.8
	Moisture (%)	27.2
	Fuel ratio (=FC/VM)	1.61
	LHV (kJ/kg)	11290
Ultimate analysis	C (%)	70.44
	H (%)	4.91
	O (%)	21.39
	N (%)	1.35
	S (%)	1.91
	HGI*	51
Physical properties	Density (g/cm^3)	1.30
	Specific heat capacity *Cp* (kJ/kg/°C)	3.37
	Average diameter (mm)	46

* Hard agrindability coefficient of coal

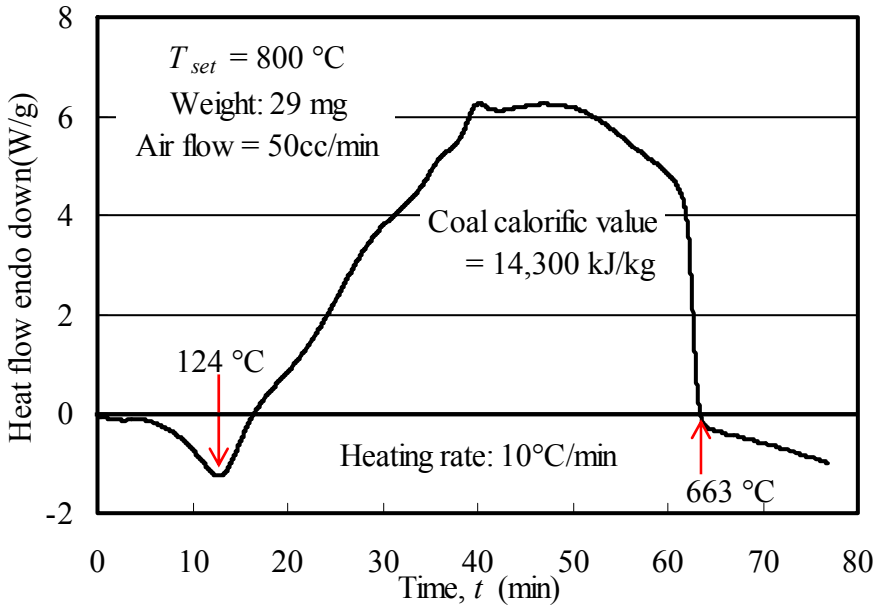

Figure 4- 1 DTA curve of UE in air atmosphere

On the other hand, DTA test also was carried out to define the coal sample. As shown in Figure 4-1, the DTA curve of the coal sample shows an endotherm peak at 124°C accompanied by the chemical reaction and water evaporation. Heat absorption was resulted in moisture mass loss of the sample and quickly weathered the coal blocks. Furthermore, the DTA curve of coal sample exhibits a major exothermal near 430°C @ 43 minutes, which indicates that the combustion has reached the climax. Evidence of coal sample activities in different heating process can be obtained in the curve. Moreover, the coal calorific value can be roughly calculated from the DTA recorded data as approximately 3434 kcal/kg. It clearly shows that analysis of DTA data can provide useful baseline information.

4.2 Experimental Apparatus

Three set of wire-mesh baskets (25, 50, 100 cm in length) were placed in different temperature environment. The UE with average particle size of 46 mm was filled in the wire-mesh basket. As shown in Figure 2-12 thermocouples were continuously monitoring the inner temperature of the coal piles.

Figure 4- 2 Photo of wire-mesh baskets (25, 50, 100 cm) for upscale experiment

In order to reduce the fluctuation range of temperature in the constant chamber (2 × 2 × 2 m), the electrical hot air generator and internal electric heaters were equipped to maintain a constant temperature. Besides, the chamber inside and outside walls were made of gypsum insulation plate. Between the gypsum insulation plate rock wool were filled.

In order to maintain the original feature of coal sample, the experiment was started as soon as the coal arrived from the mine. The coal piles were formed by filling them in the three different sizes of wire-mesh baskets (25, 50 and 100 cm in length cubic) composed of one open top and five screened faces so that air could permeate into the coal pile. Their net stock volumes were 0.015625, 0.125 and 1 m^3, respectively (see Figure 4-2).

As previously shown in Figures 2-1 and 2-2 (Chapter 2), the large cube wire-mesh baskets were set in chamber where ambient air temperature was controlled to be constant. Thermocouples 60 cm in length were used to detect internal temperatures at 6 to 9 positions including the center of the coal pile. They were installed into the coal pile from one side facing the observation window on the

door. Preheating was not applied to make the heating environment conditions same with the experiment initial design because preheating the chamber (from T_0 to T_E) was hard before carrying 1m^3 coal pile. However, heating chamber was relatively short compared with the whole process of spontaneous combustion. Thus, tests started from temperature T_0. The difference between laboratory and upscale experiments can be neglected.

The basket filled with coal was loaded into the constant temperature chamber at initial temperature T_0 (T_0 = 30°C). Each coal heating experiment using the wire-mesh baskets were done with several constant temperatures to establish the self-heating characteristics of coal samples. The coal sample and wire-mesh baskets are as shown in Figure 4- 3.

25 cm Wire-mesh basket
Coal weght: 10.8kg

50 cm Wire-mesh basket
Coal weght: 86kg

100 cm Wire-mesh basket
Coal weght: 707kg

Figure 4- 3 Photos of wire-mesh basket and loaded coal in the test (Aug. 2014)

4.3 Measurement Results and Discussions

To apply the results of laboratory experiment to estimate spontaneous combustion on industrial coal stockpiles, upscale experiment especially the 100 cm wire-mesh basket test case is particularly important to fill the gap of scales between laboratory and field piles. Nevertheless, investigations using large-scale apparatus on

self-heating of coal stockpiles are difficult due to cost and long measurement time to finish it (James et al., 2012). Based on this, in this study the upscale experiments were carried out by using fresh low-rank coal sample. The ambient-air test environment T_E of three different sizes wire-mesh baskets (25, 50 and 100cm in length) are shown in Table 4-2.

Table 4- 2 Environment temperatures (T_E) of upscale experiments

L (cm)	Environment Temperature, T_E (ºC)			T_{CSIT} (ºC)
25 cm	90ºC	100ºC	110ºC	104ºC
50 cm	90ºC	100ºC	—	94ºC
100 cm	75ºC	85ºC	—	81ºC

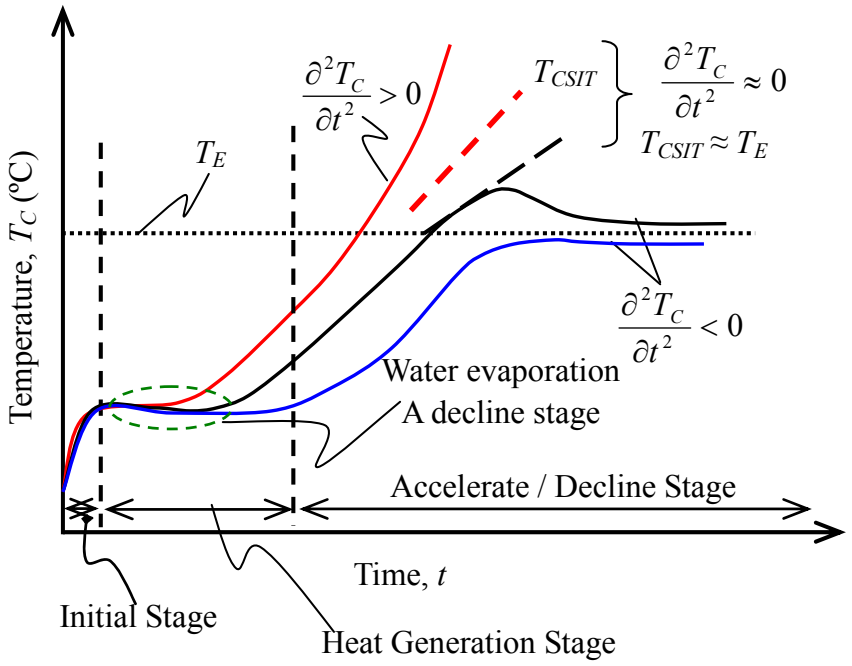

Figure 4- 4 Schematic figure of pile temperature of upscale experiment

In the upscale experiment process, the different environment temperature T_E for the piles gave effects on self-heating and also the enormous difference between the behaviors. According to the record of the thermocouple data, the pile temperature in upscale experiment was under go significantly decline period during heat exchange

process. This kind of phenomenon cannot find in the laboratory experiments. In the laboratory small size tests, coal pile surface area dominated the heat conduction process. Large heat exchange between coal pile and environment is easily to offset the heat loss from moisture evaporating. Furthermore, part of moisture was losses during the coal crush and screening process. Based on this, the upscale pile temperature rising process can be defined as Figure 4-4 shown.

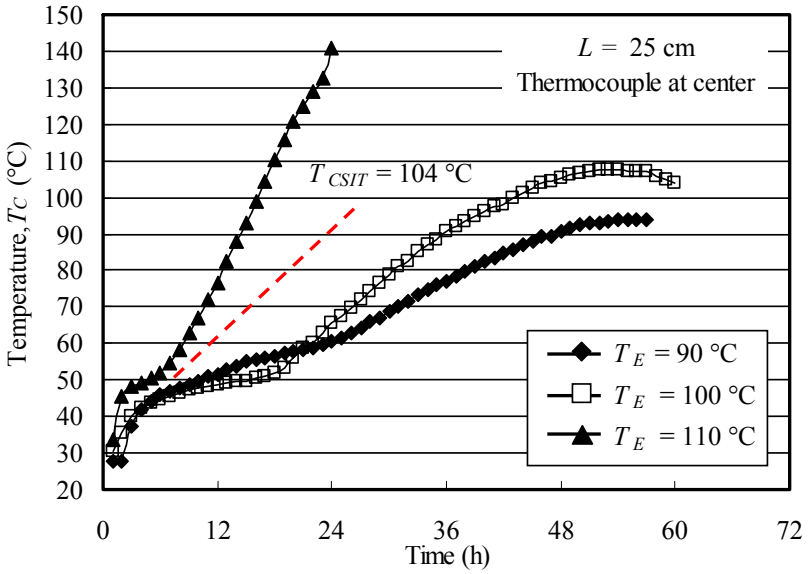

Figure 4- 5 Temperature profiles for coal sample (L = 25 cm)

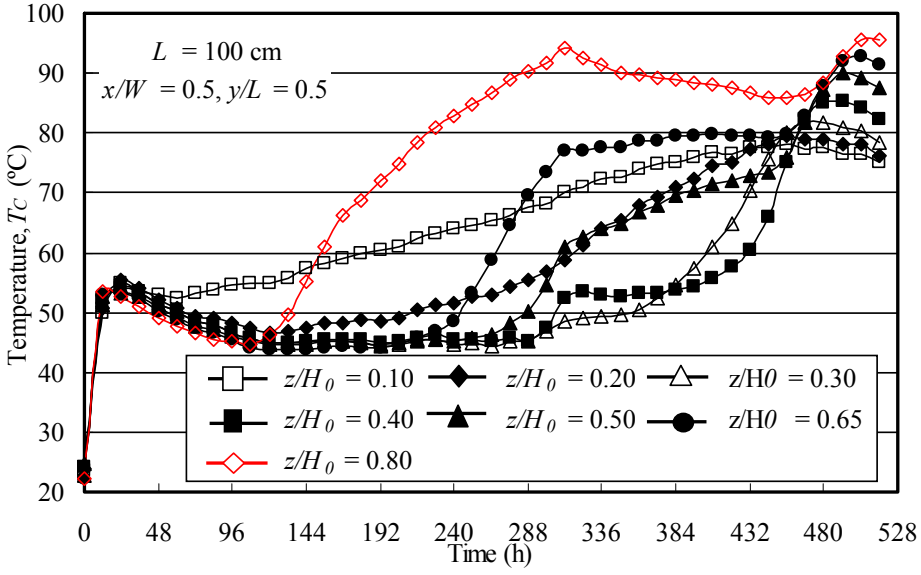

Figure 4- 6 Temperature profiles for coal sample (T_E = 75ºC)

After preheating the constant chamber, the tests of L = 25 cm and L = 50 cm wire-mesh basket at different environmental temperatures were used to investigate the process of obtaining the *CSIT* value for the coal and the subsequent kinetic analysis derived from this value. Figure 4-5 shows test results for UE of L = 25 cm at three different ambient air temperatures, were used to find the critical point of self-ignition.

For the 1 m^3 coal pile, it was hard to bring into the chamber within short time and the preheating time (30 min from T_0 to T_E) is relatively short compared with the whole time for the test (e.g. 525 h). The difference with and without preheating can be neglected. From practical experience with model calculation and the value of *CSIT* by the laboratory experiment, it can be deduced that the *CSIT* with L = 100 cm wire-mesh basket is expected to be between 70ºC to 90ºC. Considering the unknown factors, 75ºC of ambient-air temperature was firstly applied in the experiment.

Figure 4-6 shows the results of temperature for T_E = 75ºC; L = 100 cm. The position inducing early self-heating was observed to be located in the upper surface area. In the first stage, the center temperature rising was slow and the thermal conductivity of the pile had main effect in this period. The closer to the coal pile boundary, the faster the heating rate has. Natural convection in early time promoted air flow (low temperature) which causes cooling down coal temperature at the coal pile bottom; however this effect can be neglected for self-heating in the center region. Although a series of chemical reactions in heating process were hard to detected, the changes of pile volume and internal temperatures provided the information about inner phenomenon and thermal conditions. After heat transfer from lower to center area, the center temperature gradient increase speeded up significantly. After 500 hours, sample temperature reached the maximum level with a slow temperature rising rate. Then it started cooling by natural convection and finally stabilized to the slow ambient air temperature, T_E. The most notorious

phenomenon observed in coal pile was surface crushing of coal blocks.

The temperature drop is appeared after the initial preheating stage. Nevertheless, the temperature drop range and it duration time are different in each vertical position. Initially, the temperature drop gradient is around 0.1ºC/h until reaching the equilibrium temperature balancing heat loss and heat generation. On the other hand, a unique behavior was observed at z = 10 cm (z/H_0 = 0.1) and z = 20 cm (z/H_0 = 0.2) where temperatures start rising after relatively short periods (Figure 4-6). These two probes are located at the bottom of coal pile, where can obtain more heat flow by natural convection. As mentioned in chapter 2, there are heaters installed in the bottom of constant chamber, which may contribute to providing energy. As long as the heat generation and exchanging in the coal pile, moisture evaporation induced the reduction of pile volume. The hot air in the chamber going up takes away large amount of moisture from the coal. Natural convection and water evaporation from the coal that occurs is an endothermic process. Hence, the effect of natural convection and water evaporation in this is insignificant. In this case, this range has a short period temperature decrease temperature range. With the elapsed time, all showing temperatures run up reaching to a dynamic equilibrium (around 480 h). In this case, the highest temperature contains energy does not reaches the critical temperature of self-ignition, then starts to a leveled off period and finally the coal cools down as shown in Figure 4-6. Combined with the coal piles in 25 cm wire-mesh basket, the small size coal pile's temperature curves show slow temperature rising at approximately 48 ºC, which the coal moisture evaporated from coal blocks in this temperature range. In L = 25 cm wire-mesh basket case, the duration of moisture evaporation is mainly affected by ambient-air temperature, coal moisture content, porosity, and so on.

In addition to testing the coal pile self-heating, the change in coal block sizes was also studied by drying (see Figure 4-7). The drying test was using 4 coal blocks

in different size under ambient-air temperature of T_E = 110ºC for approximately 24 hours. Then, the changes in their sizes were measured after drying. As Figures 4-7 shows, the coal samples had obvious changes of blocks weathered and had crushed on their surface. Those phenomena indicate that water evaporation and a series of physical/chemical reactions were enhanced in the heating process.

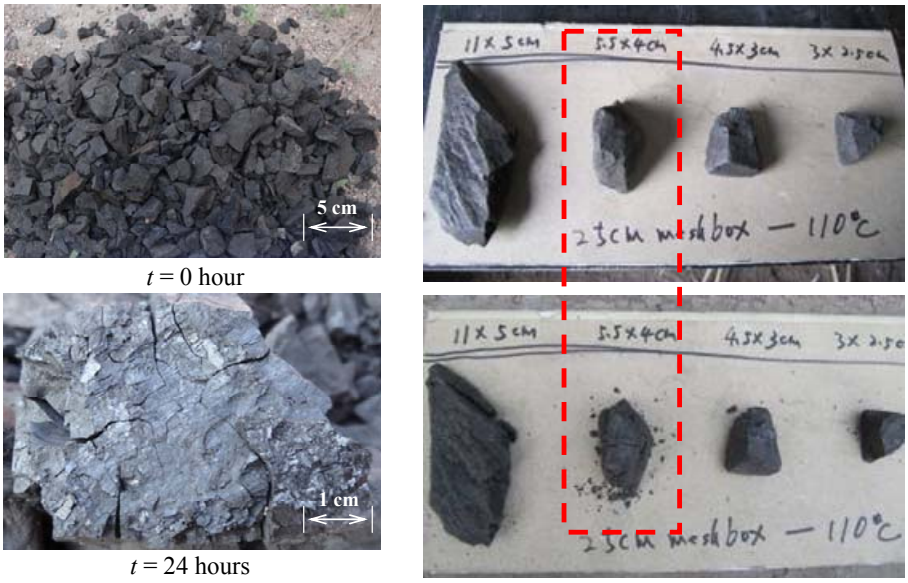

t = 0 hour

t = 24 hours

Coal in wire-mesh basket
t =0 & t = 24 hours

Drying test using coal blocks

Figure 4- 7 Examples of the coal sample changes in 110 ºC environment (Jun. 2014)

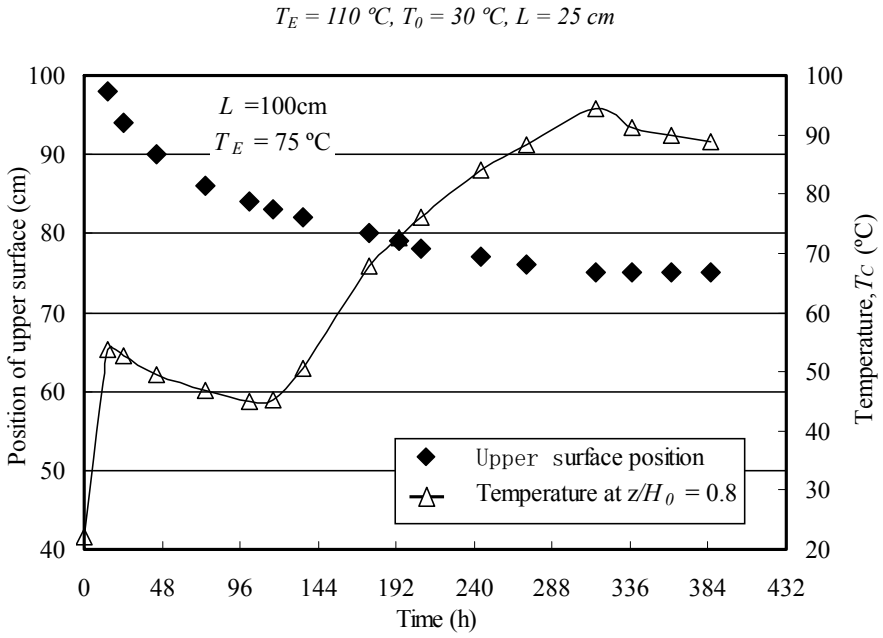

Figure 4- 8 Coal pile height vs. reciprocal temperature

Figure 4-8 shows the coal pile height versus reciprocal temperature of UE at T_E = 75ºC. The figure shows approximately a logarithmic change of coal pile height vs. time (t < 315 h). Initially, the heat conduction dominates the rise of coal pile temperature. When the self-heating starts, the heat generation makes the coal to accelerate weathering and crushing. However, this kind of phenomenon gradually disappears in the final heating process. The coal pile height H keeps 75 cm during 300~500 h, and the thermocouple tilt angle θ is 20°, approximately.

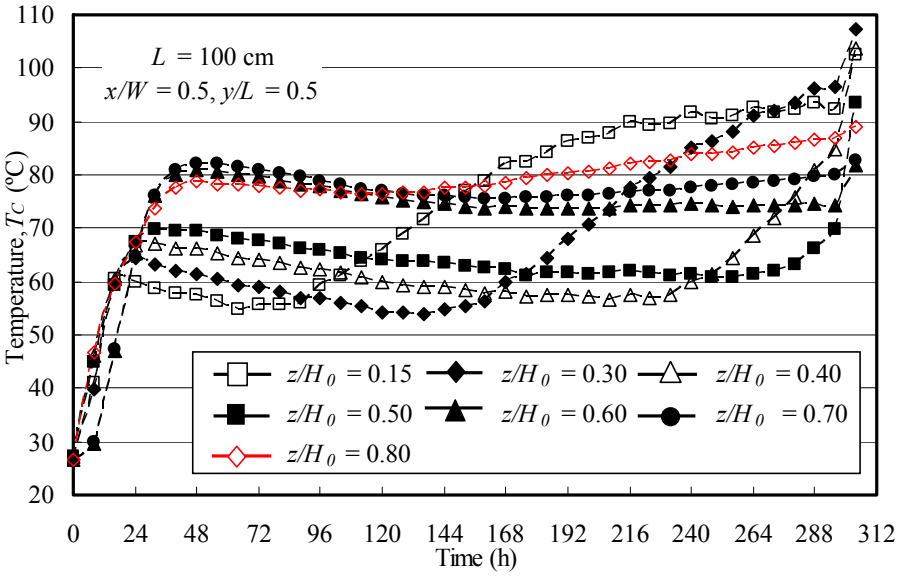

Figure 4- 9 Temperature-time profiles at different vertical positions in the coal pile (T_E= 85ºC)

Figure 4-9 shows the temperature-time curve for L = 100 cm wire-mesh basket and T_E = 85 ºC. The large heat flow causes coal crushing and the height drops from H = 100 cm to 75 cm in just only 138 hours. A very important result on the coal pile height drop is that the rapid temperature rise in the top area probably is found in the final period.

After preheating stage, the coal pile is in a temperature drop period. Moreover, it takes longer time to heat up center position in the coal pile. This is more clearly seen in Figure 4-9, in coal pile center area (z/H_0 = 0.2) the temperature increasing

start time has 7 ~ 8 hours delay. Because it has a longer distance to transmit heat and has a smaller permeability to permeate oxygen. The critical situation of temperature curve levels off, which occurs at z/H_0 = 0.15 measure area at around 60 h. As shown in Figure 4-9, this phenomenon continued 12 hours approximately then the temperature rising was accelerated. The temperature rise gradient increases gradually and finally reaches self-ignition. In this case moisture almost evaporates during the initial stage heated by hot air. Hence, transport of heat due to evaporation practically comes to a standstill then heat-collecting leads to the start of temperature climbing.

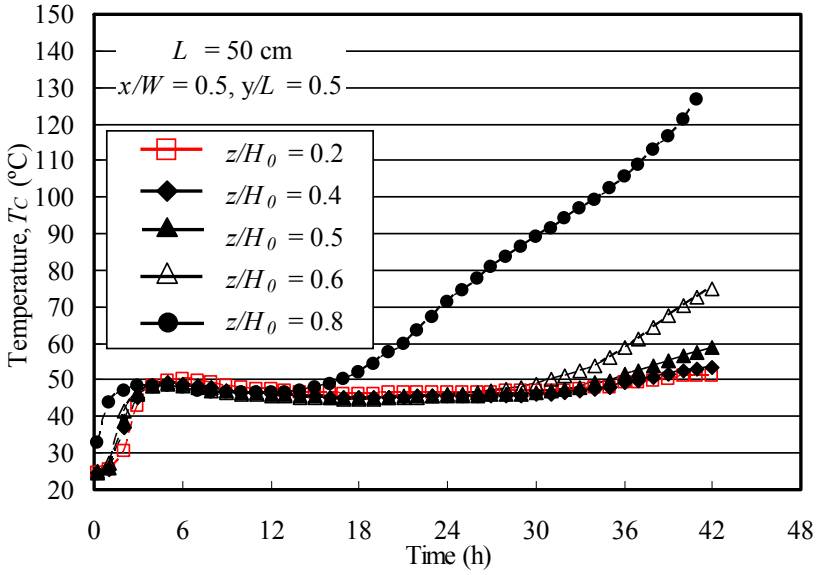

Figure 4- 10 Results of temperature profiles for coal sample (L = 50 cm)

This kind of temperature drop period also can be found in L = 50cm, T_E = 100ºC test. During the early 16 hours, temperature shows same trend stays almost constant for a while (about 10 hours). Since the moisture has an effect to inhibit the self-heating. The measured temperature decreases a little during the leveled off period as shown in Figure 4-10. At the highest probe position in the coal pile (z/H_0 = 0.8), self-heating temperature reached thermal acceleration to ignition after the coal pile temperature went up to 47ºC (16 hour). When the storage time is longer and the

moisture in the coals is decreasing, coals a shift in an equilibrium and exothermic process.

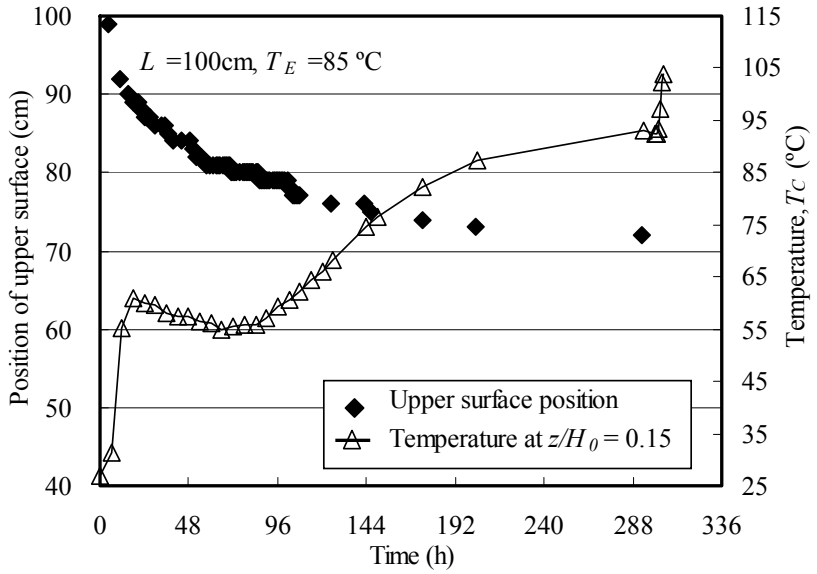

Figure 4- 11 Coal pile height vs. reciprocal temperature

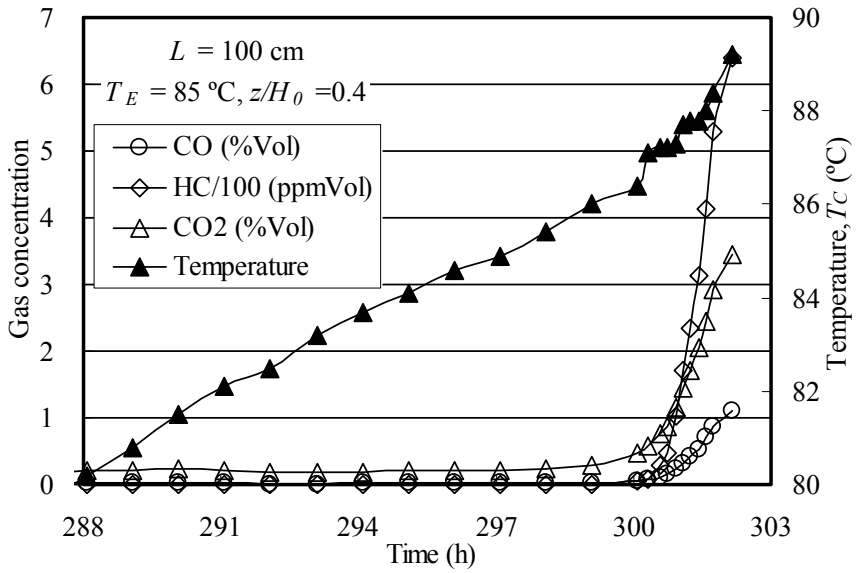

Figure 4- 12 Gas concentration and temperature at pile center

x/W = 0.5, y/L= 0.5, z/H$_0$=0.4

Based on comparison of the heat generation between z/H_0 = 0.15 and z/H_0 = 0.3; (H_0 = 100 cm), it is clearly found that deeper area has a smaller heat dissipation. The rate of heat release in the condition mainly depends on the depth and ambient air

temperature. Although surface area has enough oxygen to generate reaction heat, natural ventilation air takes heat from this area. Water evaporation is still continuing. The rest of moisture from this coal is probably formed by chemical reaction. In this case, the air cannot be saturated anymore and then rapid temperature rise occurs because transport of heat due to evaporation practically standstills. Then, self-ignition starts with a relatively short time. This phenomenon can be observed in Figure 4-9, some part area of coal pile shows rapid temperature rise and eventually ignition starts. For the verification of intensity of the reaction, environment gas compositions were also monitored. In the initial stage, the concentrations of CO, HC and CO_2 were held constant and in the same level with outdoor. Once the self-ignition started, significant climbing of concentration can be found as shown in Figure 4-12. With the active reaction of coal sample, smoke was found on 300 h. As Figure 4-12 shows, there is a dramatic increase in gases content in 301 h. The largest gradient of temperature rise was measured in the center region of the coal pile which means reaction generating heat was already out of control. A distinct open fire was observed when opening the constant chamber door, as shown in Figure 4-13(a) and (b).

(a) Door open after experiment finished

CO : 1.11 %Vol, HC : 639 ppmVol,

CO_2 : 3.44 %Vol

(b) Observation fire on the pile surface

Figure 4- 13 Photos of coal smoking

T_E = 85℃; L = 100 cm; t = 300 hours

(a) Thermocouples position in final, $\theta = 22°$

(b) Coal pile height at last, with reduction of 22 cm

Figure 4- 14 Photos of thermocouples position and coal pile height

$T_E = 85℃; L = 100cm; t = 300$ hours

Figure 4-15 Water condensation observed on the window

Reactions accompanied with heat conduction lead to heat generation and heat loss reaches dynamic equilibrium at a certain stage. Natural air convection provides more heat to the upper area and speeds up the convection air velocity. During the heating process, generated heat was used for evaporating moisture from the coals. Conversely, moisture evaporation is essentially required heat to complete this process. In such a case the temperature will decrease (at 36h) until the equilibrium temperature.

As mentioned above, during the heating process it was found that crushing and

compacting of coal sample contribute to reducing of the coal pile leads to a low oxygen permeability and diffusivity. This depleted the chemical reactions and resulted in less heat generation. This is also the reason why temperature-time curve has a drop stage after preheating in the early stage.

In Figure 4-13, the combustion region was found at the upper area (H > 40cm) where oxygen concentration always close to 20%. On the contrary, because of low porosity and lack of oxygen, center area runs a weak physical and chemical reaction. The coal pile height came down 22 cm and weight loss was 21.7% after the experiment.

The drying and crushing process was inducted by evaporating large amount of water in the coal pile as written in previous sections on small baskets. In such a case, the temperature becomes constant or shows declining until all moisture are evaporated. The exact value of time for temperature re-rising is depended on the heat generation rate and the moisture evaporation rate. By observing from the viewing window, it was easy to find water removed from coal pile (see Figure 4-15).

Directly from the experiment it can be concluded that 1m^3 coal pile in T_E = 85ºC started self-ignition at 300 hours. Finally, the thermocouple tilt angle θ was measured 22° (see Figure 4-14 (a)). Furthermore, if the reaction in heat generation stage is stable, the reaction can make to start self-ignition. It is thought that effectively controlling the reaction in this stage can prevent coal piles' spontaneous combustion. For the case of the basket of L = 100 cm ambient-air temperature T_E = 75ºC, coal heating process can be classified into four steps by their profile of the temperature-time curve.

1) Initial heating stage

During the period of this process, the coal pile temperature is lower than the

ambient temperature and down ward natural convection was induced because it has the largest temperature differences between coal pile and ambient-air environment T_E. The data shows this period was 6 hours for the L = 100 cm tests.

2) Heat generation stage

After preheating, the temperature starts climbing. A feedback for this could be a faster temperature rise rate and rapid water evaporation. In this case, the water evaporated from the coal is probably formed by reaction. Due to this active reaction, large coal blocks starts to crush and coal pile porosity starts to change. This instability is indicated by a low air saturate and a rapid temperature rise.

3) Decline stage

When the coal runs dry the rate of moisture removal falls to a lower level. More water is evaporated from the coal. In this case, part of generated heat was used for water evaporation and drying the coal for further reaction. The effect of water evaporation prevented coal pile to accumulate enough heat to accomplish the reaction. The coal blocks crushing caused by reaction and evaporation directly lead to a lower oxygen permeability of pile. The effect of oxygen concentration shortage in coal pile as reflected in a temperature drop. It can be seen from Figure 4-9 that the temperature starts to drop at 6 hours and the largest temperature drop was 11ºC.

4) Accelerate or decline stage

The initial process of this stage is similar to the initial stage. Under former three stages reaction, large coal blocks were already crushed and powdered into smaller sized coals and coal pile porosity was further reduced and oxidation is depleted to keep heat generation. Furthermore, evaporation causes heat transportation that practically leads to a standstill state and then the heat conduction dominates the temperature change. In this situation, self-ignition is ready to occur.

Otherwise, the coal pile temperature would be leveled off for a while and finally cooled. When coal at the center of pile is preheated slowly without oxygen, a high temperature spot at the center may be generated (Sasaki et al. 2003).

Figure 4- 16 Schematic of thermocouple position change

L = 50 cm, T_E = *100* ºC

After the experiment, the used coal samples were characterized and weighted before removing them from the chamber to the safety area. Moreover, original fresh and used coal samples were kept in order to measure their differences. For example, in the test of L = 50cm and T_E = 100ºC, coal pile weight loss was 22.9% (from 86.28 kg to 66.52 kg). On the other hand, the tilt angle was θ = 15°, because reducing of coal pile volume induced drop the thermocouple (see Figure 4-16).

4.4 Critical Self-ignition Temperature for L = 100 cm Basket

Initially, the coal pile temperature is equal to the environment's T_0. So the coal pile internal needs time to gather heat to reaches T_E. Evidence of such time is seen in Figure 4-17, obtained from data in different pile positions.

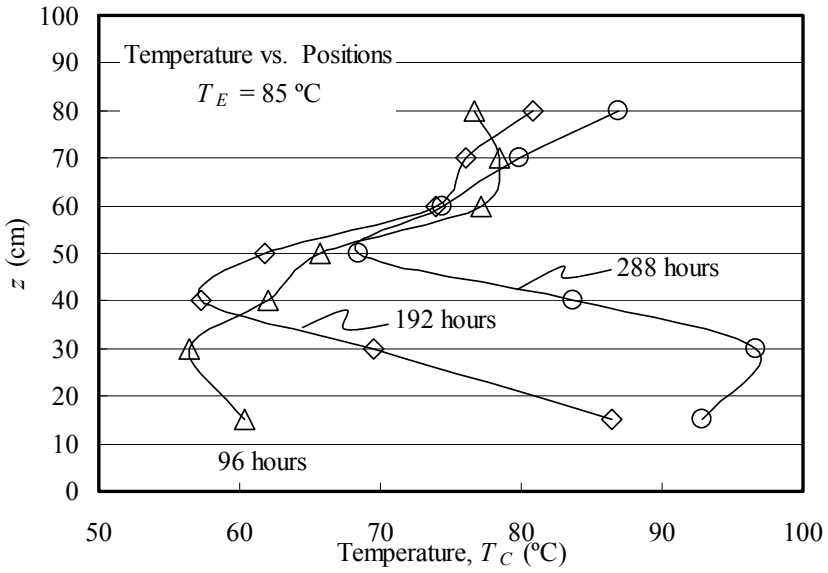

Figure 4- 17 Temperature distribution of thermocouple position

H: Coal pile original height; T_E = *85* ºC*; L= 100* cm

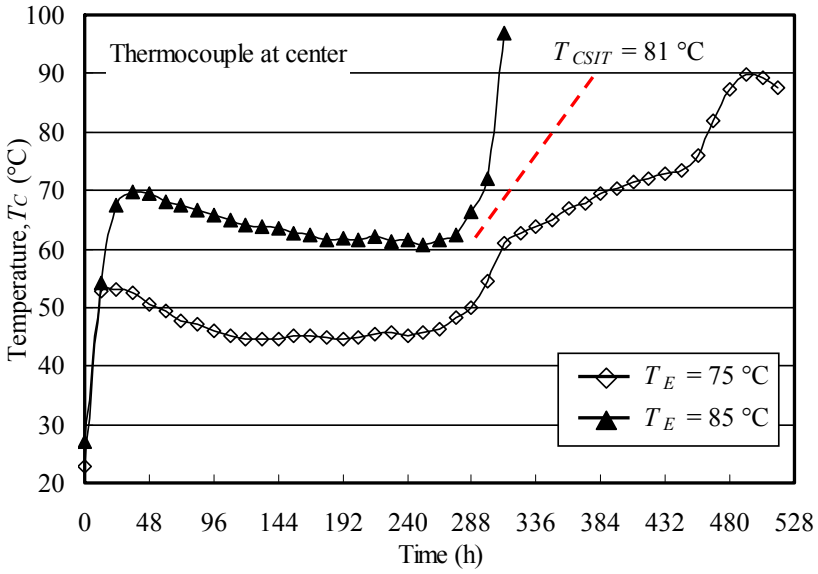

Figure 4- 18 Critical self-ignition temperature measured by center temperature (T_C) using the wire-mesh basket (L = 100cm)

Figure 4- 18 illustrates the critical self-ignition temperature range of 1m^3 coal pile. In this case, the value of 1m^3 coal pile critical self-ignition temperature is determined to be 81ºC (354 K).

By analyzing the three upscale results for different sizes and ambient-air

temperatures (H_0 = 25 cm, T_E = 110ºC); (H_0 = 50 cm T_E = 100ºC) and (H_0 = 100 cm, T_E = 85ºC), it can be summarized that the temperature rise curve can be divided into three stages. The first stage dominated thermal conduction; chemical reaction, thermal conductivity & moisture evaporation coexisted heat generation stage and heat conduction & self-heating reaction based accelerate or decline stage. It can be found that temperature drop in the heat generation stage in L = 25 cm test shows a different trend because of its smaller volume. The strong natural convection in chamber evaporated moisture of coal pile in a short time. Furthermore, the 110ºC ambient-air temperature is high enough to heat up water to steam. Based on these factors L = 25 cm wire-mesh basket showed an anomalous temperature rise in heat generation stage.

4.5 Evaluation of Critical Self-ignition Temperature for Upscale Stockpiles

The relationship of coal weight loss and the size of coal pile for ignition case are shown in Figure 4-19. The larger wire-mesh basket size the smaller weight loss ratio. By combining Figure 4-19 with measurement result of temperature for each size coal pile weight loss during the storage period can be evaluated for larger coal stock pile.

Based on the Frank-Kamenetskii's model, critical self-ignition temperature can be formulated from heat balance at the temperature between heat generation and heat loss rates of the coal pile. By plotting $\ln\left(\frac{\delta_c (T_{CSIT})^2}{r^2}\right)$ against $(T_{CSIT})^{-1}$, value of β and activation energy, E, can be obtained from the value of intercept and slope of the line from the semi-log, respectively. Finally, heat generating rate, Q, and critical self-ignition temperature or T_{CSIT} can be obtained as a function of r. It predicts *CSIT* for larger volume of coal piles.

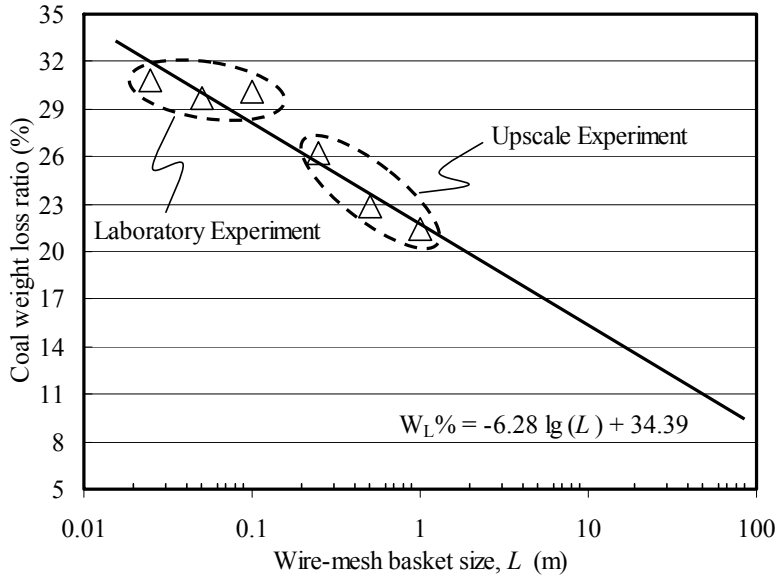

Figure 4- 19 Coal weight loss ratio of coal (W_L) versus size of wire-mesh basket

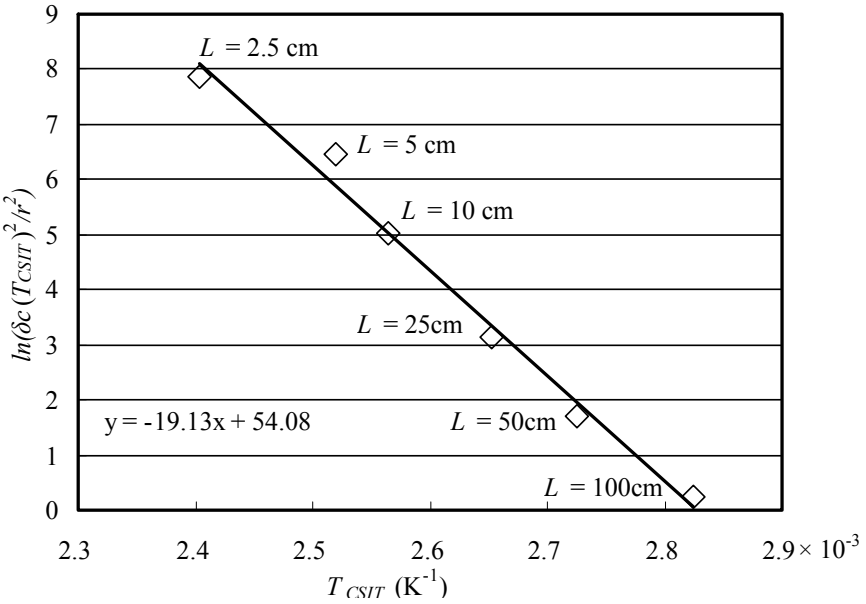

Figure 4- 20 Plotting $\ln\left(\delta_c (T_{CSIT})^2 / r^2\right)$ against $(T_{CSIT})^{-1}$ based on critical self-ignition temperature, $x = \dfrac{1000}{T_{CSIT}}$; $y = \ln\left(\dfrac{\delta_c (T_{CSIT})^2}{r^2}\right)$

By analyzing the coal inside temperature and application of Fourier equation boundary conditions the self-heating data of the coal can be calculated. As shown in Figure 4-20, the results shows that a distinct linear relationship exists between critical self-ignition temperature (*CSIT*) and wire-mesh basket size. The value of

CSIT was measured low for the large coal pile size and high for the small coal pile size. As shown in Figure 4-20, the relationship is formulated by Equation (4-1), which yields the activation energy is given by Equation (4-2).

$$\ln\left(\frac{\delta_c T_{CSIT}^2}{r^2}\right) = 67.90 - 1.913\times10^4 \frac{1}{T_{CSIT}} \tag{4-1}$$

$$E = 160\,\mathrm{kJ/mol} \tag{4-2}$$

Figure 4-21 shows the two lines on *CSIT* vs. pile volume that are formulated with the laboratory experiment and both test of laboratory and upscale, respectively. For 1m^3 basket, the *CSIT* of laboratory experiment prediction result is 2°C deviation to that by both tests. This means the methodology and theory used in the research are reliable and useful. As the test practical, the laboratory experiment can be to simulate *CSIT*.

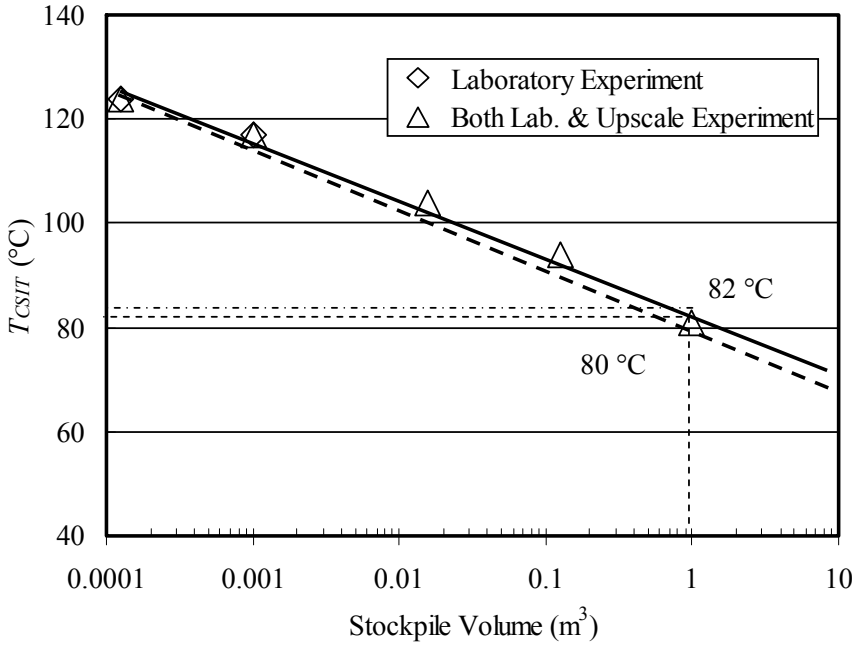

Figure 4- 21 *CSIT* vs. coal stockpile volume

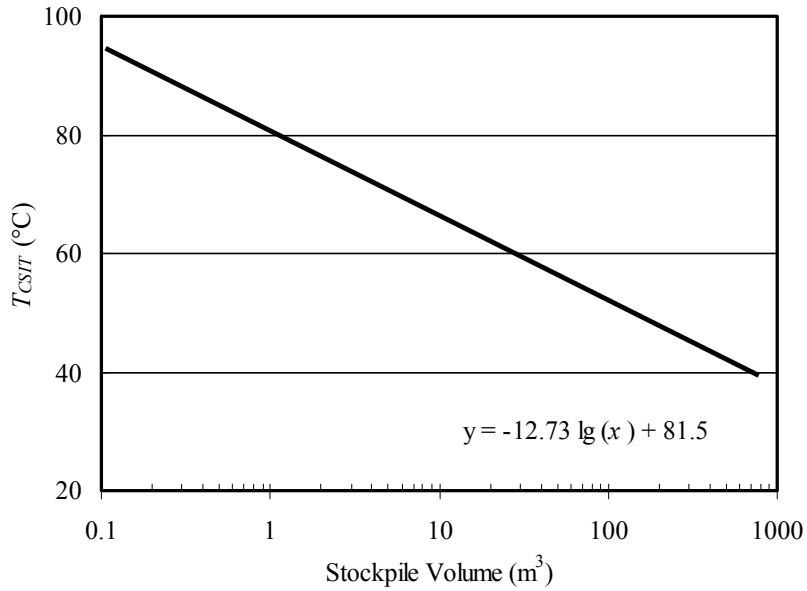

Figure 4- 22 Prediction of critical self-ignition temperature expanding to coal pile volume up to 1,000 m^3

The relation of

$$(T_{CSIT} - 273)\ °C = -12.73 \lg (x) + 81.5 \quad (4\text{-}3)$$

between critical self-ignition temperature (= (T_{CSIT} – 273) °C) and stockpile volume V has been obtained from Equations (4-1) and (4-2) for stockpile volumes extrapolated over $1m^3$ as shown in Figure 4-22. The critical self-ignition temperature decreases with stockpile volume, while the elapsed time to get to critical self-ignition temperature increases with stockpile volume. Thus, preserving a larger volume of coal stock has a larger possibility to induce spontaneous combustion, but it takes longer elapsed time to get it.

4.6 Conclusions

The critical self-ignition temperature (*CSIT*) of coal is important to evaluate the possibility of spontaneous combustion of coal stockpiles. In this chapter, based on results of the upscale experiments using the wire-mesh basket tests with

Frank-Kameneskii equation, the values of *CSIT* were evaluated for the coal sample UE.

The values of *CSIT* by the upscale experiments presented more reliable relationships between *CSIT* and pile size or volume for the coal sample UE, because it is expected to be able to apply it to larger coal stock pile used in coal industries. The activation energy of the UE sample was evaluated as about 200 kJ/mol.

Based on temperature-time curves, CO and CO_2 gas concentrations and decreasing height of the pile, the heating process observed in the upscale experiment was classified into three stages as initial preheating, heat generation and accelerate/decline stages. Moreover, coal pile weight loss ratio and size relationship was evaluated as $W_L\% = -6.28 \lg(L) + 34.39$, which indicates the moisture approximate loss from coal piles during the storage period.

The larger coal pile volume, the more possibility to induce spontaneous combustion of coal piles has. However, moisture has an important role on the self-heating process of the coal samples. The moisture make slow down the coal temperature rise due to latent heat to evaporate the moisture.

Based on the Frank-Kamenetskii equation, the equation shows *CSIT* as function of pile size or volume was presented to predict *CSIT* for larger stockpile volumes in order of 100 m^3.

Chapter 5: Preventing Spontaneous Combustion of Residual Coal in Goaf

5.1 Introduction

It is well known that the key area relating to underground coal mine fire is goaf areas because there is always a potential to induce spontaneous combustion of residual coal in it. According to the statistics of Chinese coal production, 90% of total coal production is underground mines. There are around 600 state-owned key coalmines of which 25.1% are highly gassy mines and 17% are gas out-burst mines, approximately. In Chinese underground coal mines, serious accidents have occurred especially in the last ten years. Since they produce a large amount of coal to meet domestic demand, the safety efforts are not sufficient. In particular, most of the accidents were directly or indirectly related to coal spontaneous combustion in goaf areas. In this chapter, a preventing method for spontaneous combustion of residual coal at a goaf in coal mine based on critical self-ignition temperature theory has been developed.

In spontaneous combustion zone the airflow velocity is very small always less than 0.24 m/min (Qi et al., 2009). It is useful to divide the goaf area into different parts based on the distribution of O_2 and CO concentration for studying the coal spontaneous combustion. Pan et al. (2013) classified the goaf area to radiating and asphyxiation zones by O_2 concentrations larger than 18% and less than 7%, respectively.

O_2 participated in chemical reaction in goaf area comes from working faces and other areas' air leakage. If the residual coal in appropriate environment can easier to generate heat it has a higher potential of spontaneous combustion. The reaction inside coal mainly accompanies heat generation, if the heat is higher than the coal's activation energy, self-ignition will start. How to enlarge the coal activation energy

and how to decrease the air leakage are the main challenges to prevent the goaf residual coal spontaneous combustion.

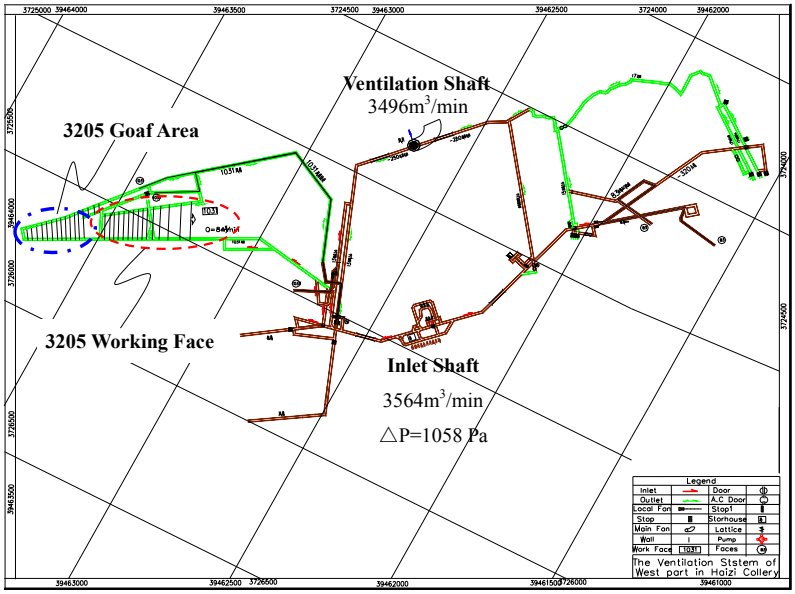

Figure 5- 1 Plan of mining in Haizi coal mine

As shown in Figure 5-1, the Haizi coal mine area is nearly 6.44 km^2 consisting of 1,200 to 5,200 m along the strike and 0 to 1,700 m in tendency. Its coal seams are cleft by three normal faults that formed an isolated blocked area like a triangle coal-bearing zone. The current level operation working faces are located -320m from the surface. Average self-ignition point of the produced lignite coal is 275 °C. And the elapsed time after contacting air to spontaneous combustion in a pail has been estimated to be roughly 1 to 1.5 month. Based on the mine operation record data, spontaneous combustion phenomenon has been frequently observed at working faces during 2002 to 2013.

The first step of this study was to analyze ventilation network airflows in the mine using the simulator MIVENA (Sasaki et al., 2002), especially pressure drop at a working face was studied to control leakage airflow into a goaf area. The FLUENT was also used to simulate leakage flow in the goaf area with comparing monitoring data by the tube bundle gas monitoring system. Finally the effectiveness of slurry

grout injection into the goaf area has been investigated to change the coal average activation energy as an economical method to prevent spontaneous combustion of residual coal in the goaf.

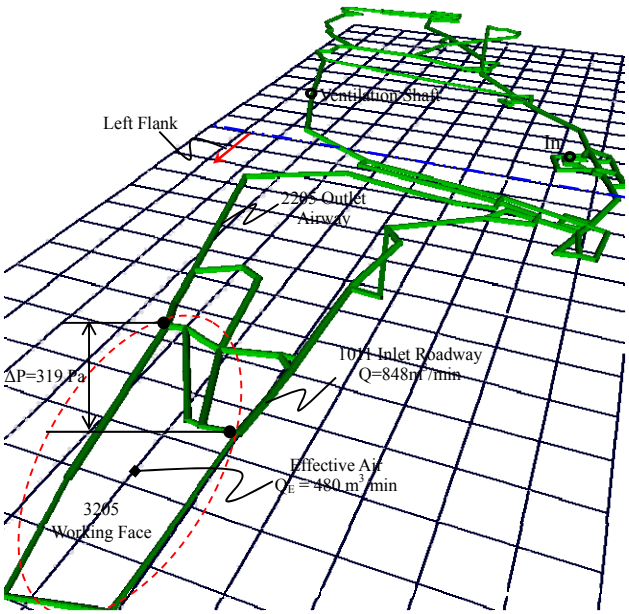

Figure 5- 2 Three Dimensional network airways diagram provided by the MIVENA system

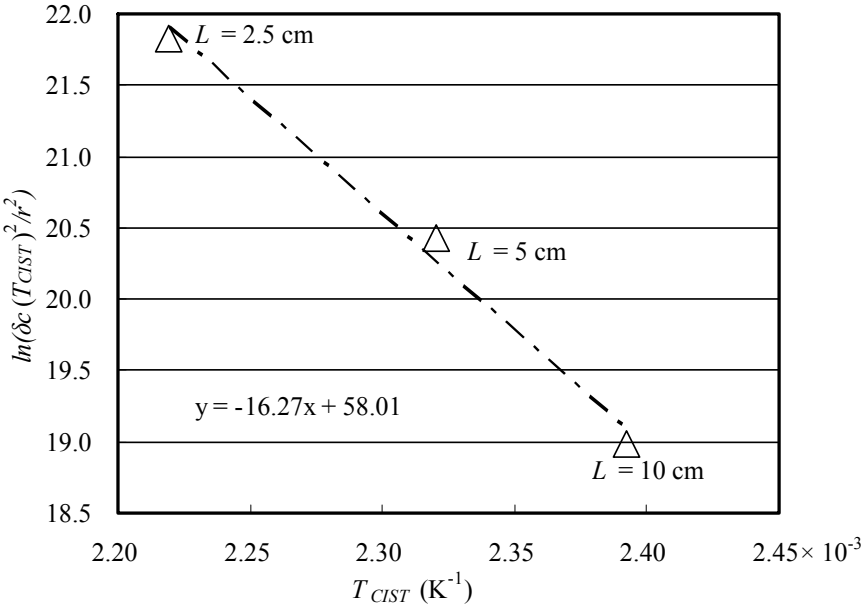

Figure 5- 3 Plotting $\ln\left(\delta_c (T_{CSIT})^2 / r^2\right)$ against $(T_{CSIT})^{-1}$ based on critical self-ignition temperature, $x = \dfrac{1000}{T_{CSIT}}$; $y = \ln\left(\dfrac{\delta_c (T_{CSIT})^2}{r^2}\right)$

5.2 Coal Properties

The characteristics of Haizi coal mine sample are listed in Table 5-1. The coal was crushed into the average size of 0.48 mm. The coal piles were formed by filling them in the three different sized of wire-mesh baskets to test the critical self-igniting temperature in the laboratory.

Table 5- 1 Density, specific heat capacity and proximate analyses of coal sample

NE	Density ρ(g/cm^3)	Heat Capacity *Cp* (kJ/kg/°C)	Fixed Carbon (%)	Ash (%)	Volatile Matter (%)	Moisture (%)
Lignite	1.290	2.181	54.0	6.98	33.62	5.53

By using the test result $\ln\left(\delta_c (T_{CSIT})^2 / r^2\right)$ against $(T_{CSIT})^{-1}$ was plotted as Figure 5-3 shows. So the coal sample activation energy (E) can be calculated.

$$\ln\left(\frac{\delta_c T_{CSIT}^2}{r^2}\right) = 58.01 - 1.627\times10^4 \frac{1}{T_{CSIT}};\quad E = 135.2\,\text{kJ/mol} \tag{5-1}$$

As mentioned in chapter 2, coal critical self-ignition temperature (*CSIT*) is mainly affected by the coal pile volume (V) and thermal diffusivity (α) of sample. Coal thermal conductivity is depended on coal porosity, ε, and specific internal surface in it (Sasaki et al., 2011). The effective thermal conductivity (λ) of residual coal was defined as, $\lambda = \lambda coal\ (1-\varepsilon) + \varepsilon\lambda air$, and volumetric heat capacity, ρCp, and thermal diffusivity can be rewritten as

$$\rho Cp = \xi\rho_{air} Cp_{air} + (1-\xi)\rho_{coal} Cp_{coal},\quad \alpha = \lambda/\rho Cp \tag{5-2}$$

According to the Equation 5-2, it can be concluded that the goaf residual coal critical self-ignition temperature (*CSIT*) is affected by coal thermal diffusivity and coal porosity.

5.3 Mine Ventilation Network Analysis and Goaf Area Three Zones

The centralized ventilation system is used with a main intake shaft for fresh ventilation air and an exhausting shaft utilized only for exhausting airflow in the coal mine. The total intake airflow $Q = 3564 m^3/min$ operated by total pressure loss of $\Delta P =$ 1058Pa.

Especially, the airflow around the #3205 working face, that is a fully-mechanized coal cutting faces, was focused by changing conditions with working face operation. After that, simulated data was used to control airflows in the working face considering whole ventilation airflows in the network.

Based on the Chinese safety regulations (State Administration of Coalmine Safety, China, 2011) for coal mine ventilation, airflow velocity must satisfy the range of 0.25 m/s to 4m/s. Herein, the coal mine's evaluated air quantity through the goaf was 480 m^3/min that meets the regulation mentioned above, because the air leakage was estimated as $368 m^3/min$ (see Figure 5-2).

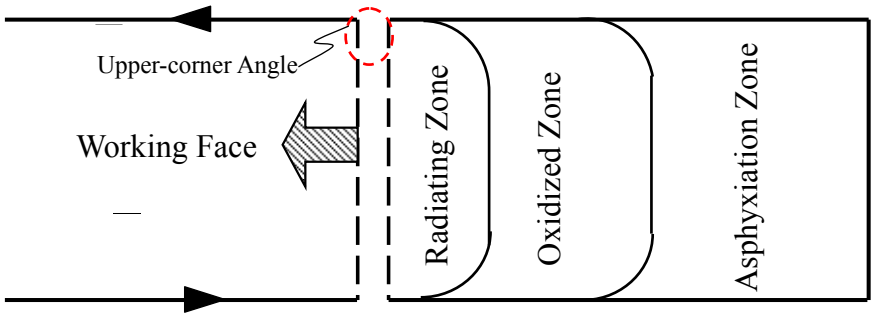

Figure 5- 4 Schematic of three zones in the goaf

Table 5- 2 Chinese safety standards for divided goaf zones

Zone	Oxygen concentration	Airflow velocity	Temperature Gradient $d\theta/dt$
Radiating	—	$v > 0.02$m/s	—
Oxidized	$O_2 \geq 8\%$	$0.02\text{m/s} \geq v \geq 0.001\text{m/s}$	$d\theta/dt > 1$°C/day
Asphyxiation	$O_2 < 8\%$	$v < 0.001$m/s	—

Goaf area is changing with the moving of working face. Air leakage at the working faces supplies oxygen to the residual coal in the goaf area and coal seams close to the goaf, and it may lead to coal spontaneous combustion in the goaf area which can be classified into three zones as radiating zone, oxidized zone and asphyxiation zone as shown in Figure 5-4 (Qin et al., 2009; Wu et al., 2011; He et al., 2008; Mu, 2013; Sasaki et al., 2011). As experiment and analysis result shows, oxidized zone has high potential to generate starting heat for self-ignition (He et al., 2008). These three zones can be characterized by flow velocity of air leakage (V), oxygen concentration in the goaf area and rate of temperature rise that are evaluated by the method defined in the Coal Mine Safety Regulation of China as shown in Table 5-1.

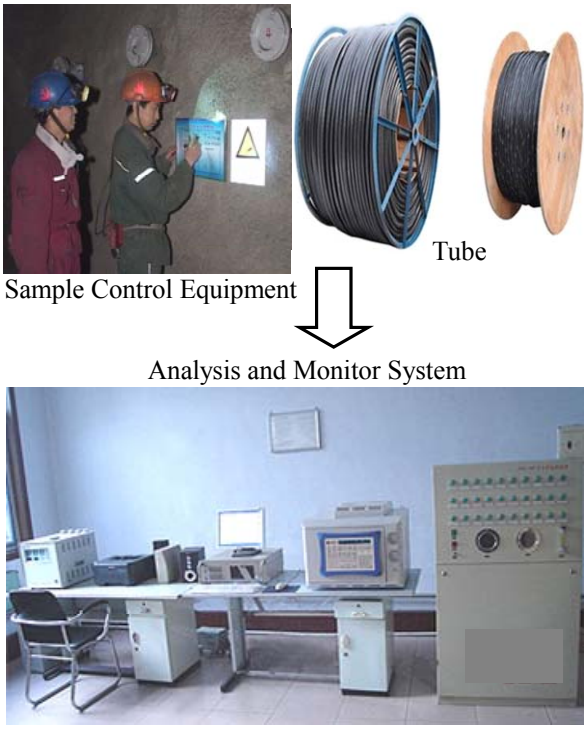

Figure 5- 5 The tube bundle gas monitoring system for goaf area in the coal mine (Dec. 2013)

5.4 Oxidized Zone Border Demarcation in Goaf Area

5.4.1 Oxygen concentration detection in goaf

The tube bundle gas monitoring system (Figure 5- 5) has been used to monitor the coal spontaneous combustion process in the goaf, continuously. It can detect the early stage coal spontaneous combustion based on monitoring oxidation products, such as CO, and then make an alarm to the mine engineers (Nordon 1979; Weishauptovü et al., 1998; Alexeev et al., 2004). Numerous gas contents, such as O_2, N_2, CO, CH_4, CO_2, C_2H_4, C_2H_6 etc., are measured to detect the spontaneous combustion of coal at the monitoring spot. Gas concentration changes and distribution in the goaf area were used to divide it into three zones, and discuss its pros and cons for controlling the spontaneous combustion of coal (Li et al., 2009).

About 50 gas monitor points were installed, especially in the goaf areas by the monitoring system shown in Figure 5-6. The measurement used continuous monitoring of gas compositions in three months to pick up data detecting spontaneous combustion.

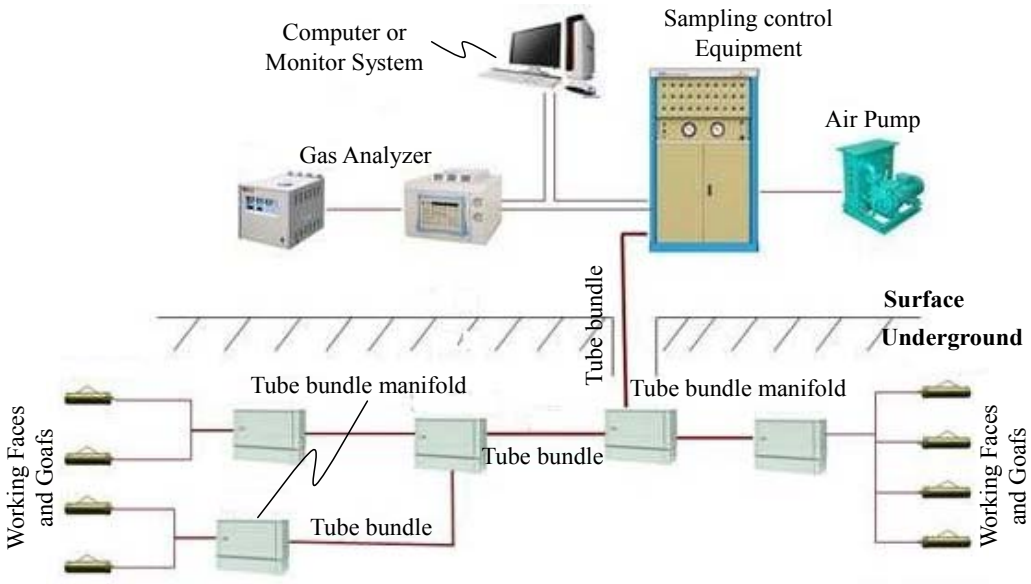

Figure 5- 6 Schematic of the tube bundle gas monitoring system

The measured oxygen concentration distribution in the goaf area is shown in

Figure 5- 7 in which the horizontal axis is the distance along the #3205 working face from its upstream corner and the vertical axis is distance from working face in the goaf. The contour lines of oxygen concentration were drawn by cubic spline function fitting the limited monitoring data (around 30). There was a relatively higher temperature range in the goaf area where O_2 concentration was over 10% compared with others in which oxygen concentration still not goes up to this level. Therefore, the goaf area can be divided into two zones by considering the contour line of 10% concentration of oxygen. The determination of boundary line between the oxidized and asphyxiation zones in the goaf was relatively easy using the oxygen concentration curves, while the radiating zone boundary demarcation was difficult due to high oxygen concentration range close to 21% of air. The oxidized zone which O_2 concentration is over 10% shows a potential zone in which spontaneous combustion can be started in a few days, however, the other zones showed a stable condition in terms of the temperature.

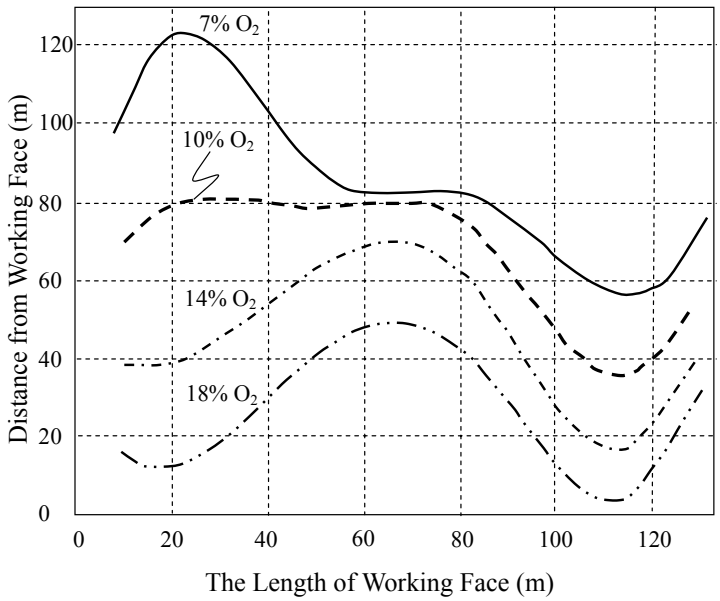

Figure 5- 7 Distribution of oxygen concentration in #3205 goaf area (by Measurement, Dec. 2013)

5.4.2 Goaf air flow simulation

As described in previous chapter, the radiating zone boundary is difficult to determine by using the oxygen distribution curve. In this research, the numerical simulation by FLUENT (Li et al., 2007) was taken into account to define the boundary.

FLUENT presents a 2-dimensional numerical simulation model in which the goaf was assumed as a zone of porous media composed of collapsed rock and un-mined coal, and uniform permeability was given for the goaf area based on the measured data (Gao et al., 2010). The goaf average porosity was set as 0.3 according to the empirical formula and measurement data (Ren et al., 2013). On the other hand, oxygen concentration of 10%O_2 was used for compacted area based on the gas monitoring data recorded by the tube bundle system. The airflow is leaked through a working face into goaf area (Zhao et al., 2008). Furthermore, airflow in the goaf was treated as laminar flow expressed by Darcy's law (Lan, 2007). Based on the monitoring data, the numerical simulation results by the ventilation simulator MIVENA, inlet airflow and its velocity into the #3205 face were evaluated as 852 m^3/min and 1.3 m/s, respectively. Meanwhile, the differential pressure along the working face was simulated as 319 Pa (see Figure 5-2).

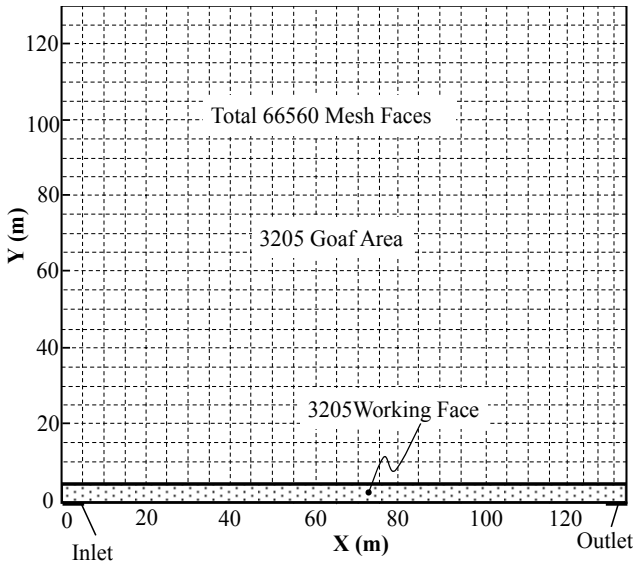

Figure 5- 8 Gird block model of analysis area and definition of coordinate (*X,Y*) (by Gambit)

The numerical simulations on airflow leakage distribution in goaf area were carried out using with the above airflow conditions by the FULENT using the grid block size of 0.5 m × 0.5 m as showed in Figure 5-8.

In the monitoring result shown in Figure 5-7, the area where air leakage velocity is over 0.001 m/s corresponding to 7% O_2 is located 97 m away from the #1011 inlet roadway and #2205 outlet airway, while this area was 79 m away from the middle of #3205 working face. The oxidation zone boundary is located at 74 to 92 m far from the working face.

Goaf area was assumed as a continuous porous media. According to oxygen concentration and the air leakage condition, flow energy and concentration equations in the goaf can be expressed as (Pan et al., 2013)

$$\begin{cases} C_g\left(\dfrac{\partial}{\partial X}(ut)+\dfrac{\partial}{\partial Y}(vt)\right)=\lambda\left(\dfrac{\partial^2 v}{\partial X^2}+\dfrac{\partial^2 v}{\partial Y^2}\right)+\dfrac{(b_2+b_1\beta)w(O_2)}{H} \\ \dfrac{\partial}{\partial X}(uc)+\dfrac{\partial}{\partial Y}(vc)=D\left(\dfrac{\partial^2 c}{\partial X^2}+\dfrac{\partial^2 c}{\partial Y^2}\right)+W \end{cases} \tag{5-3}$$

where,

u: X direction speed, (m/s);

v: Y direction speed, (m/s);

b_1: Heat producted by chemical reaction, (J/kg);

b_2: Heat adsorbed by chemical reaction, (J/kg);

β: Consumed oxygen, (mol/m^3);

H: The width of working face, (m);

C_g: The equivalent specific heat capacity of gas in goaf, (kJ/kg/°C);

λ: Effective thermal conductivity of porous media, (W/(m·K));

W: The source term of O_2 and CO concentrations (mol/m^3).

The coal in goaf area starts self-heating by oxidation. CO was generated by the chemical reaction. The O_2 and CO reaction equations are as shown in Equation (5-4)

$$\begin{cases} W_{O_2} = -\left(\dfrac{r_0 H_1 c(O_2)}{c(O_2)_0} + \dfrac{nHW_{CH_4}}{c - c(O_2)} \right) \dfrac{c(O_2)}{H} \\ W_{CO} = 2\beta W_{O_2} - \dfrac{1}{H} W_1 c(CO) \end{cases} \tag{5-4}$$

where,

W_{O_2} : The source term equation for O_2;

W_{CO}: The source term equation for CO;

W_{CH4}: The source term equation for CO;

r_0: Oxygen consumption speed of losse coal in standard air, (mol/m^{3}h);

$C(O_2)_0$: The standard O_2 concentration in air, (mol/m^3);

n: The probability of interval in goaf, (n = 1.5);

W_1: CO adsorption intensity in goaf, (mol/m^{3}h).

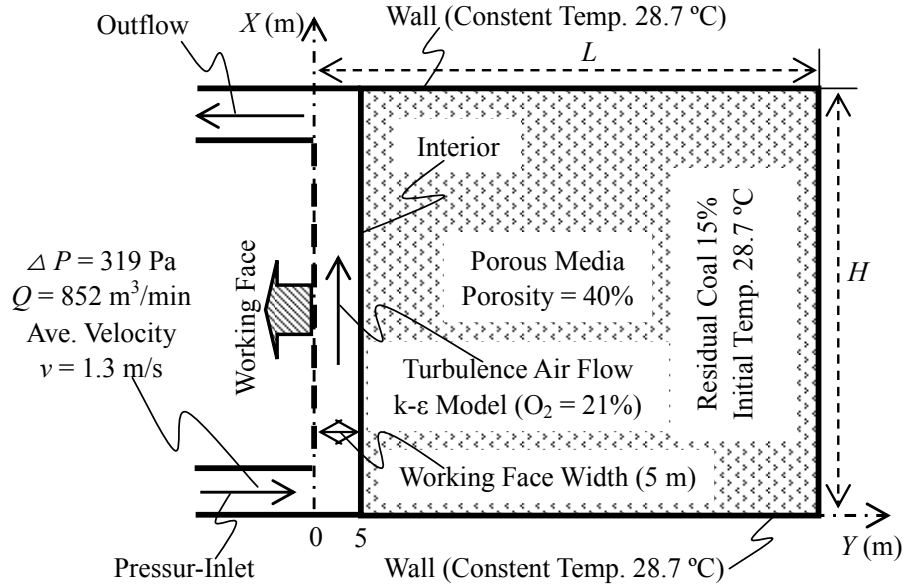

Figure 5- 9 Numerical model of goaf area and boundary conditions for FLUENT simulations

H: The width of working face (m); L: The length of goaf (m)

As shown in Figure 5-9, airflow along the working face was treated as turbulent flow, because airflow velocity and airway size are large enough. In the FULENT, the standard κ-ε model was chosen to simulate the airflow in the working face. The boundary conditions were assumed in the numerical model was shown in Figure 5-9.

In this case, the boundary conditions in the model are given as follows;

(a) $X = 0$, $Y = 0 \sim L$; wall boundary, constant temperature 28.7 ºC

(b) $X = H$, $Y = 0 \sim L$; wall boundary, constant temperature 28.7 ºC

(c) $X = 0 \sim H$, $Y = L$; wall boundary, $\frac{\partial u}{\partial X} = 0; \frac{\partial v}{\partial Y} = 0$, $O_2\% \approx 0\ \%$

(d) $X = 0 \sim H$, $Y = 5$; interior, pressure boundary, $\Delta P = 319$ Pa

(e) $X = 0 \sim H$, $Y = 0 \sim 5$; porous media, porosity = 100 %, $O_2\% = 21\ \%$

(f) $X = 0 \sim H$, $Y = 5 \sim L$; porous media, porosity = 40%, initial temp.= 28.7 ºC

(g) Pressure-Inlet; $Q = 852$ m^3/min, $v = 1.3$ m/s

5.4.3 Simulation results and analysis

Figure 5-10 shows the simulation result of the airflow velocity distribution in the goaf along the #3205 working face. The flow quantity of air leakage into the goaf is increasing with the pressure drop along the working face. Thus, controlling airflow in the working face can reduce air leakage which can provide oxygen to residual coal reaction in goaf.

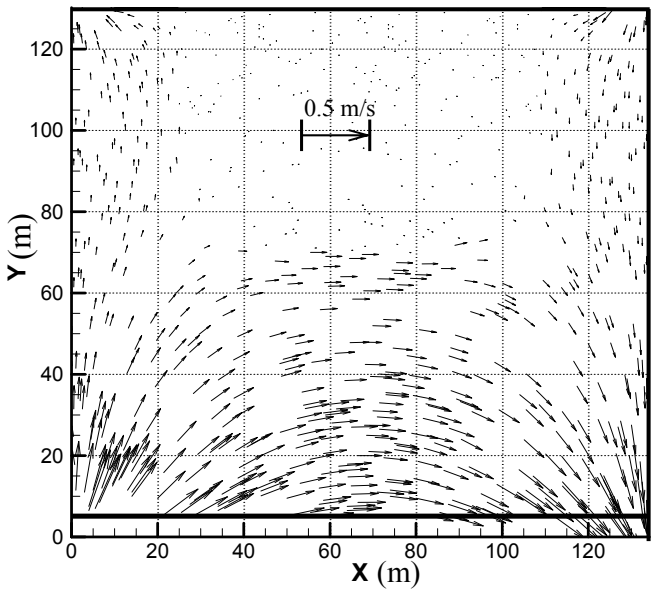

Figure 5- 10 Air leakage flow velocity vector in goaf simulated by FLUENT

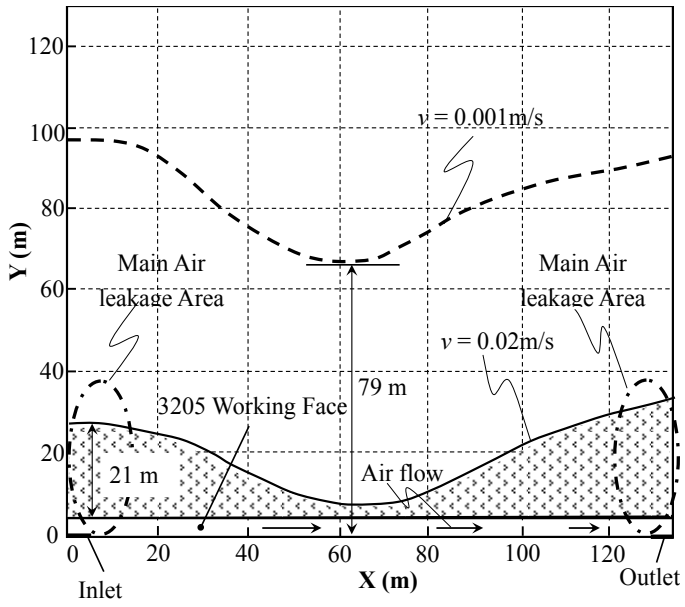

Figure 5- 11 Contour lines of air leakage velocity in a goaf (unit: m/sec) simulated by FLUENT

As shown in Figure 5-11, air leakage is observed at the zone located 20 m away from the #3205 working face. And velocity is reduced with increasing distance from the 3205 working face. The working face 134 m in length was modeled between #1011 inlet and #2205 outlet airways. The position showing the minimum airflow leakage velocity of 0.001 m/s is located at the middle of #3205 working face. Figure

5-10 also indicates a larger amount of air leakage and higher velocity at inlet and exhaust ends in the #3205 working face. The air leakage velocity equals to 1.2 m/min (= 0.02 m/s) at the position 26 m away from the #1011 inlet roadway and #2205 outlet airway corners and 10 m far from the #3205 working face.

The calculated width of oxidized zone boundary in the #3205 working face is approximately 5 to 21 m. Then, according to the oxygen concentration curves in goaf presented in Figure 5-7, the air leakage velocity of 0.001 m/s shows approximately 7% O_2. The deep oxidation zone boundary is located at 74 to 92 m far from the #3205 working face. Figure 5-12 shows that the farthest boundary of the oxidation zone with 10% O_2 is located at the area 80m away from the #3205 working face. However, the nearest one, which next to the radiating zone is about 30 m far from the #3205 working face. By drawing the boundary lines, it is clear that the width of oxidation zone becomes narrower with increasing distance from both ends of the working face. After deciding the oxidation zone area, appropriate methods should be applied in order to change the residual coal activation energy and porosity to prevent the coal spontaneous combustion in it (see Figure 5-13).

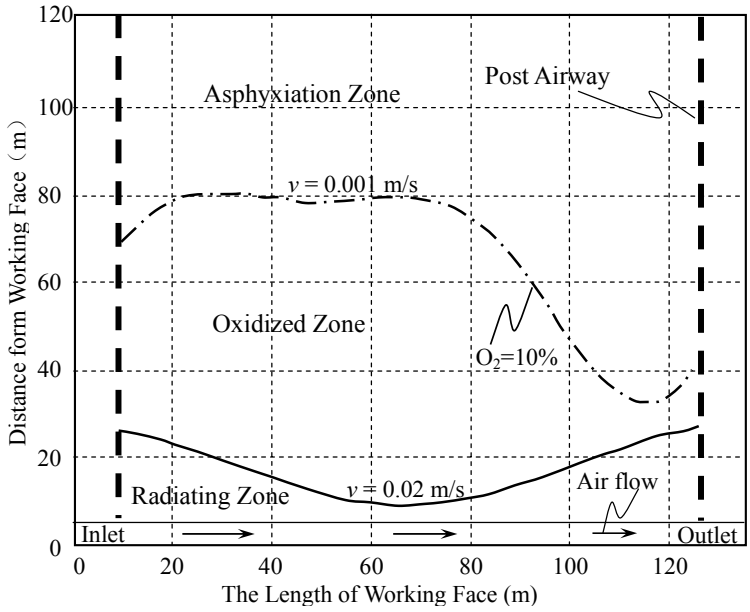

Figure 5- 12 Schematic of “Three zones” in goaf area

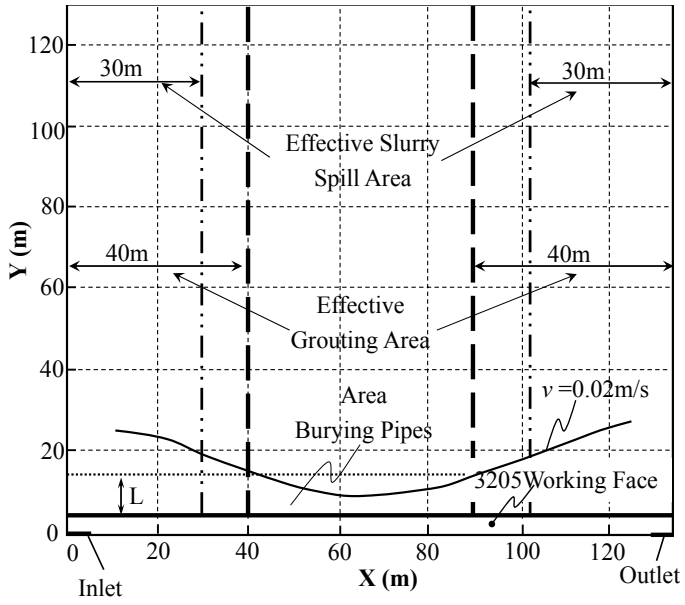

Figure 5- 13 Grouting area and pipe bury diagram

5.5 Preventing Method for Goaf Fire

5.5.1 Injecting grouting slurry into goaf area

The grouting filling method using pulp slurry was chosen as the best method to prevent spontaneous combustion of residual coal in the goaf area. The slurry grouting in the goaf especially in oxidation zone area can reduce the goaf area porosity. Low porosity has a smaller O_2 concentration, which promotes a weak chemical reaction. On the other hand, slurry mixed with residual coal has a lower thermal conductivity and higher average activation energy. Such feedbacks between a narrow oxidation zone and less O_2 concentration can lead to a higher coal critical self-ignition temperature.

In the grouting filling system, the pulp slurry was transferred by natural hydraulic head between the surface and goafs. The slurry pool of 200 m^3 in volume was constructed on the level +32.7m. The pipes to transport the slurry were vinyl tubes of 2.5 inches in diameter. Total length of the slurry pipeline is Lp = 1994 m and the vertical level difference is Hp = 330.7 m, thus the slurry line coefficient is

given by $Np = Lp / Hp = 6.03$.

The goaf area was filled with grouting slurry to prevent the coal spontaneous combustion of residual coal by installing the pipe end at the position 40 m away from both ends of the #3205 working face (see Figure 5-13). And the distance between the filling area and the working face was controlled to be longer than 10 m, because grouting slurry moved 15 to 20 m toward the working face. When a spontaneous combustion is found in the goaf, the working face and goaf area must be spilled with slurry immediately. To operate grouting slurry to be effective, the required amount of solid pulp is given by

$$Q = KmLHC \tag{5-5}$$

where,

Q : Amount of solid pulp (m^3);
m : Coal seam thickness (m = 4.36m);
L : Grouting zone strike length (L =1058m);
C: Coal recovery ratio, 86%;
H: Grouting zone inclination length (H =133.7m);
K: Krouting coefficient (generally 0.1 to 0.5), (K= 0.3).

Also based on the regulation, the required amount of water is given by

$$Q_w = K_w Q\delta \tag{5-6}$$

where,

Qw: Amount of water, (m^3);
Kw: Coefficient of water reserve (= 1.10 to 1.25);
δ: Water and soil ratio (= 2 to 5, average ≈ 3).

The amount of solid pulp for the goaf area was roughly calculated from Equation (5-5) as

$Q = 0.3 \times 4.36 \times 1058 \times 133.7 \times 0.86 = 159{,}100\ (m^3)$

By substituting above values into Equation (5-6), the amount of water, *Qw*, was also calculated from Equation (5-6) as

$Q_w = 1.2 \times 159{,}000 \times 3 = 577{,}600\ (m^3)$

Thus, total amount of grouting slurry was calculated as;

$Q_T = Q + Q_w = 736{,}700\ (m^3)$

5.5.2 Grouting simulation result verification

Figure 5-14 shows the numerical simulation result of velocity contour lines after filling with the grouting slurry by FLUENT. When the goaf is assumed to be filled uniformly with grouting slurry, the oxidation zone exists only in a very small area just behind the #3205 working face. This result shows that the slurry grouting is a useful and effective method to prevent the coal spontaneous combustion in the goaf. The area of oxidation zone is affected by porosity in the goaf area. Figure 5-15 shows the numerical simulation result of the relationship between the area of oxidation zone and goaf porosity. The area increases exponentially with increasing goaf porosity. It shows that filling mined-out goaf area after coal cutting by grouting slurry reduced the area of oxidation zone and decreases the risk of spontaneous combustion of residual coal in goaf areas. It is also expected that reducing air leakage from the working face by controlling ventilation pressure and airflow rate is effective to prevent spontaneous combustion.

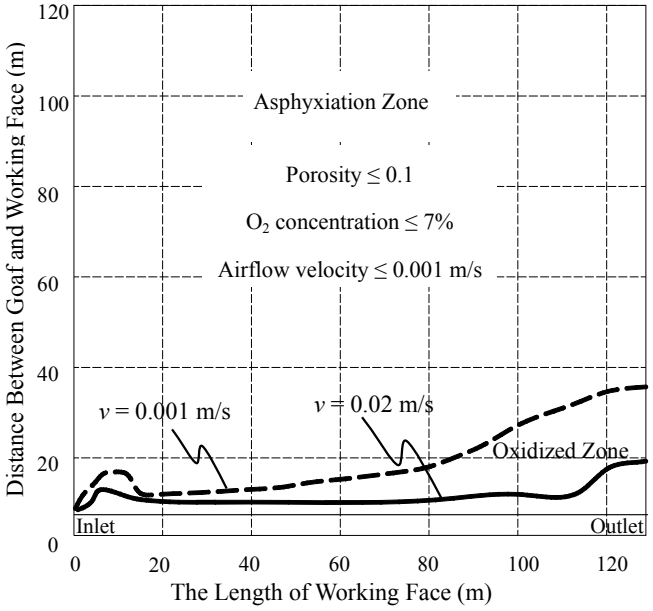

Figure 5- 14 Contour lines of air leakage velocity after grouting slurry (goaf porosity is 0.1)

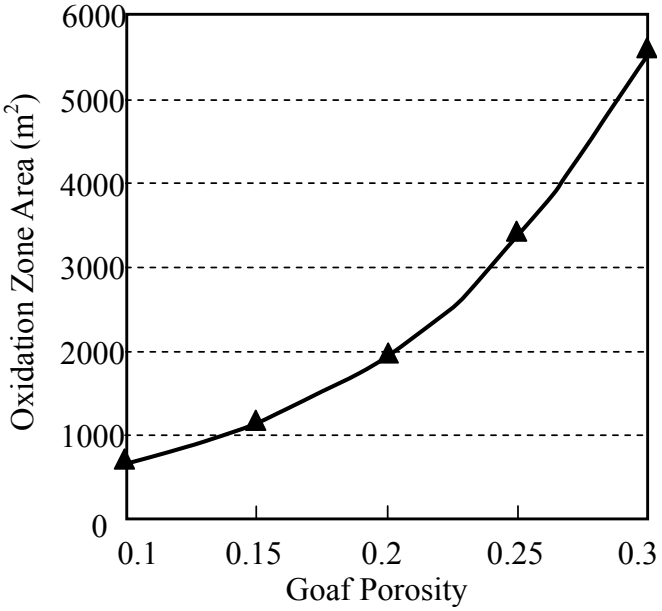

Figure 5- 15 Area of oxidation zone vs. goaf porosity

5.6 Conclusions

In this chapter, an effective and economical method to prevent spontaneous combustion of residual coal in a goaf area was investigated based on experimental proved critical self-ignition temperature theory and numerical predictions of

MIVENA and FLUENT. The characteristics of oxidation and temperature rising in the goaf area in the coal mine have been studied by combining the tube bundle gas monitoring results and numerical simulation results. Furthermore, dividing the goaf area into three zones, that are radiating, oxidized and asphyxiation zones, were discussed in considerations of spontaneous combustion of residual coal. After deciding the oxidation zone area, injecting grouting slurry method was used to change the residual coal activation energy and porosity to prevent the coal spontaneous combustion. The slurry grouting in the goaf especially in oxidation zone area reduces the goaf area porosity and coal thermal conductivity improves that can lead to self-ignition. It was proved that filling porosity in the goaf area by injecting grouting slurry has a function of preventing the coal spontaneous combustion of residual coal in the goaf area.

Chapter 6 : Conclusions

Spontaneous combustion of low rank coal, such as lignite, is a naturally occurring process caused by the oxidation during coal mining, transportation and piling. Because low rank coal has huge reserves in the world and it is expected to be one of future energies, there still need more researches on self-heating and spontaneous combustion to produce, store and transport it safely. The coal pile self-ignition is mainly dominated by its volume through its. It has been required to a carry upscale experiment using a pile volume in 1 m^3 order, because the pile volume is a major parameter to induce spontaneous combustion. Based on Frank-Kamenetskii (F-K) equation formulated from applying Arrhenius equation and heat conduction law, the laboratory and upscale experiments by wire-mesh basket tests were used to analyze the values of *CSIT*. The conclusions of this dissertation are as follows.

The coal pile volume and coal thermal diffusivity affect the *CSIT* of coal piles the volume has a dominated effect on it. Moreover, natural air convection induced by temperature difference between out and inside of the pile is another minor phenomenon that affects the temperature rising over *CSIT*. On the other hand, the laboratory and upscale experiments setting approximately the same coal size ratio (S_C / L) is expected to make the similar reaction. Thus, *CSIT* can be treated together both laboratory and upscale with neglecting the value of L.

In the laboratory experiment using the wire-mesh baskets (2.5, 5 and 10 cm in length) by the wire-mesh basket test, four lignite samples named as LE-1, LE-2, NE, and UE and one sub-bituminous coal named SE were pulverized with the average of 0.48 mm in size were tested in hot ambient air at atmospheric to estimate *CSIT*. By measuring the center temperature-time curves of coal samples from room temperature to the ambient temperature (140°C) step by step with temperature gradient of 10°C/hour to evaluate the *CSIT*. The sample LE-1 showed faster

temperature rise than other samples due to higher thermal conductivity in the pile. LE-2 was delayed to get to the environmental ambient air temperature (T_E). Based on the center temperature-time curves of three cubic piles 2.5, 5.0 and 10cm in size, values of *CSIT* for LE-1 were obtained as 143, 124 and 117 ºC, respectively. The equation of *CSIT* vs. pile size depends on coal properties such as activation energy and moisture content.

The results of upscale experiments using the wire-mesh baskets (25, 50 and 100 cm) proved that upscale experiment for *CSIT* is reliable more than laboratory experiments. The reductions of coal pile height or volume were also measured to analyze characteristic diversification of the coal piles. Based on recorded data on temperature and CO, CO_2 and HC gas concentration in the upscale experiment, it was confirms that the thermal process of self-heating consists three stages named as initial, heat generation and accelerate/decline stages. Moreover, the relation between coal pile weight loss ratio and pile size relationship was evaluated as $W_L\% = -6.28 \lg(L) + 34.39$ for UE. The moisture evaporation makes slow down of the coal temperature rising in the early stage. The larger of coal piles volume, the more serious impact on temperature-time curve. Coal pile test results were used to evaluate *CSIT* of the coal samples with a function of stockpile volume. It was found that the value of *CSIT* is reliable by the upscale experiment using the wire-mesh basket $1m^3$ in volume to extrapolate that of industrial coal stockpile with volume less than 1,000 m^3. Moisture has an important role on the self-heating process especially in low rank coal.

Based on F-K equation, the value of *CSIT* was applied to the numerical simulation using simulator MIVENA and FLUENT on spontaneous combustion in a goaf area at an underground coal mine to avoid fire from residual coals. Based on the simulation results and data measured by a tube-bundle system, the goaf area can be classified into three zone on O_2 concentration. Grouting filling method was

evaluated to prevent the goaf residual coal spontaneous combustion. The slurry grouting especially into the oxidation zone area reduced the goaf area porosity from 0.4 to 0.1. Measurement results of oxygen concentration using tube-bundle system proved that filling porosity in the goaf area with injecting grouting slurry is effective and economical to prevent spontaneous combustion in the goaf area.

REFERENCES

D. Frank-Kamenetzkii, Wärme- und Stoffübertragung in der chemischen Kinetik (in German), Springer Verlag: Berlin, 1959.

H. Münzner, W. Peters, Zur kinetic der kohlenoxydation im temperaturbereich 30 – 100°C, *Brenstoff-Chemie,* Vol. 12(46), 1965.

P. Gray and P. Lee, Thermal explosion theory, Oxidation and Combustion Reviews (ed: CFH Tipper), Elsevier: Amsterdam, vol. 21, 1967.

H. Münzner, Der Einfluss von fremdstoffen auf das selbstentzündungs verhalten von steinkohle, *Glückauf-Forschungshefte*, pp. 42-44, 1972.

P. Norder, A model for the self-heating reaction of coal and char, *Fuel*, vol. 58, pp.456-464, 1979.

H. Miyakoshi, T. Isobe, and K. Ostsuka, Relationship between oxygen adsorption and physico-chemical properties of coal, *Journal of MMIJ,* vol. 100-1161, pp. 1057-1062, 1984.

J. Cox, C. Nelson, Coal weathering: causes, effects and implications, *Chemistry Society, Division Fuel Chemistry,* Vol. 29(1), 1984.

P. Bowes, Self-heating: evaluating and controlling the hazards, H.M.S.O.: London, 1984.

K. Brooks, D. Glasser, A simplified model of spontaneous combustion in coal stockpiles, *Fuel*, vol. 65, pp. 1035-1041, 1986.

D. Schmal, A model for the spontaneous heating of stored coal. PhD thesis, University of Delft, 1987.

K. Laidler, Chemical Kinetics,Third Edition, Harper & Row, pp. 42, 1987.

K. Brooks, S. Bradshaw, D. Glasser, Spontaneous combustion of coal stock piles. An usual chemical reaction engineering problem, *Chemical Engineering Science,* vol.43, 1988.

S. Bradshaw, D. Glasser, K. Brooks, Self-ignition and convection patterns in an infinite coal, *Chemical Engineering Communications*, vol.105, 1991.

D. Thomas, A. Tytko, M. Mulligan, P. Green, The effect of oxidation on the thermoplastic and cooking properties of coal at elevated pressures, *Fuel,* vol. 71 (2) pp. 169, 1992.

S. Pisupati, A. Scaroni, Effects of natural weathering and low temperature oxidation on some aspects of the combustion behaviour of bituminous coals, *Fuel*, vol. 72(6), pp. 779, 1993.

J. Riley, J. Reasoner, S. Fatemi, and G. Yates, Self-heating of coal in barges, *No Name*, pp. 162-167, 1996.

S. Krishnaswamy, P. Agarwal, R. Gunn, Low-temperature oxidation of coal: 3. Modelling spontaneous combustion in coal stockpiles, *Fuel*, vol. 75 (3), 1996.

State Administration of Coalmine Safety, China, Technical Specification of Fire Fighting by Grouting in Coal Mines MT/T 702—1997, Standards Press of China, Beijing, 1998.

S. Yang, R. Zhang, Z. Di, Mechanism analysis of coal spontaneous combustion and flame retard of conventional fire preventing and extinguishing measures, *Journal of China Coal Society*, vol. 23(6), pp. 576-580, 1998.

Z. Weishauptovü, J. Medek, Bound forms of methane in the porous system of coal,

Fuel, vol. 77, pp. 71-76, 1998.

J. Deng, J. Xu, Y. Zang, L. Li, Experimental and numerical analysis on the shortest spontaneous combustion period of coal, *Journal of China Coal Society*, vol. 3, pp. 69-75, 1999.

J. Golas and J. Needham, Science and Civilisation in China, Cambridge University Press, pp. 186-191, 1999.

V. Fierro, J. Miranda, C. Romero, J. Andrés, A. Arriaga, D. Schmal, G.. Visser, Prevention of spontaneous combustion in coal stockpiles: Experimental results in coal storage yard, *Fuel Processing Technology,* vol. 59, pp. 23-34, 1999.

B. Moghtaderi, B. Dlugogorski, E. Kennedy, Effects of wind flow on self-heating characteristics of coal stockpiles, *Process Safety and Environmental Protection*, vol. 78, pp. 445-453, 2000.

S. Banerjee, Prevention and Combating Mine Fires, CRC Press, 2000.

Y. Tan, Disaster and contral of spontaneous combustion in coal dield, *Coal Geology & Exploraton,* vol. 28(6), pp. 8-10, 2000.

J. Warnatz, U. Maas, and R. Dibble, Combustion: Physical and Chemical Fundamentals, Modeling and Simulation, Experiments, Pollutant Formation (3rd ed.), Springer-Verlag, Berlin, 2001.

V. Fierro, J. Miranda, C. Romero, J. Andrés, A .Arriaga, D. Schmal, Model predictions and experimental results on self-heating prevention of stockpiled coals, *Fuel*, vol. 80(1), pp. 125-134, 2001.

K. Sasaki, C. Dindiwe, An integrated mine ventilation simulator “MIVENA Ver.6” with applications, *Proceeding of the North American/Ninth U.S. Mine Ventilation*

Symposium, pp. 181-188, 2002.

V. Misra, L. Sukla, Mineral Biotechnology, Allied Publishers, ISBN 10: 8177643495 / ISBN 13: 9788177643497, 2002.

V. Babrauskas, Ignition Handbook, Fire Science Publishers/Society of Fire Protection Engineers, Issaquah WA, 2003.

Y. Çengel, Heat Transfer: A Practical Approach, *McGraw-Hill*, 2003.

A. Alexeev, E. Ulyanova, G.. Starikov, Latent methane in fossil coals, *Fuel*, vol. 83, pp. 1407-1411, 2004.

D. Yap, Master of the extremophiles. The World & I, vol. 19(2), pp. 140-147, 2004. Retrieved from http://search.proquest.com/docview/235847005?accountid=27835

B. Beamish, and D.Blazak, Relationship between ash content and R_{70} self-heating rate of Callide Coal, *International Journal of Coal Geology,* vol. 64(1-2), pp. 126-132, 2005.

Z. Li, Z. Lu, Q. Wu, Numerical simulation study of goaf methane drainage and spontaneous combustion coupling, *Journal of China University of Mining and Technology*, vol. 17, pp. 503-507, 2007.

Z. Lan, Numerical simulation of gas concentration field in multi-source and multi-congruence goaf, *Journal of China Coal Society*, vol. 32, pp. 62-67, 2007.

Eberhard Lindner, Chemie für Ingenieure, Lindner Verlag Karlsruhe, pp. 258, 2008.

Q. Wang, J. Sun, and S. Guo, Spontaneous combustion identification of stored wet cotton using a C_{80} calorimeter. I*ndustrial crops and products*, vol. 28(3), pp. 268-272, 2008.

X. He, R. Zhang, X. Pei, Y. Sun, B. Tong, H. Huang, Numerical simulation for determining Three zones in the goaf at a fully-mechanized coal face, *Journal of China University of Mining and Technology*, vol. 18(2), pp. 199-203, 2008.

X. Huang, R. Finkelman, Understanding the chemical properties of macerals and minerals in coal and its potential application for occupational lung disease prevention, *Journal of Toxicology and Environmental Health, Part B*, vol.11, pp. 45-67, 2008.

Y. Zhao, J. Zhang, C. Chou, Trace element emissions from spontaneous combustion of gob piles in coalmines, *International Journal of Coal Geology*, vol. 73, pp. 52–62, 2008.

A. Jain, Assesment of spontaneous heating susceptibility of coals using differential thermal analysis (Doctoral dissertation, National Institute of Technology Rourkela), 2009.

B. Qin, Q. Sun, D. Wang, L. Zhang, Q. Xu, Analysis and key control technologies to prevent spontaneous combustion occurring at a fully mechanized caving face with large obliquity in deep mines, *Mining Science and Technology*, vol.19(4), pp. 446-451, 2009.

K. Lu, T. Chen, and K. Hu, Investigation of the decomposition reaction and dust explosion characteristics of crystalline benzoyl peroxides, *Journal of hazardous materials*, vol. 161(1), pp. 246-256, 2009.

L. Qi, X. Chen, Theory analysis on spontaneous combustion zone width in the middle of goaf, *Proceedings of 6th International Conference on Mining Science and Technology*, pp. 322-327, 2009.

Y. Fei, A. Aziz, S. Nasir, W. Jackson, M. Marshall, J. Hulston, A. Chaffee, The

spontaneous combustion behavior of some low rank coals and a range of dried products, *Fuel*, vol. 88, pp. 1650-1655, 2009.

Z. Li, Y. Wang, N. Song, Y. Yang, Y. Yang, Experiment study of model compound oxidation on spontaneous combustion of coal, *Procedia Earth and Planetary Science*, vol. 1, pp. 123-129, 2009.

J. Gao, H. Wang, Influence of permeability distribution on airflow field of leakage in gob, *China Safety Science Journal*, Vol.20(3), pp. 81-85, 2010.

International Energy Annual 2006, Energy Information Administration. 2008. Archived from the original on 23 May 2011.

K. Sasaki, and Y. Sugai, Equivalent oxidation exposure-time for low temperature spontaneous combustion of coal, Heat Analysis and Thermodynamic Effects (ed: A Ahsan), InTech, pp. 235-254, 2011.

R. Lakra, Assesment of spontaneous heating of some Indian coking and non-coking coals (Doctoral dissertation, National Institute of Technology Rourkela), 2011.

State Administration of Coalmine Safety, China, Law of The People's Republic of China On Safety in Mines, China Coal Industry Publishing House, Beijing, 2011.

Tamburello, S. Michael, On determining spontaneous ignition in porous materials, master thesis, Department of Fire Protection Engineering, University of Maryland, College Park, MD, 2011.

Y. Pandit, Y .Badhe, B. Sharma, S. Tambe, and B. Kulkarni, Classification of Indian power coals using K-means clustering and Self Organizing Map neural network, *Fuel*, vol. 90(1), pp. 339-347, 2011.

Y. Wu, J. Wu, D. Zhang, C. Zhou, J. Liu, Distribution law of gas and change rule of

"Three zones" in the goaf of fully mechanized top-coal caving working face under the continuous nitrogen injection, *Journal of China Coal Society*, vol. 6, pp. 964-967, 2011.

B. Ambedkar, Experimental Studies on Ultrasonic Coal Beneficiation. Ultrasonic Coal-Wash for De-Ashing and De-Sulfurization. Springer Berlin Heidelberg, ISBN 9783642250163, pp. 41-71, 2012.

G.. James, J. Warden, S. Tamburello, T. Minnich, Spontaneous ignition in fire investigation, *The U.S. Department of Justice Report*, 2012.

G. Speight, The chemistry and technology of coal, Third Edition, CRC Press, ISBN 9781439836460, 2012.

R. Deckers, C. Debeissat, P. Fortin, C. Moonen, and F. Couillaud, Arrhenius analysis of the relationship between hyperthermia and Hsp70 promoter activation: A comparison between ex vivo and in vivo data, *International Journal of Hyperthermia*, vol. 28(5), pp. 441-450, 2012.

S. Dave, D. Tipre, Coal mine drainage pollution and its remediation, Microorganisms in environmental management, Springer Netherlands, pp. 719-743, 2012.

U. Green , Z. Aizenshtat, L. Metzger, and H. Cohen, Field andlLaboratory simulation study of hot spots in stockpiled bituminous coal, *Energy Fuels,* vol. 26 (12), pp. 7230–7235, 2012.

B. Beamish, P. McLellan, H. Endara, U. Turunc, M. Raab, and R. Beamish, Delaying spontaneous combustion of reactive coals through inhibition, *2013 Coal Operators' Conference,* University of Wollongong, Wollongong Australia 2013, pp. 221-226, 2013.

M. Saucedo , J. Lim, J. Dennis, S. Scott, CO_2-gasification of a lignite coal in the presence of an iron-based oxygen carrier for chemical-looping combustion, *Fuel,* vol 127, pp. 186-201, 2013.

R. Pan, Y. Chen, M. Yu, Lu, K. Yang, New technological partition for "Three zones" spontaneous combustion in goaf, *International Journal of Mining Science and Technology*, vol. 23, pp. 489-493, 2013.

W. Ren, Y. Zhao, Z. Feng, Namerical simulation of flow field in goaf based on FLUENT, *Safety in Coal Mines*, Vol.44(6), pp. 26-29, 2013.

Y. Mu, Spontaneous combustion characteristics and air leakage control technology of half isolated island fully mechanized caving face, *Advanced Materials Research*, vol. 718-720, pp. 1639-1644, 2013.

China Industry Research, China Coal Industry Report 2014, *http://www.cir.cn/2014-04/MeiTan-HangYeYanJiuBaoGao650.html*, 2014.

Coal, Encyclopedia Britannica, http://global.britannica.com/science/coal-fossil-fuel, 2014.

D. Ussiri, P. Jacinthe, R. Lal, Methods for determination of coal carbon in reclaimed minesoils: A review, *Groderma*, vol 214-215, pp. 155-167, 2014.

International energy statistics, U.S. Energy Information Administration, 2014.

K. Sasaki, Y. Wang, Y. Sugai, and X. Zhang, Numerical modelling of low rank coal for spontaneous combustion, *2014 Coal Operators' Conference,* University of Wollongong, Wollongong Australia 2014, pp. 344-349, 2014.

S. Ray, D. Panigrahi, and A. Varma, An ecectro-chemical method for determining the susceptibility of Indian coals to spontaneous heating, *International Journal of*

Coal Geology, vol.128-129, pp. 68-80, 2014.